NUWC-NPT Technical Report 10,845
15 March 1995

Wave Propagation in a Fluid-Loaded, Homogeneous, Transversely Isotropic, Elastic Cylinder of Arbitrary Thickness

Marilyn J. Berliner
Submarine Sonar Department

Naval Undersea Warfare Center Division
Newport, Rhode Island

PREFACE

This report was prepared as a Ph.D. dissertation for the degree of Doctor of Philosophy in Mechanical Engineering awarded by the University of Connecticut. The major advisor for this work was Professor Roman Solecki. Associate advisors were Michael L. Accorsi and Robert G. Jeffers. The study was partially sponsored by the Office of Naval Research in Washington, DC.

The technical reviewer for this report was Bruce E. Sandman (Code 814) of NUWC Division Newport.

The author gratefully acknowledges Dr. Sandman for his careful review of the manuscript.

Reviewed and Approved: 15 March 1995

R. J. Martin
Acting Head, Submarine Sonar Department

REPORT DOCUMENTATION PAGE

Form Approved
OMB No. 0704-0188

1. AGENCY USE ONLY (Leave Blank)	2. REPORT DATE	3. REPORT TYPE AND DATES COVERED
	15 March 1995	Ph.D Thesis

4. TITLE AND SUBTITLE

Wave Propagation in a Fluid-Loaded, Homogeneous, Transversely Isotropic, Elastic Cylinder of Arbitrary Thickness

5. FUNDING NUMBERS

6. AUTHOR(S)

Dr. Marilyn J. Berliner

7. PERFORMING ORGANIZATION NAME(S) AND ADDRESS(ES)

Naval Undersea Warfare Center
Detachment New London
New London, Connecticut 06320

8. PERFORMING ORGANIZATION REPORT NUMBER

TR 10,845

9. SPONSORING/MONITORING AGENCY NAME(S) AND ADDRESS(ES)

Office of Naval Research
800 No. Quincy St.
Arlington, VA 22217-5000

10. SPONSORING/MONITORING AGENCY REPORT NUMBER

11. SUPPLEMENTARY NOTES

12a. DISTRIBUTION/AVAILABILITY STATEMENT

Approved for public release; distribution is unlimited.

12b. DISTRIBUTION CODE

13. ABSTRACT (Maximum 200 words)

The problem of wave propagation in an infinite, fluid-loaded, homogeneous, transversely isotropic cylinder is studied within the framework of the linearized, three-dimensional theory of elasticity. The equations of motion of the cylinder are formulated using the constitutive equations of a transversely isotropic material with a preferred material direction collinear with the longitudinal axis of the cylinder. The equations of motion of the internal and external fluids are formulated using the constitutive equations of an inviscid fluid. Displacement potentials are used to solve the equations of motion of the cylinder and the fluids. The frequency equation of the coupled system, consisting of the cylinder and the internal and external fluids, is developed under the assumption of perfect-slip boundary conditions at the fluid-solid interfaces. This frequency equation is general in axial wavenumber k, circumferential wavenumber n, cylinder wall thickness h, and radial frequency ω.

Cut-off frequencies and frequency spectra are computed for the n=1 modes in hollow cylinders, hypothetical fluid columns, fluid-filled cylinders, and cylinders that are fluid filled and immersed in fluid. Numerical results are obtained for two isotropic cylinders (composed of steel and soft (linear) rubber) and for a highly anisotropic, fiber-reinforced cylinder.

The results for the n=1 modes in hollow isotropic cylinders and fluid-filled isotropic cylinders are found to compare very well with known results. The results for the n=1 modes in isotropic cylinders that are fluid filled and immersed in fluid are compared to known results for the n=0 modes in isotropic cylinders with the same fluid-loading boundary conditions.

The results for the n=1 modes in the fiber-reinforced cylinder are compared to the results for the isotopic cylinders. It is shown that the characteristics of wave propagation in the fiber-reinforced cylinder, with and without fluid loading, is markedly different from the characteristics of wave propagation in the isotropic cylinders.

14. SUBJECT TERMS

Anisotropic Cylinder, Fluid Loading, Nonaxisymmetric Modes, Wave Propagation

15. NUMBER OF PAGES
142

16. PRICE CODE

17. SECURITY CLASSIFICATION OF REPORT	18. SECURITY CLASSIFICATION OF THIS PAGE	19. SECURITY CLASSIFICATION OF ABSTRACT	20. LIMITATION OF ABSTRACT
UNCLASSIFIED	**UNCLASSIFIED**	**UNCLASSIFIED**	**SAR**

TABLE OF CONTENTS

LIST OF NOMENCLATURE

a	inner radius of the cylinder
b	outer radius of the cylinder
B^f	adiabatic bulk modulus of the fluid
B_T	transverse bulk modulus of a transversely isotropic material
c	phase velocity
c_e	group velocity
$\hat{c}$	normalized phase velocity, Ω/δ
c_T	shear wave velocity, $\sqrt{c_{44}/\rho}$
C_i	material constants of a homogeneous, transversely isotropic materia ($i = 1, 2, \ldots, 5$)
c_1, c_2	acoustic phase velocities of the inner and outer fluids, respectively
c_{ij}	elastic moduli of the solid
c_{ijkl}	components of the elasticity tensor
E	Young's modulus
E_L	longitudinal Young's modulus of a transversely isotropic material
E_T	transverse Young's modulus of a transversely isotropic material
G_L	longitudinal shear modulus of a transversely isotropic material
G_T	transverse shear modulus of a transversely isotropic material
h	wall thickness of the cylinder

i	imaginary number, $i = \sqrt{-1}$
k	axial wavenumber
m_i	direction cosines of the preferred direction vector of a transversely isotropic material
n	circumferential wavenumber
p_i	excess acoustic pressure in the fluid (i = 1, 2)
q^2	$(\rho\omega^2 - c_{44}\, k^2)/c_{66}$
r, θ, z	cylindrical coordinates
s	ratio of the inner to outer radius of the cylinder
t	time
u_i	displacement components of the cylinder
u_i^f	displacement components of the fluid
$W_n(\xi_i r)$	Bessel functions $J_n(\xi_i r)$ or $I_n(\xi_i r)$, (i = 1, 2, or 3)
$Z_n(\xi_i r)$	Bessel functions $Y_n(\xi_i r)$ or $K_n(\xi_i r)$, (i = 1, 2, or 3)
$W_n(\xi_4 r)$	Bessel functions $J_n(\xi_4 r)$ or $I_n(\xi_4 r)$
$Z_n(\xi_5 r)$	Bessel functions $H_n^1(\xi_5 r)$ or $K_n(\xi_5 r)$
α^2	$\omega^2/c_1^2 - k^2$
β^2	$\omega^2/c_2^2 - k^2$
δ	normalized wavenumber, $\delta = kh$

δ_{ij}	Kronecker's delta
ε_{ij}	components of the strain tensor
ζ_i	constants defined by equations 2.23, (i = 1, 2)
η_i	constants defined by equations 2.38, (i = 1, 2)
ν	Poisson's ratio
ν_L	longitudinal Poisson's ratio of a transversely isotropic material
ν_T	transverse Poisson's ratio of a transversely isotropic material
ξ_i	ζ_i, when ζ_i is real or complex; $\lvert\zeta_i\rvert$, when ζ_i is imaginary, (i = 1, 2)
ξ_3	q, when q is real or complex; |q|, when q is imaginary
ξ_4	α, when α is real or complex; $\lvert\alpha\rvert$, when α is imaginary
ξ_5	β, when β is real or complex; $\lvert\beta\rvert$, when β is imaginary
ρ, ρ_1^f, ρ_2^f	density of cylinder, and inner and outer fluids, respectively
τ_{ij}	components of the cylinder stress tensor
τ_{ij}^f	components of the fluid stress tensor
ϕ	displacement potential of the cylinder
ϕ_i^f	scalar function
ψ	displacement potential of the cylinder
ω	radian frequency
Ω	normalized frequency, $(\omega h)/c_T$

LIST OF FIGURES

1. INTRODUCTION

1.1 GOALS AND OBJECTIVES

The objective of this dissertation is to describe wave propagation in a fluid-loaded, homogeneous, transversely isotropic, elastic cylinder of arbitrary thickness and to investigate the effects of fluid loading on the cut-off frequencies and phase velocities of various axial shear and plane strain modes.

In particular, the goal is to investigate the cut-off frequencies and phase velocities of the flexural modes (n=1, where *n* is the circumferential wavenumber) of wave propagation in the coupled system consisting of a *fiber-reinforced* cylinder that is filled with and immersed in an inviscid fluid. To assist in the interpretation of the numerical results, an analysis of the n=1 modes of wave propagation in fluid-loaded *isotropic* cylinders, with properties of steel and of soft (linear) rubber, is also conducted.

Since the primary interest is in the propagating modes, branches extending into the imaginary and complex wavenumber domains are not included in this study. However, the attenuation of these modes due to the external fluid loading can be obtained directly from the imaginary part of the complex frequency.

1.2 BACKGROUND

1.2.1 Basic concepts in wave propagation

The following definitions are provided as background information. The text by Achenbach (1990) provides a comprehensive study on wave propagation in elastic solids.

1.2.1.1 Phase velocity

A traveling, mechanical wave in one dimension is defined by an expression of the type $f = f(\omega t - kz)$, where f, as a function of the spatial coordinate *z*, time *t*, wavenumber *k*, and radian frequency ω, generally denotes a displacement, a particle velocity, or a stress component. The argument $\omega t - kz$ is the phase of the wave function. Points of constant phase are propagated with the phase velocity

$$c = \omega/k. \tag{1.1}$$

In an inviscid, compressible fluid, the phase velocity is the velocity of sound in the fluid (or the acoustic phase velocity).

If $c = \omega/k$ is complex, the wave function is attenuated. The phase velocity is the real part of *c*. The attenuation is defined by the imaginary part of *c*. Normally, the attenuation is written as an exponential decay as a function of time *t* or of the spatial coordinate *z*.

1.2.1.2 Dispersion

If the phase velocity depends on the wavenumber, the system is said to be dispersive. Dispersion occurs in inelastic (dissipative) materials and in elastic waveguides, where a waveguide is any extended body with a cross section of finite dimensions (such as an infinite plate and an infinitely long cylinder).

1.2.1.3 Group velocity

Group velocity is the velocity of energy transmission in the system. Group velocity

is defined as

$$c_e = d\omega/dk. \tag{1.2}$$

Using $\omega = ck$, we can write the group velocity as

$$c_e = c + k\, dc/dk. \tag{1.3}$$

If there is dispersion, the group velocity is different from the phase velocity.

1.2.1.4 Frequency equation

The frequency equation is an expression relating ω to k in waveguides. The frequency equation is generally derived from the equations of motion and the boundary conditions of the system.

1.2.1.5 Branches and dispersion curves

Solution of the frequency equation yields an infinite number of continuous curves called branches. A branch displays the relationship between wavenumber and frequency for a particular mode of propagation. If the branch is dispersive, it is sometimes called a dispersion curve.

1.2.1.6 Frequency spectrum

A collection of branches is the frequency spectrum of the system. A complete frequency spectrum includes branches extending into the imaginary and complex wavenumber domains.

1.2.1.7 Cut-off frequency

Cut-off frequencies are the frequencies corresponding to a zero wavenumber. For a particular mode, the cut-off frequency is the frequency where the wavenumber of the branch changes from real to imaginary (or complex).

1.2.2 Transversely isotropic materials

Many natural and artificial materials are transversely isotropic. For example, hexagonal crystals, including beryllium, cadmium, magnesium, titanium and zinc, are transversely isotropic. Ice is also transversely isotropic.

A unidirectional, fiber-reinforced composite material is transversely isotropic. This type of material is highly anisotropic because the stiffness and strength in the fiber direction are of the order of the values for the fiber, and are thus very high, and the stiffness and strength transverse to the fiber direction are of the order of the values for the matrix, and are thus much lower. Carbon and graphite, which are often used in fiber-reinforced materials, are themselves transversely isotropic.

1.2.2.1 Constitutive behavior of transversely isotropic materials

In its most general form (here, and in the following, we use the Cartesian coordinate system), Hooke's law can be written as

$$\tau_{ij} = c_{ijkl}\varepsilon_{kl}, \tag{1.4}$$

where τ_{ij} are the components of the stress tensor, ε_{kl} are the components of the strain tensor, and c_{ijkl} are the components of the elasticity tensor. Note that Einstein's sum-

mation convention applies to equations 1.4 and to all subsequent equations that are written in tensor notation, unless noted otherwise.

The components of the stress and strain tensor are symmetric, that is

$$\begin{aligned} \tau_{ij} &= \tau_{ji} \\ \varepsilon_{kl} &= \varepsilon_{lk}, \end{aligned} \tag{1.5}$$

so that

$$c_{ijkl} = c_{jikl} = c_{klij} = c_{ijlk}. \tag{1.6}$$

As a result, there are at most 36 independent components of the elasticity tensor in the general Hooke's law for anisotropic materials. The existence of a strain-energy density function

$$W = \frac{1}{2} c_{ijkl} \varepsilon_{ij} \varepsilon_{kl} \tag{1.7}$$

further reduces the maximum number of independent components to 21.

Because of the symmetries in the components c_{ijkl}, a shortened matrix notation has been introduced to describe the stress-strain relation for an anisotropic material (Payton 1983). In this notation, pairs of subscripts involving the numbers 1, 2, and 3 are replaced by 1, 2, 3, 4, 5, and 6 as follows

$$\begin{aligned} &(11) \leftrightarrow 1,\ (22) \leftrightarrow 2,\ (33) \leftrightarrow 3,\ (23) = (32) \leftrightarrow 4, \\ &(31) = (13) \leftrightarrow 5 \text{ and, } (12) = (21) \leftrightarrow 6, \end{aligned} \tag{1.8}$$

so that, for example,

$$c_{1232} = c_{64}. \tag{1.9}$$

Using the shortened notation, we write equations 1.4 as

$$\tau_i = c_{ij}\varepsilon_j, \tag{1.10}$$

where $i, j = 1, 2, \ldots, 6$, and

$$\begin{aligned} \tau_{11} &= \tau_1 \qquad \tau_{22} = \tau_2 \qquad \tau_{33} = \tau_3 \\ \tau_{23} &= \tau_4 \qquad \tau_{31} = \tau_5 \qquad \tau_{12} = \tau_6, \end{aligned} \tag{1.11}$$

and

$$\begin{aligned} \varepsilon_{11} &= \varepsilon_1 \qquad \varepsilon_{22} = \varepsilon_2 \qquad \varepsilon_{33} = \varepsilon_3 \\ 2\varepsilon_{23} &= \varepsilon_4 \qquad 2\varepsilon_{31} = \varepsilon_5 \qquad 2\varepsilon_{12} = \varepsilon_6. \end{aligned} \tag{1.12}$$

The components c_{ij} in equations 1.10 are called the elastic moduli of the material. When the elastic moduli are independent of position, the medium is said to be elastically homogeneous and the components c_{ij} are the elastic constants of the material.

When the material is elastically symmetric in certain directions, the number of independent elastic moduli in equations 1.10 is further reduced. For instance, when there is one plane of elastic symmetry in the material, there are 13 independent elastic moduli

and the material is called monoclinic. When there is elastic symmetry with respect to three mutually perpendicular planes, the number of independent elastic moduli reduces to 9 and the material is called orthotropic. If, at every point in the material, there is one plane in which the elastic moduli are equal in all directions, the material is called transversely isotropic and the number of elastic moduli reduces to 5. The unit vector normal to the special plane of isotropy in a transversely isotropic material is called the preferred direction of the material. Comprehensive discussions of material symmetry and elastic moduli can be found in Jones (1975), Christensen (1979) and Sokolnikoff (1987).

1.2.2.2 Constraints on the elastic moduli

The elastic moduli c_{ij} are positive definite when

$$c_{ij}x_i x_j > 0, \ (i, j = 1, 2, \ldots, 6), \tag{1.13}$$

for arbitrary, non-zero vectors x_i. Physically this corresponds to the requirement that the strain-energy density function must remain positive in order that this energy be minimal in a state of equilibrium. The necessary and sufficient conditions on the elements c_{ij}, in order that the quadratic form (equation 1.13) be positive definite, are that all of the determinants,

$$c_{11}, \begin{vmatrix} c_{11} & c_{12} \\ c_{21} & c_{22} \end{vmatrix}, \begin{vmatrix} c_{11} & c_{12} & c_{13} \\ c_{21} & c_{22} & c_{23} \\ c_{31} & c_{32} & c_{33} \end{vmatrix}, \ldots, |c_{ij}|, \tag{1.14}$$

remain positive (Kreyszig 1972). The specific constraints on the elastic moduli of a transversely isotropic material are discussed in chapter 3.

1.2.2.3 Effective elastic constants of homogeneous composite materials

When we speak of the elastic constants of a homogeneous, composite material, we really mean the *effective* elastic constants of the material. Before defining the effective elastic constants of a homogeneous, composite material, it is first necessary to explain what is meant by a composite material versus a composite body.

A composite body consists of two or more materials that are macroscopically distinct and are joined together in order to achieve some useful property. The properties that may be emphasized include wear resistance, thermal insulation, acoustic insulation, and low weight. Examples of a composite body include bimetals, clad metals, and laminated glass.

In a composite material, it is possible to define a representative volume element (Hashin 1983). Representative volume elements are large compared to the dimensions of the components of the composite material. A necessary characteristic of a composite material is statistical homogeneity. In a statistically homogeneous composite material all global characteristics such as volume fractions, two-point correlations, etc., are the same in any representative volume element, irrespective of its position within the material. Examples of a composite material include fibrous composites and particulate composites.

The effective elastic constants of a composite material define the relations between averages of field variables such as stress and strain, when the spatial variation of these

field variables is statistically homogeneous. The use of effective elastic constants to define the relations between field variables, when the composite material is subjected to arbitrary boundary conditions and, therefore, the internal field variables are no longer statistically homogeneous, is discussed by Hashin (1983) and is summarized in the following paragraphs.

In the classical continuum mechanics of homogeneous materials, it is always assumed that the continua retain their properties regardless of specimen size. All real materials, however, have microstructure. Metals, for example, are actually polycrystalline aggregates and are heterogeneous materials that are statistically homogeneous. Therefore, the differential element of the theory of elasticity is actually a representative volume element. The effective elastic moduli of this representative volume element are the elastic moduli of the theory of elasticity.

The classical approach, then, in the analysis of homogeneous composite materials, is to assume that the field equations of elasticity are valid, with the effective properties of the composite material replacing the usual elastic properties of a homogeneous continuum.

1.2.2.4 Wave propagation in composite materials

The dynamic response of deformable composite materials can be broadly divided into two categories (Christensen 1979). If the wavelength of the response of the material is long compared to the scale of the representative volume element, the material response is governed by the effective properties of the material. In this case, the equations of motion of the composite material are identical to those of homogeneous materials.

If the wavelength of the response is not ideally long with respect to the representative volume element, very complicated dynamic effects occur. These effects include wave reflection and refraction at the interfaces of the components of the composite material. These phenomena are most important in the field of ultrasonics.

In this study, we restrict our analysis to the wavenumber and frequency domains such that wavelengths are long enough so that we can assume that the material response is governed by the effective material properties.

1.2.3 Previous investigations into wave propagation in cylinders

1.2.3.1 Shells and cylinders in a vacuum

Various models have been developed to investigate the free wave propagation in hollow circular cylinders in a vacuum. Many of the earlier models were based on assumptions that restricted their validity to low frequencies of shells whose thickness is small compared to the inner radius, (Love 1944, Junger and Rosato 1954, Naghdi and Berry 1954, Lin and Morgan 1956a, Naghdi and Cooper 1956, Mirsky and Herrmann 1957, Cooper and Naghdi 1957, Herrmann and Mirsky 1956). Later, Mirsky and Herrmann (1958) investigated wave propagation in a thick-walled shell but restricted their analysis to the lowest or fundamental mode.

Other approximate models have been developed based on the theory of elasticity. Bird (1960) and Bird *et al.* (1960) used a perturbation theory that lead to results involving algebraic and trigonometric functions. McNiven *et al.* (1966a) expanded the displacements in a series of orthogonal polynomials. McFadden (1954) and Gazis (1958) investigated several modes of the plane strain vibrations of finite or infinite cylinders

using the theory of elasticity, but excluded displacements in the axial direction. Finally, investigations of the axisymmetric and nonaxisymmetric modes of wave propagation in hollow cylinders, based on the three-dimensional equations of elasticity, were conducted by Armenakas *et al.* (1969), Gazis (1959a, b) and by Kumar and Stephens (1972).

Almost all of the above investigations were restricted to the purely real dispersion curves, i.e. involving relationships only between real wavenumbers and real frequencies. However, the investigations of McNiven *et al.* (1966b) and Kumar and Stephens (1972) encompassed purely real, purely imaginary and complex dispersion curves.

1.2.3.2 Fluid-filled shells and cylinders

Wave propagation in fluid-filled tubes has been investigated since the time of Young (1808), who produced a comprehensive analysis of the influence of wall compliance on blood flow in human arteries. Since that time, the subject of blood flow has been studied extensively, (see Skalak (1966) for a survey of the literature on blood flow). Examples of other studies includes that of Fay *et al.* (1947) and Jacobi (1949) who used various approximations, such as a restriction to low frequencies or ignoring the Poisson's coupling of the shell, in their investigations of axisymmetric wave propagation in tubes. Thomson (1953) introduced the effects of Poisson's ratio and evaluated the phase velocities of the first three axisymmetric "fluid" waves. Later, Lin and Morgan (1956b) studied the axisymmetric wave propagation in a fluid-filled shell without the approximations introduced by previous authors.

Kumar (1971, 1972) investigated the axisymmetric and nonaxisymmetric wave

propagation in a fluid-filled cylinder of arbitrary thickness, within the framework of the theory of elasticity, and analyzed the cut-off frequencies and the real, imaginary, and complex dispersion curves as functions of wall thickness. More recently, Fuller and Fahy (1982) investigated the real, imaginary, and complex dispersion behavior and energy distributions of axisymmetric and nonaxisymmetric waves in thin-walled cylindrical elastic shells, filled with a fluid, as functions of frequency and material parameters.

1.2.3.3 Shells and cylinders immersed in a fluid

Many of the early investigators of the vibrations of thin and thick shells surrounded by a fluid were interested in the application of the results to acoustic waveguides and underwater sound sources. Junger's (1952a, b) early analysis of thin shells considered only axisymmetric, radial motion of the shell. Junger (1953) later considered the three-dimensional thin shell problem. In this study, Junger did not address the fluid-solid interaction problem but, instead, assumed that the shell had known displacements. Bleich and Baron (1954) extended the work of Junger (1953) by utilizing the modes of vibration of the thin shell in a vacuum as generalized coordinates and emphasized the structural response of the shell rather than the acoustic response of the fluid. Greenspon (1960) studied the case of the axisymmetric vibration of a thick cylindrical shell in water for the purpose of gaining insight into the shell behavior and specialized the results for applications to underwater sound sources and transducers. Greenspon (1961) extended this investigation into the more general type of deformation corresponding to higher order circumferential modes of vibration of thin and thick shells in water. The text by Junger and Feit (1986) provides a comprehensive study on the vibration of

plates and shells in a vacuum and in water and of the sound radiation into the fluid.

1.2.3.4 Shells and cylinders that are fluid-filled and immersed in a fluid

Due to the complexity of the geometry, there have been few investigations into the wave propagation in circular cylinders, of arbitrary thickness, with fluid loading on the inner and the outer surfaces. Chandra and Kumar (1976) investigated the dispersion of axisymmetric waves in fluid-filled cylinders that had external fluid loading. They found that the effect of the surrounding fluid on the fluid-filled cylinder increased with a decrease in the wall thickness of the cylinder and extended their results into the complex wavenumber domain. Sinha *et al.* (1992) also investigated the case of axisymmetric wave propagation in a fluid-loaded cylinder of fixed wall thickness. In their study, the boundary conditions increased in complexity from a hollow cylinder in a vacuum to a fluid-filled cylinder, a hollow cylinder with fluid loading on the outer surface, and a cylinder with fluid loading on the inner and the outer surfaces. A comparison of the analytical results were made to experimental data by Plona *et al.* (1992).

1.2.3.5 Anisotropic cylinders

All of the investigations, discussed so far, have dealt with cylinders composed of isotropic materials. A limited amount of investigations exists in the area of wave propagation in cylinders composed of anisotropic materials, particularly based on the three-dimensional theory of elasticity. Chree (1890) may have been the first investigator of axisymmetric wave propagation in an anisotropic bar. In this analysis, the equations of motion of a transversely isotropic bar, of any cross section, were developed and then specialized for the case of a circular rod. Approximate solutions were obtained by ex-

panding the displacements in powers of the radius r. Later, Morse (1954) developed the exact solution of the problem studied by Chree (1890) and showed that the solution reduced to the Pochhammer solution for the isotropic case. No numerical results were presented by either Chree (1890) or Morse (1954). Mirsky (1965a, b) investigated axisymmetric and nonaxisymmetric wave propagation in transversely isotropic cylinders and used displacement potentials to solve the equations of motion. Fraser (1980) used the method of eigenfunction expansion to separate the equations of motion of an anisotropic cylinder and specialized the results to a transversely isotropic material. However, he did not analyze the dispersion of the modes of vibration. Axisymmetric wave propagation in orthotropic cylinders was studied by Mirsky (1964) who obtained closed-form solutions of the equations of motion in terms of infinite series using the method of Frobenius. Armenakas and Reitz (1973) expanded the displacements of the cylinder into a power series of the radial coordinate to study wave propagation with an arbitrary number of circumferential modes in an orthotropic cylinder. However, none of the above investigations included the effects of fluid loading on either the internal or external surfaces of the cylinder.

To the author's knowledge, wave propagation in fluid-loaded, transversely isotropic cylinders has not been investigated, to date, within the framework of the theory of elasticity,

1.3 OVERVIEW OF THE DISSERTATION

In chapter 2, the displacement equations of motion of the cylinder are formulated using the constitutive equations of a transversely isotropic material with a preferred ma-

terial direction collinear with the longitudinal axis of the cylinder. The displacement equations of motion of the internal and external fluids are formulated using the constitutive equations of an irrotational, inviscid fluid. Displacement potentials are used to solve the equations of motion of the cylinder and of the fluids. The frequency equation of the coupled system, consisting of the cylinder and the inner and outer fluids, is developed under the assumption of perfect-slip boundary conditions at the fluid-solid interfaces. This frequency equation is general in axial wavenumber k, circumferential wavenumber n, wall thickness h, and radian frequency ω.

In chapter 3, the frequency equation is specialized for the case of material isotropy and for the n=1, nonaxisymmetric modes of wave propagation. Cut-off frequencies are computed for the first four plane strain modes and the first two axial shear modes, as functions of two different Poisson's ratios and the ratio of the cylinder inner to outer radius. In particular, Poissons's ratios for steel and for rubber are used in these computations. The frequency spectrum of wave propagation in a hollow cylinder, a hypothetical fluid column, a fluid-filled cylinder, and a cylinder that is fluid-filled and immersed in fluid, is computed for each of the two materials.

In chapter 4, the cut-off frequencies and frequency spectrum are computed for the n=1, nonaxisymmetric modes of wave propagation in a homogeneous, transversely isotropic cylinder that is fluid-filled and immersed in fluid. The particular geometry that is investigated is a fiber-reinforced cylinder with the fibers aligned parallel to the longitudinal axis of the cylinder. The effective elastic constants are computed using the individual elastic constants of the matrix and reinforcing fibers and the volume fractions

of each of the two components. The numerical results are compared to those obtained for the two isotropic materials.

A summary and conclusions of the results of chapters 2 to 4 are provided in chapter 5 and a discussion of recommendations for continued investigations are provided in chapter 6.

The Mathematica programming language (Wolfram 1991) was used extensively throughout this investigation. The symbolic computation capabilities of Mathematica were first used to assist in the manipulation of algebraic formulas in the analytical formulation of the problem. Next, Mathematica's numerical capabilities, including computations of complex Bessel functions, were used for the root searches of the complex frequency equation.

2. ANALYTICAL FORMULATION

We begin this chapter with the physical description and assumptions of the behavior of the coupled system consisting of a hollow cylinder filled with and immersed in an inviscid fluid. We then develop the displacement equations of motion of the cylinder using the constitutive equations of a linearly elastic, homogeneous, transversely isotropic material, and the assumed displacement forms. Solutions of the equations of motion are used to derive the displacement components and surface stresses on the cylinder. Next, we develop the displacement equations of motion of the internal and external fluids, using the constitutive equations of an irrotational, inviscid fluid, and the assumed displacement forms. Solutions of the equations of motion of the internal and the external fluids provides their respective displacement components and pressures.

The frequency equation of the system is developed by coupling the cylinder to the fluids through the boundary conditions at the cylinder's inner and outer surfaces. The classical approach is used to deal with the inviscid fluid-solid interface. That is, perfect-slip boundary conditions are assumed allowing for discontinuity in the planar displacement components. Application of these boundary conditions results in a system of eight, linear, homogeneous, algebraic equations in the unknown wave amplitudes. The solutions of these equations are discussed in chapters 3 and 4.

2.1 SYSTEM GEOMETRY

The system consists of an infinitely long, hollow, linearly elastic, transversely isotropic cylinder with inner radius a, and outer radius b. The cylinder is filled with an ir-

rotational, inviscid fluid with a density ρ_1^f and an acoustic phase velocity c_1. The cylinder is also immersed in a second, irrotational, inviscid fluid with a density ρ_2^f and an acoustic phase velocity c_2. The system is assumed to be linear so that the linearized, three-dimensional, stress equations of motion can be utilized for the cylinder and the fluids. The system displacements and stresses are defined by the cylindrical coordinates, r, θ, z. The cylindrical coordinate directions are designated as the 1, 2, and 3 directions, respectively.

2.2 EQUATIONS OF MOTION OF THE CYLINDER

2.2.1 Three-dimensional dynamic equations of elasticity

The three-dimensional stress equations of motion and strain-displacement relationships of a linearly elastic, solid medium are

$$\tau_{ij,j} = \rho \ddot{u}_i , \tag{2.1}$$

and

$$\varepsilon_{ij} = \frac{1}{2}(u_{i,j} + u_{j,i}) , \tag{2.2}$$

respectively, where τ_{ij} are the components of the stress tensor, ε_{ij} are the components of the strain tensor, u_i are the displacement components, and ρ is the density. It should be noted that Einstein's summation convention applies to equations 2.1 and 2.2 and to

all other equations that are written in tensor notation, and that $\tau_{ij,j}$ denotes $\partial\tau_{ij}/\partial x_j$, etc.

Equations 2.1 and 2.2 are written in cylindrical coordinates as

$$\begin{aligned}
\tau_{rr,r} + \frac{1}{r}\tau_{r\theta,\theta} + \tau_{rz,z} + \frac{1}{r}(\tau_{rr} - \tau_{\theta\theta}) &= \rho\ddot{u}_r \\
\tau_{\theta z,z} + \frac{1}{r}\tau_{\theta\theta,\theta} + \frac{2}{r}\tau_{r\theta} + \tau_{r\theta,r} &= \rho\ddot{u}_\theta \\
\tau_{zz,z} + \frac{1}{r}\tau_{\theta z,\theta} + \frac{1}{r}\tau_{rz} + \tau_{rz,r} &= \rho\ddot{u}_z,
\end{aligned} \tag{2.3}$$

and

$$\begin{aligned}
\varepsilon_r = u_{r,r} \qquad \varepsilon_\theta &= \frac{u_r}{r} + \frac{1}{r}u_{\theta,\theta} \qquad \varepsilon_z = u_{z,z} \\
2\varepsilon_{r\theta} = 2\varepsilon_{\theta r} &= u_{\theta,r} - \frac{u_\theta}{r} + \frac{1}{r}u_{r,\theta} \\
2\varepsilon_{\theta z} = 2\varepsilon_{z\theta} &= \frac{1}{r}u_{z,\theta} + u_{\theta,z} \\
2\varepsilon_{zr} = 2\varepsilon_{rz} &= u_{r,z} + u_{z,r},
\end{aligned} \tag{2.4}$$

respectively.

2.2.2 Constitutive equations

The constitutive equations of a general anisotropic material are

$$\tau_{ij} = c_{ijkl}\varepsilon_{kl}, \tag{2.5}$$

where c_{ijkl} are the components of the elasticity tensor. As discussed in chapter 1, when the medium is homogeneous the components of the elasticity tensor are constant and, when the medium is homogeneous and transversely isotropic only 5 of the elastic constants are independent.

Homogeneous, transversely isotropic materials have one plane in which the elastic constants are equal in all directions. The unit vector, normal to the special plane of isotropy in a transversely isotropic material, is called the preferred direction of the material. When the preferred direction of a transversely isotropic material is given by a unit vector {m}, the constitutive equations, 2.5, can be written as (Sutcu 1992)

$$\begin{aligned}\tau_{ij} = {} & \delta_{ij}\left(C_1\varepsilon_{kk} + C_2 m_p m_q \varepsilon_{pq}\right) + m_i m_j \left(C_2\varepsilon_{kk} + C_3 m_p m_q \varepsilon_{pq}\right) + C_4\varepsilon_{ij} \\ & + C_5\left(m_i m_p \varepsilon_{pj} + m_j m_p \varepsilon_{pi}\right),\end{aligned} \tag{2.6}$$

where the constants C_1, C_2, C_3, C_4, and C_5, are related to the more familiar engineering constants as

$$\begin{aligned} C_1 &= B_T - G_T \\ C_2 &= (2\nu_L - 1)B_T + G_T \\ C_3 &= E_L + (2\nu_L - 1)^2 B_T - 4G_L + G_T \\ C_4 &= 2G_T \\ C_5 &= 2G_L - 2G_T. \end{aligned} \tag{2.7}$$

The definitions of the engineering constants on the right-hand side of equations 2.7 are

B_T = the transverse bulk modulus,

G_L = the longitudinal shear modulus,

G_T = the transverse shear modulus,

E_L = the longitudinal Young's modulus,

E_T = the transverse Young's modulus,

ν_L = the longitudinal Poisson's ratio,

ν_T = the transverse Poisson's ratio,

where "transverse" refers to properties in the plane of isotropy and "longitudinal" refers to properties along the material preferred direction.

When the preferred direction vector {m} is collinear with the z, or the 3, direction of the cylinder, i.e. m_1=0, m_2=0, and m_3=1, equations 2.6 become

$$\begin{aligned} \tau_{rr} &= c_{11}\varepsilon_{rr} + c_{12}\varepsilon_{\theta\theta} + c_{13}\varepsilon_{zz} \\ \tau_{\theta\theta} &= c_{12}\varepsilon_{rr} + c_{11}\varepsilon_{\theta\theta} + c_{13}\varepsilon_{zz} \\ \tau_{zz} &= c_{13}\varepsilon_{rr} + c_{13}\varepsilon_{\theta\theta} + c_{33}\varepsilon_{zz} \\ \tau_{\theta z} = 2c_{44}\varepsilon_{\theta z} \qquad \tau_{zr} &= 2c_{44}\varepsilon_{zr} \qquad \tau_{r\theta} = 2c_{66}\varepsilon_{r\theta}\,, \end{aligned} \tag{2.8}$$

where

$$\begin{aligned} \tau_{11} = \tau_{rr} \qquad \tau_{22} = \tau_{\theta\theta} \qquad \tau_{33} = \tau_{zz} \\ \tau_{23} = \tau_{\theta z} \qquad \tau_{31} = \tau_{zr} \qquad \tau_{12} = \tau_{r\theta}\,, \end{aligned} \tag{2.9}$$

$$\begin{aligned} \varepsilon_{11} &= \varepsilon_{rr} \qquad \varepsilon_{22} = \varepsilon_{\theta\theta} \qquad \varepsilon_{33} = \varepsilon_{zz} \\ \varepsilon_{23} &= \varepsilon_{\theta z} \qquad \varepsilon_{31} = \varepsilon_{zr} \qquad \varepsilon_{12} = \varepsilon_{r\theta}\,, \end{aligned} \tag{2.10}$$

and where

$$\begin{aligned} c_{11} &= C_1 + C_4 = B_T + G_T \\ c_{12} &= C_1 = B_T - G_T \\ c_{13} &= C_1 + C_2 = 2B_T\nu_L \\ c_{33} &= C_1 + 2C_2 + C_3 + C_4 + 2C_5 = E_L + 4B_T\nu_L^2 \\ c_{44} &= \frac{(C_4 + C_5)}{2} = G_L \\ c_{66} &= \frac{C_4}{2} = G_T = (c_{11} - c_{12})/2. \end{aligned} \tag{2.11}$$

A Mathematica program (Wolfram 1991) was developed to expand equations 2.6 for any unit vector {m} and to provide the resulting elastic constants in terms of the engineering constants. This program is provided in appendix D.

Substitution of the constitutive equations, 2.8, and the strain-displacement relationships, 2.4, into the stress equations of motion, 2.3, results in the following displacement equations of motion,

$$c_{11}\left(u_{r,rr}+\frac{1}{r}u_{r,r}-\frac{u_r}{r^2}\right)+\frac{c_{66}}{r^2}u_{r,\theta\theta}+c_{44}u_{r,zz}+\frac{1}{r}(c_{66}+c_{12})\,u_{\theta,r\theta}$$
$$-\frac{1}{r^2}(c_{66}+c_{11})\,u_{\theta,\theta}+(c_{44}+c_{13})\,u_{z,rz}=\rho\ddot{u}_r$$

$$\frac{1}{r}(c_{66}+c_{12})\,u_{r,r\theta}+\frac{1}{r^2}(c_{66}+c_{11})\,u_{r,\theta}+c_{66}\left(u_{\theta,rr}+\frac{1}{r}u_{\theta,r}-\frac{u_\theta}{r^2}\right) \qquad (2.12)$$
$$+\frac{c_{11}}{r^2}u_{\theta,\theta\theta}+c_{44}u_{\theta,zz}+\frac{1}{r}(c_{44}+c_{13})\,u_{z,\theta z}=\rho\ddot{u}_\theta$$

$$(c_{44}+c_{13})\,u_{r,rz}+\frac{1}{r}(c_{44}+c_{13})\,u_{r,z}+\frac{1}{r}(c_{44}+c_{13})\,u_{\theta,\theta z}$$
$$+c_{44}\left(u_{z,rr}+\frac{1}{r}u_{z,r}+\frac{1}{r^2}u_{z,\theta\theta}\right)+c_{33}u_{z,zz}=\rho\ddot{u}_z.$$

2.2.3 Displacement potentials

To uncouple equations 2.12, we follow Mirsky (1965) who assumed the following displacement forms,

$$\begin{aligned}
u_r(r,\theta,z,t) &= \left(\phi(r,\theta)_{,r}+\frac{1}{r}\psi(r,\theta)_{,\theta}\right)\cos(\omega t+kz)\\
u_\theta(r,\theta,z,t) &= \left(\frac{1}{r}\phi(r,\theta)_{,\theta}-\psi(r,\theta)_{,r}\right)\cos(\omega t+kz) \qquad (2.13)\\
u_z(r,\theta,z,t) &= \eta\phi(r,\theta)\sin(\omega t+kz),
\end{aligned}$$

where $\phi(r,\theta)$ and $\psi(r,\theta)$ are displacement potentials and η is an arbitrary constant.

For mathematical convenience we will use an exponential dependence on z and on t so that the assumed displacement forms become

$$\begin{aligned} u_r(r,\theta,z,t) &= \left(\phi(r,\theta)_{,r} + \frac{1}{r}\psi(r,\theta)_{,\theta}\right)e^{-i(\omega t - kz)} \\ u_\theta(r,\theta,z,t) &= \left(\frac{1}{r}\phi(r,\theta)_{,\theta} - \psi(r,\theta)_{,r}\right)e^{-i(\omega t - kz)} \\ u_z(r,\theta,z,t) &= \eta\phi(r,\theta)\,e^{-i(\omega t - kz)}. \end{aligned} \tag{2.14}$$

With this notation, complex phase velocities can be handled in a straightforward manner.

When equations 2.14 are substituted into equations 2.12, and the results are simplified, the equations of motion of the displacement potentials are found to be

$$\begin{aligned} &\left[c_{11}\nabla^2\phi(r,\theta) + \{\rho\omega^2 - k^2c_{44} + i\eta k(c_{13}+c_{44})\}\phi(r,\theta)\right]_{,r} \\ &\quad + \frac{1}{r}\left[c_{66}\nabla^2\psi(r,\theta) + \left(\rho\omega^2 - k^2c_{44}\right)\psi(r,\theta)\right]_{,\theta} = 0 \\ &\frac{1}{r}\left[c_{11}\nabla^2\phi(r,\theta) + \{\rho\omega^2 - k^2c_{44} + i\eta k(c_{13}+c_{44})\}\phi(r,\theta)\right]_{,\theta} \\ &\quad - \left[c_{66}\nabla^2\psi(r,\theta) + \left(\rho\omega^2 - k^2c_{44}\right)\psi(r,\theta)\right]_{,r} = 0 \\ &\left[ik(c_{13}+c_{44}) + \eta c_{44}\right]\nabla^2\phi(r,\theta) + \left(\rho\omega^2 - k^2c_{33}\right)\eta\phi(r,\theta) = 0, \end{aligned} \tag{2.15}$$

where

$$\nabla^2 = (\ )_{,rr} + \frac{1}{r}(\ )_{,r} + \frac{1}{r^2}(\ )_{,\theta\theta} \tag{2.16}$$

is the two-dimensional Laplacian operator, and where the exponential dependence on t and z has been suppressed.

The first two equations of the set 2.15 are satisfied if, in particular,

$$c_{11}\nabla^2\phi(r,\theta) + \left[\rho\omega^2 - k^2 c_{44} + i\eta k(c_{13}+c_{44})\right]\phi(r,\theta) = 0, \tag{2.17}$$

and if

$$c_{66}\nabla^2\psi(r,\theta) + \left(\rho\omega^2 - k^2 c_{44}\right)\psi(r,\theta) = 0. \tag{2.18}$$

The last equation of the set 2.15 is consistent with equation 2.17 when η is the solution of

$$\frac{\eta\left(\rho\omega^2 - k^2 c_{33}\right)}{ik(c_{13}+c_{44}) + \eta c_{44}} = \frac{\rho\omega^2 - k^2 c_{44} + i\eta k(c_{13}+c_{44})}{c_{11}} \equiv \zeta^2. \tag{2.19}$$

After solving for η from

$$\frac{\rho\omega^2 - k^2 c_{44} + i\eta k\,(c_{13} + c_{44})}{c_{11}} = \zeta^2, \tag{2.20}$$

and substituting the solution into

$$\frac{\eta\left(\rho\omega^2 - k^2 c_{33}\right)}{ik\,(c_{13} + c_{44}) + \eta c_{44}} = \zeta^2, \tag{2.21}$$

we find that ζ^2 satisfies the equation

$$\begin{aligned}(c_{11}c_{44})\,\zeta^4 - \left[(c_{11} + c_{44})\,\rho\omega^2 + \left(c_{13}^2 + 2c_{13}c_{44} - c_{11}c_{33}\right)k^2\right]\zeta^2 \\ + \left(\rho\omega^2 - c_{33}k^2\right)\left(\rho\omega^2 - c_{44}k^2\right) = 0.\end{aligned} \tag{2.22}$$

The solutions of ζ^2 are

$$\begin{aligned}\zeta_1^2 &= \frac{-B - \sqrt{B^2 - 4AC}}{2A} \\ \zeta_2^2 &= \frac{-B + \sqrt{B^2 - 4AC}}{2A}\end{aligned} \tag{2.23}$$

where

$$
\begin{aligned}
A &= (c_{11}c_{44}) \\
B &= -\left[(c_{11} + c_{44})\rho\omega^2 + \left(c_{13}^2 + 2c_{13}c_{44} - c_{11}c_{33} \right)k^2 \right] \\
C &= \left(\rho\omega^2 - c_{33}k^2 \right)\left(\rho\omega^2 - c_{44}k^2 \right).
\end{aligned}
\tag{2.24}
$$

From equations 2.17, the third equation of the set 2.15 and equation 2.18, the equations of motion of the displacement potentials $\phi_1(r,\theta)$ (corresponding to ζ_1^2 from equation 2.20), $\phi_2(r,\theta)$ (corresponding to ζ_2^2 from equation 2.21), and $\psi(r,\theta)$, can be shown to be

$$
\begin{aligned}
\nabla^2\phi_1(r,\theta) + \zeta_1^2\phi_1(r,\theta) &= 0 \\
\nabla^2\phi_2(r,\theta) + \zeta_2^2\phi_2(r,\theta) &= 0 \\
\nabla^2\psi(r,\theta) + q^2\psi(r,\theta) &= 0,
\end{aligned}
\tag{2.25}
$$

where

$$
q^2 = \frac{\left(\rho\omega^2 - c_{44}k^2 \right)}{c_{66}}. \tag{2.26}
$$

2.2.4 Solutions of the equations of motion of the cylinder

We first consider the solution of $\phi_1(r, \theta)$. In view of the finite cross-sectional dimensions of the cylinder, we assume a separation of variables solution in r and θ, i.e.

$$\phi_1(r, \theta) = \Phi_1(r)\Theta_1(\theta). \tag{2.27}$$

Substitution of equation 2.27 into the first equation of set 2.25, results in

$$\begin{aligned} &\Theta_1(\theta)_{,\theta\theta} + n^2\Theta_1(\theta) = 0 \\ &\Phi_1(r)_{,rr} + \frac{1}{r}\Phi_1(r)_{,r} - \frac{n^2}{r^2}\Phi_1(r) + \zeta_1^2\Phi_1(r) = 0. \end{aligned} \tag{2.28}$$

The solutions of the first equation in set 2.28 are sines and cosines of argument $n\theta$. Because the solutions should be continuous functions of θ with continuous derivatives, n can only be zero or an integer. The second equation of set 2.28 is Bessel's equation of order n when ζ_1 is real or complex, and is the modified Bessel's equation of order n when ζ_1 is imaginary. The solution of $\Phi_1(r)$ is

$$\Phi_1(r) = A_1 W_n(\xi_1 r) + B_1 Z_n(\xi_1 r), \tag{2.29}$$

where $\xi_1 = \zeta_1$ and W_n and Z_n are the Bessel functions J_n and Y_n, respectively, when ζ_1 is real or complex, and $\xi_1 = |\zeta_1|$ and W_n and Z_n are the modified Bessel functions I_n and K_n, respectively, when ζ_1 is imaginary.

Assuming a separation of variables solution for $\phi_2(r,\theta)$ and $\psi(r,\theta)$ in r and θ results in

$$\Phi_2(r) = A_2 W_n(\xi_2 r) + B_2 Z_n(\xi_2 r), \tag{2.30}$$

and

$$\Psi(r) = A_3 W_n(\xi_3 r) + B_3 Z_n(\xi_3 r). \tag{2.31}$$

In equation 2.30, $\xi_2 = \zeta_2$ and W_n and Z_n are the Bessel functions J_n and Y_n, respectively, when ζ_2 is real or complex, and $\xi_2 = |\zeta_2|$ and W_n and Z_n are the modified Bessel functions I_n and K_n, respectively, when ζ_2 is imaginary. In equation 2.31, $\xi_3 = q$ and W_n and Z_n are the Bessel functions J_n and Y_n, respectively, when q is real or complex, and $\xi_3 = |q|$ and W_n and Z_n are the Bessel functions I_n and K_n, respectively, when q is imaginary.

The sine or cosine dependence on θ in $\phi_1(r,\theta)$, $\phi_2(r,\theta)$, and $\psi(r,\theta)$ must be chosen so that they satisfy equation 2.14. It is evident that a cosine dependence on θ in $\phi_1(r,\theta)$ and in $\phi_2(r,\theta)$ is consistent with a sine dependence on θ in $\psi(r,\theta)$, and vice versa. In this investigation, we use the following set of solutions of the displacement potentials,

$$\phi_1(r,\theta) = (A_1 W_n(\xi_1 r) + B_1 Z_n(\xi_1 r))\cos(n\theta), \tag{2.32}$$

$$\phi_2(r,\theta) = (A_2 W_n(\xi_2 r) + B_2 Z_n(\xi_2 r))\cos(n\theta), \tag{2.33}$$

and

$$\psi(r,\theta) = (A_3 W_n(\xi_3 r) + B_3 Z_n(\xi_3 r))\sin(n\theta). \tag{2.34}$$

2.2.5 Cylinder displacements and surface stresses

When equations 2.32, 2.33 and 2.34 are inserted into equations 2.14, the cylinder displacements become

$$\begin{aligned} u_r(r,\theta,z,t) = \{ & A_1 W_n(\xi_1 r)_{,r} + B_1 Z_n(\xi_1 r)_{,r} \\ & + A_2 W_n(\xi_2 r)_{,r} + B_2 Z_n(\xi_2 r)_{,r} \\ & + \frac{n}{r}[A_3 W_n(\xi_3 r) + B_3 Z_n(\xi_3 r)] \} \cos(n\theta)\, e^{-i(\omega t - kz)}, \end{aligned} \tag{2.35}$$

$$u_\theta(r,\theta,z,t) = \{-\frac{n}{r}[A_1 W_n(\xi_1 r) + B_1 Z_n(\xi_1 r)]$$

$$-\frac{n}{r}[A_2 W_n(\xi_2 r) + B_2 Z_n(\xi_2 r)] \qquad (2.36)$$

$$-[A_3 W_n(\xi_3 r)_{,r} + B_3 Z_n(\xi_3 r)_{,r}]\ \}\sin(n\theta)\, e^{-i(\omega t - kz)},$$

and

$$u_z(r,\theta,z,t) = \{\eta_1[A_1 W_n(\xi_1 r) + B_1 Z_n(\xi_1 r)]$$

$$+\eta_2[A_2 W_n(\xi_2 r) + B_2 Z_n(\xi_2 r)]\ \}\cos(n\theta)\, e^{-i(\omega t - kz)}, \qquad (2.37)$$

where, from equations 2.20 and 2.21, we have

$$\eta_1 = \frac{ik\zeta_1^2(c_{13}+c_{44})}{\left(\rho\omega^2 - c_{33}k^2 - c_{44}\zeta_1^2\right)}$$

$$\eta_2 = \frac{i\left(-c_{44}k^2 + \rho\omega^2 - c_{11}\zeta_2^2\right)}{(c_{13}+c_{44})k}. \qquad (2.38)$$

Next, when equations 2.35, 2.36, and 2.37 are inserted into equations 2.4 and 2.8, and simplified, the surface stresses, τ_{rr}, τ_{zr}, and $\tau_{r\theta}$ become

$$\begin{aligned}\tau_{rr} = \{ & 2c_{66}\frac{n}{r}\Big(A_3 W_n(\xi_3 r)_{,r} + B_3 Z_n(\xi_3 r)_{,r} - \frac{1}{r}[A_3 W_n(\xi_3 r) \\ & + B_3 Z_n(\xi_3 r)\ ]\ ) - 2\frac{c_{66}}{r}[A_1 W_n(\xi_1 r)_{,r} + B_1 Z_n(\xi_1 r)_{,r} \\ & + A_2 W_n(\xi_2 r)_{,r} + B_2 Z_n(\xi_2 r)_{,r}\ ] + 2c_{66}\frac{n^2}{r^2}[A_1 W_n(\xi_1 r) + B_1 Z_n(\xi_1 r) \\ & + A_2 W_n(\xi_2 r) + B_2 Z_n(\xi_2 r)\ ] + \Big(ic_{13}\eta_1 k - c_{11}\zeta_1^2\Big)[A_1 W_n(\xi_1 r) \\ & + B_1 Z_n(\xi_1 r)\ ] + \Big(ic_{13}\eta_2 k - c_{11}\zeta_2^2\Big)\Big[A_2 W_n(\xi_2 r) + B_2 Z_n(\xi_2 r)\ ]\ \} \\ & \cos(n\theta)\, e^{-i(\omega t - kz)},\end{aligned} \tag{2.39}$$

$$\begin{aligned}\tau_{zr} = c_{44}\{ & (\eta_1 + ik)\ [A_1 W_n(\xi_1 r)_{,r} + B_1 Z_n(\xi_1 r)_{,r}\ ] \\ & + (\eta_2 + ik)\ [A_2 W_n(\xi_2 r)_{,r} + B_2 Z_n(\xi_2 r)_{,r}\ ] \\ & + ik\frac{n}{r}[A_3 W_n(\xi_3 r) + B_3 Z_n(\xi_3 r)]\ \}\cos(n\theta)\, e^{-i(\omega t - kz)},\end{aligned} \tag{2.40}$$

and

$$\tau_{r\theta} = c_{66}\{2\frac{n}{r^2}[A_1 W_n(\xi_1 r) + B_1 Z_n(\xi_1 r) + A_2 W_n(\xi_2 r) + B_2 Z_n(\xi_2 r)\,]$$
$$-2\frac{n}{r}[A_1 W_n(\xi_1 r)_{,r} + B_1 Z_n(\xi_1 r)_{,r} + A_2 W_n(\xi_2 r)_{,r} + B_2 Z_n(\xi_2 r)_{,r}\,]$$
$$+q^2\Big[A_3 W_n(\xi_3 r) + B_3 Z_n(\xi_3 r)\,\Big] + \frac{2}{r}[A_3 W_n(\xi_3 r)_{,r} + B_3 Z_n(\xi_3 r)_{,r}\,] \tag{2.41}$$
$$-2\frac{n^2}{r^2}\Big[A_3 W_n(\xi_3 r) + B_3 Z_n(\xi_3 r)\,\Big]\}\sin(n\theta)\, e^{-i(\omega t - kz)}.$$

2.3 EQUATIONS OF MOTION OF THE FLUID

2.3.1 Stress equations of motion and acoustic pressure

The three-dimensional stress equations of motion of and excess acoustic pressure in a linear, irrotational, inviscid fluid are

$$\tau^f_{ij,j} = \rho^f \ddot{u}^f_i, \tag{2.42}$$

and

$$p = -B^f u^f_{i,i}, \tag{2.43}$$

respectively.

2.3.2 Constitutive equations

The constitutive equations of an inviscid fluid are

$$\tau_{ij}^{f} = -p\delta_{ij}. \tag{2.44}$$

We note that the stress tensor for an inviscid fluid is isotropic. That is, the components of the stress tensor, in any rectangular Cartesian system, are unaltered by orthogonal transformations of the coordinates.

Substitution of equations 2.43 and 2.44 into 2.42 provides the displacement equation of motion

$$B^{f} u_{j,ji}^{f} = \rho^{f} \ddot{u}_{i}^{f}, \tag{2.45}$$

where B^f is the adiabatic bulk modulus of the fluid.

2.3.3 Displacement potentials

In investigations of wave propagation in an inviscid fluid, it is generally assumed (Kumar 1972, Chandra and Kumar 1976, Sinha *et al.* 1992) the displacements to be of the form,

$$u_{i}^{f}(r, \theta, z, t) = \phi^{f}(r, \theta, z, t)_{,i} \tag{2.46}$$

where it should be noted that, because the fluid is irrotational, $\phi^f(r,\theta,z,t)$ must be a scalar function.

Upon substitution of 2.46 into 2.45, it can be shown that $\phi^f(r,\theta,z,t)$ must satisfy the

wave equation, that is

$$\phi^f(r, \theta, z, t)_{,ii} - \frac{1}{c^2}\ddot{\phi}^f(r, \theta, z, t) = 0, \tag{2.47}$$

where

$$c^2 = \frac{B^f}{\rho^f} \tag{2.48}$$

is the acoustic phase velocity in the fluid, and where, in cylindrical coordinates,

$$(\ )_{,ii} = (\ )_{,rr} + \frac{1}{r}(\ )_{,r} + \frac{1}{r^2}(\ )_{,\theta\theta} + (\ )_{,zz}. \tag{2.49}$$

2.3.4 Solution of the equations of motion of the fluids

The radial displacement of the fluids and of the cylinder must be continuous at the fluid-solid interfaces. Upon inspection of equations 2.35 and 2.46, it is evident that $\phi^f(r,\theta,z,t)$ must be of the form

$$\phi^f(r, \theta, z, t) = \Phi^f(r) \cos(n\theta)\, e^{-i(\omega t - kz)}. \quad (2.50)$$

When equation 2.50 is substituted into 2.47, we have

$$\left[\Phi^f(r)_{,rr} + \frac{1}{r}\Phi^f(r)_{,r} + \left(\frac{\omega^2}{c^2} - k^2 - \frac{n^2}{r^2}\right)\Phi^f(r)\right]\cos(n\theta)\, e^{-i(\omega t - kz)} = 0. \quad (2.51)$$

Equation 2.51 must be valid for all θ, t, and z, so that

$$\left[\Phi^f(r)_{,rr} + \frac{1}{r}\Phi^f(r)_{,r} + \left(\frac{\omega^2}{c^2} - k^2 - \frac{n^2}{r^2}\right)\Phi^f(r)\right] = 0. \quad (2.52)$$

Equation 2.52 is Bessel's equation of order n when $\omega^2/c^2 - k^2$ is real or complex, and is the modified Bessel's equation of order n when $\omega^2/c^2 - k^2$ is imaginary.

2.3.4.1 Inner fluid

The solution of equation 2.52 for a fluid column must remain finite as $r \to 0$. The Bessel function of the second kind $Y_n(\xi_4 r)$, and the modified Bessel function of the

second kind $K_n(\xi_4 r)$, are unbounded when $r = 0$. Therefore, the solution of equation 2.52 for the inner fluid is

$$\Phi_1^f(r) = D_1 W_n(\xi_4 r), \tag{2.53}$$

where $\xi_4 = \alpha$ and W_n is the Bessel function J_n, when α is real or complex, and $\xi_4 = |\alpha|$ and W_n is the modified Bessel function I_n, when α is imaginary, and where

$$\alpha^2 = \frac{\omega^2}{c_1^2} - k^2. \tag{2.54}$$

2.3.4.2 Outer fluid

The solution of equation 2.52 for outgoing waves in an infinite fluid must remain finite as $r \to \infty$. The modified Bessel function $I_n(\xi_5 r)$ is unbounded when $r \to \infty$. Therefore, the solution of equation 2.52 for the outer fluid is

$$\Phi_2^f(r) = D_2 W_n(\xi_5 r), \tag{2.55}$$

where $\xi_5 = \beta$ and W_n is the Hankel function of the first kind H_n^1, when β is real or complex, and $\xi_5 = |\beta|$ and W_n is the modified Bessel function K_n, when β is imaginary, and where

$$\beta^2 = \frac{\omega^2}{c_2^2} - k^2. \tag{2.56}$$

2.3.5 Displacements and pressures in the fluids

The relevant displacement and pressure components for the inner and outer fluids are as follows.

2.3.5.1 Inner fluid

When equations 2.50 and 2.53 are substituted into equation 2.46, the radial component of displacement for the inner fluid becomes

$$u_r^f(r, \theta, z, t) = D_1 W_n (\xi_4 r)_{,r} \cos(n\theta)\, e^{-i(\omega t - kz)}, \tag{2.57}$$

and, when equations 2.44 and 2.57 are substituted into equation 2.42, the pressure in the inner fluid becomes

$$p_1 = \rho_1^f \omega^2 D_1 W_n (\xi_4 r) \cos(n\theta)\, e^{-i(\omega t - kz)}. \tag{2.58}$$

2.3.5.2 Outer fluid

When equations 2.50 and 2.55 are substituted into equation 2.46, the radial component of displacement for the outer fluid becomes

$$u_r^f(r, \theta, z, t) = D_2 W_n (\xi_5 r)_{,r} \cos(n\theta)\, e^{-i(\omega t - kz)}, \tag{2.59}$$

and, when equations 2.44 and 2.59 are substituted into equation 2.42, the pressure in the outer fluid becomes

$$p_2 = \rho_2^f \omega^2 D_2 W_n (\xi_5 r) \cos(n\theta)\, e^{-i(\omega t - kz)}. \tag{2.60}$$

2.4 BOUNDARY CONDITIONS

To complete the analytical formulation of the frequency equation of the coupled system requires consideration of the boundary conditions at the inner and outer surfaces of the cylinder. In a solid-solid interface problem, the continuity conditions require that the three displacement components and the three surface stress components must be equal. The same would be true if the fluid were viscous.

However, the classical approach with an inviscid fluid-solid interface is to employ perfect-slip boundary conditions that allows discontinuity in planar displacement components. That is, the radial component of displacement of the fluid and solid must be equal at the interfaces, however the circumferential and longitudinal components are discontinuous. The three surface stresses must also be equal. However, we earlier observed that the stress tensor for an inviscid fluid is isotropic. Therefore, the shear stresses in the inner and outer fluids are identically zero.

These boundary conditions can be written as

$$[\tau_{rr}, \tau_{zr}, \tau_{r\theta}, u_r]_{r=a} = \left[-p_1, 0, 0, u_r^f\right]_{r=a}, \tag{2.61}$$

and

$$[\tau_{rr}, \tau_{zr}, \tau_{r\theta}, u_r]_{r=b} = \left[-p_2, 0, 0, u_r^f\right]_{r=b}. \tag{2.62}$$

Equations 2.61 and 2.62 represent a system of eight linear, algebraic equations in unknown wave amplitudes that in matrix form are

$$[L]\{c\} = \{0\}, \tag{2.63}$$

where $[L]$ is a 8 x 8 matrix whose components are found from equations 2.35 and 2.39 to 2.41, and from equations 2.57 to 2.60, and where $\{c\}$ is an 8 x 1 column vector of the unknown amplitude coefficients A_1, B_1, A_2, B_2, A_3, B_3, D_1, and D_2. The components of $[L]$ are defined in appendix A.

The solution of equation 2.63 is nontrivial when the determinant of the coefficients of the wave amplitudes $\{c\}$ vanishes, i.e. when,

$$|L| = 0. \tag{2.64}$$

Equation 2.64 is the frequency equation of the coupled system consisting of a transversely isotropic cylinder filled with and immersed in an inviscid fluid. To the author's knowledge, this frequency equation has not been developed before within the framework of the theory of elasticity.

3. COMPUTATIONAL RESULTS FOR ISOTROPIC CYLINDERS

We begin our investigations by specializing the coupled system for the case of an isotropic cylinder filled with and immersed in an inviscid fluid, and the equations of motion of the n=1, nonaxisymmetric modes of wave propagation. The cut-off frequencies are computed for a ratio of inner to outer radius s ranging from 0 to 0.9, which corresponds to cylinders ranging from solid to thin-walled. The frequency spectra are computed for relatively thick cylinders, with a ratio of inner to outer radius of 0.8, consisting of two different materials, namely a soft (linear) rubber and steel. The relevant properties of the two solid materials and of the inner and outer fluids are provided in appendix C.

Numerical results are obtained for a hollow cylinder in a vacuum, a hypothetical fluid column, a fluid-filled cylinder, and a cylinder that is fluid-filled and immersed in fluid. These individual cases provide a logical progression to systems of increasing difficulty.

To assist in the interpretation of the results for the relatively complex case of a cylinder that is fluid-filled and immersed in fluid, in terms of the results for simpler configurations, the names of the modes are consistent from configuration to configuration whenever the cut-off frequencies of the modes can be approximately traced back to the corresponding cut-off frequencies for a simpler configuration. The results for the isotropic cylinders will be used as an aid to the interpretation of the results for a cylinder of a transversely isotropic material.

The numerical results are presented in and discussed as functions of normalized frequency Ω, normalized wavenumber δ, normalized phase velocity $\hat{c}$, and the ratio of the cylinder's inner to outer radius *s*, where these normalized variables are defined as

a = inner radius,
b = outer radius,
$s = \frac{a}{b}$, ratio of inner and outer radius,
$h = b - a$, cylinder thickness,
$\Omega = \frac{\omega h}{c_T}$, normalized frequency,
$\delta = kh$, normalized wavenumber,
$\hat{c} = \frac{\Omega}{\delta} = \frac{c}{c_T}$, normalized phase velocity,

and where

$$c_T^2 = \frac{c_{44}}{\rho} \tag{3.1}$$

is the shear wave velocity in the material.

3.1 ISOTROPIC BEHAVIOR

We specialize the cylinder's constitutive behavior from transversely isotropic to isotropic by reducing the number of elastic constants from five to two using the following relationships

$$
\begin{aligned}
c_{33} &= c_{11} \\
c_{13} &= c_{12} \\
c_{44} &= c_{66} = \frac{(c_{11} - c_{12})}{2}.
\end{aligned}
\tag{3.2}
$$

These elastic constants are written in terms of engineering constants (also known as technical constants) as follows,

$$
\begin{aligned}
c_{11} &= \frac{E(1-\nu)}{(1+\nu)(1-2\nu)} \\
c_{12} &= \frac{E\nu}{(1+\nu)(1-2\nu)} \\
c_{44} &= \frac{E}{2(1+\nu)},
\end{aligned}
\tag{3.3}
$$

where E is the Young's modulus and ν is the Poisson's ratio of the isotropic material. By normalizing c_{11} and c_{12} to c_{44}, these elastic constants simplify to

$$
\begin{aligned}
c_{11} &= \frac{2(1-\nu)}{(1-2\nu)} c_{44} \\
c_{12} &= \frac{2\nu}{(1-2\nu)} c_{44}.
\end{aligned}
\tag{3.4}
$$

Substitution of equations 3.2 and 3.4 into equations 2.23, 2.26 and 2.38 results in

$$\zeta_1^2 \to \frac{\rho\omega^2}{c_{44}} - k^2 = \frac{\omega^2}{c_T^2} - k^2$$

$$\zeta_2^2 \to \frac{\rho\omega^2}{c_{11}} - k^2 = \frac{(1-2\nu)}{2(1-\nu)}\frac{\rho\omega^2}{c_{44}} - k^2 = \frac{(1-2\nu)}{2(1-\nu)}\frac{\omega^2}{c_T^2} - k^2$$

$$q^2 \to \frac{\rho\omega^2}{c_{44}} - k^2 = \frac{\omega^2}{c_T^2} - k^2 \qquad (3.5)$$

$$ik\eta_1 \to \frac{\rho\omega^2}{c_{44}} - k^2 = \frac{\omega^2}{c_T^2} - k^2$$

$$ik\eta_2 \to -k^2.$$

3.2 A HOLLOW CYLINDER IN A VACUUM

We first consider the case of a hollow cylinder with no external or internal fluid loading. For this set of boundary conditions, the frequency equation is

$$|L| = \begin{vmatrix} L_{11} & L_{12} & L_{13} & L_{14} & L_{15} & L_{16} \\ L_{21} & L_{22} & L_{23} & L_{24} & L_{25} & L_{26} \\ L_{31} & L_{32} & L_{33} & L_{34} & L_{35} & L_{36} \\ L_{51} & L_{52} & L_{53} & L_{54} & L_{55} & L_{56} \\ L_{61} & L_{62} & L_{63} & L_{64} & L_{65} & L_{66} \\ L_{71} & L_{72} & L_{73} & L_{74} & L_{75} & L_{76} \end{vmatrix} = 0, \qquad (3.6)$$

where the simplified variables in equations 3.5 are substituted appropriately into the components of the determinant.

3.2.1 Cut-off frequencies

We begin by solving for the cut-off frequencies of equation 3.6. When the wave-number is zero, the variables in equations 3.5 further reduce to

$$\begin{aligned}
\zeta_1^2 &\to \frac{\omega^2}{c_T^2} \\
\zeta_2^2 &\to \frac{(1-2\nu)}{2(1-\nu)}\frac{\omega^2}{c_T^2} \\
q^2 &\to \frac{\omega^2}{c_T^2} \\
ik\eta_1 &\to \frac{\omega^2}{c_T^2} \\
ik\eta_2 &\to 0
\end{aligned} \tag{3.7}$$

and L_{23}, L_{24}, L_{25}, L_{26}, L_{63}, L_{64}, L_{65}, and L_{66} are zero. Equation 3.6 separates into the product of two sub-determinants

$$Det_1 Det_2 = 0 \tag{3.8}$$

where

$$\mathrm{Det}_1 = \begin{vmatrix} L_{13} & L_{14} & L_{15} & L_{16} \\ L_{33} & L_{34} & L_{35} & L_{36} \\ L_{53} & L_{54} & L_{55} & L_{56} \\ L_{73} & L_{74} & L_{75} & L_{76} \end{vmatrix} \tag{3.9}$$

and

$$\mathrm{Det}_2 = \begin{vmatrix} L_{21} & L_{22} \\ L_{61} & L_{62} \end{vmatrix}. \tag{3.10}$$

Equation 3.8 is satisfied if either Det_1 or Det_2 is equal to zero. The case $\mathrm{Det}_1 = 0$ corresponds to plane strain vibrations (Gazis 1958) in which the displacement component u_z is equal to zero. The case $\mathrm{Det}_2 = 0$ corresponds to axial (or longitudinal) shear vibration involving only longitudinal displacements u_z. When the variables in equations 3.7 are substituted into equation 3.10, we find that the only material variable in Det_2 is the shear wave velocity in the material. Therefore, the normalized cut-off frequencies for the axial shear modes are the same for any isotropic material. Although the plane strain and axial shear modes are uncoupled in the limiting case of zero wavenumber (corresponding to rigid body motion), these modes are coupled at all other wavenumbers.

There is an infinite number of cut-off frequencies that are the solutions of setting Det_1 or Det_2 to zero. For the case of a hollow cylinder in a vacuum, we have solved for the first four cut-off frequencies for the plane strain modes and the first two cut-off frequencies for the axial shear modes. It should be noted that the cut-off frequency for the first plane strain mode is zero. A plot of these cut-off frequencies for a Poisson's ratio of 0.3 (representative of steel) and for a Poisson's ratio of 0.45 (representative of rubber), as functions of the ratio of the inner radius and outer radius of the cylinder, is shown in figure 1. (Note that figures 1-10 are located at the end of chapter 3, starting on page 65).

The cut-off frequencies are normalized to the shear wave velocity in each material. Using the material properties for rubber and for steel, provided in appendix C, along with equation 3.1, the shear wave velocities in the two materials are

$$c_T = 72 \text{ m/sec, for rubber}$$
$$c_T = 3218 \text{ m/sec, for steel.}$$

The normalized cut-off frequencies for the axial modes are the same for either material type, as was discussed above. The normalized cut-off frequencies for the second and third plane strain modes are similar for both materials, with those for rubber being somewhat greater than those for steel. The normalized cut-off frequencies for the second and third plane strain modes, of the two materials, become asymptotically close as the thickness of the cylinder wall decreases. The normalized cut-off frequencies for the

fourth plane strain mode are quite different for the two materials, particularly as the wall thickness increases. As the wall thickness decreases, the normalized cut-off frequencies of the fourth plane strain modes, for both materials, become essentially constant, but not equal.

The results, shown in figure 1, for $\nu = 0.3$, agree with those of Armenakas *et al.* (1969), Gazis (1959), and Kumar and Stephens (1972). Kumar and Stephens (1972) also investigated the variation of cut-off frequencies as functions of Poisson's ratio as Poisson's ratio was varied from 0 to 0.5, for the case of a ratio of inner radius to outer radius of 0.5. Their results showed that, in general, the cut-off frequencies increased with an increasing Poisson's ratio.

The cut-off frequencies for s=0.8 will be used to identify the modes in the frequency spectrum for each material.

3.2.2 Frequency spectra

Next we develop the branches of the frequency spectrum for each material by numerically searching for the frequencies, which are solutions of equation 3.6, for real wavenumbers from 0 to π. Figures 2 and 3 are plots of the frequency spectrum for the three lowest modes (first two plane strain modes and first axial mode) in a cylinder made of a soft rubber and steel, respectively.

In both figures, the first branch, labeled S_1, corresponds to the first plane strain mode. This mode is a flexural mode with large radial displacements and a zero cut-off frequency. The second branch, labeled S_2, corresponds to an axial shear mode with large axial displacements and whose cut-off frequency is the lowest solution of setting

Det_2 equal to zero. For both materials the normalized cut-off frequency for S_2 is

$$\Omega \cong 0.223 \ .$$

The third branch, labeled S_3, corresponds to the second plane strain mode. This mode is a "breathing mode" with large tangential displacements. The cut-off frequency for S_3 is the lowest, non-zero solution of setting Det_1 equal to zero. The normalized cut-off frequencies for the two materials are

$$\Omega \cong 0.5953, \text{ for rubber}$$
$$\Omega \cong 0.5274, \text{ for steel.}$$

For both materials, S_2 and S_3 have group velocities that are vanishingly small in the neighborhood of the cut-off frequencies.

The low wavenumber behavior of the S_1, S_2, and S_3 modes corresponds to that contained in a bending shell theory in which the radial component of displacement is assumed constant through the thickness, while the axial and tangential components are assumed to vary linearly through the thickness (Armenakas, 1969).

By comparing figures 2 and 3, we can examine the differences in the wave propagation characteristics of hollow cylinders of rubber and of steel. For instance, the normalized phase velocity of S_1, for both rubber and steel, is essentially identical in the low wavenumber domain. At higher wavenumbers, the normalized phase velocity of the flexural wave of a steel cylinder is less than that of a rubber cylinder of comparable

thickness. The normalized cut-off frequency and normalized phase velocity, over all wavenumbers, of S_2 is identical for both materials and is asymptotic to the shear wave velocity in each material at high wavenumbers. The normalized cut-off frequency and normalized phase velocity of S_3 for the steel cylinder is lower than for the rubber cylinder, over all wavenumbers shown.

The frequency spectrum for the steel cylinder compares very well with that of previous investigators (Gazis 1959, Armenakas *et al.* 1969, and Kumar and Stephens 1972). These numerical results are included here for completeness and as an aid to the interpretation of the results for more complicated geometries. The frequency spectrum for the thick rubber cylinder, to the author's knowledge, has not been presented before.

3.3 A HYPOTHETICAL FLUID COLUMN

Earlier studies by Kumar (1971, 1972), Chandra and Kumar (1976), and Sinha *et al.* (1992) have shown that the presence of an inner fluid may introduce modes of wave propagation that are not present in a hollow cylinder in a vacuum. These additional modes originate from modes in the fluid column. Therefore, we next consider the cut-off frequencies and frequency spectrum of a hypothetical, cylindrical fluid column.

This information will be useful to the interpretation of the frequency spectrum of the case of a fluid-filled cylinder.

3.3.1 Pressure-release boundary conditions

The case of a cylindrical fluid column with a pressure-release boundary condition requires the pressure at the inner fluid-solid interface to vanish while the radial displacement remains arbitrary. Since the pressure must be zero for all θ, z, and t, equation

2.58, at the inner radius and n=1, reduces to

$$W_1(\xi_4 a) = 0, \tag{3.11}$$

or

$$\xi_4 a = x_1, x_2, x_3, \ldots, \tag{3.12}$$

where $x_1, x_2, x_3, \ldots$ are the zeroes of $W_1(\xi_4 a)$. If $W_1(\xi_4 a) = I_1(\xi_4 a)$ then $x_1, x_2, x_3, \ldots$, are all complex (Abramowitz and Stegun 1972) and, from equation 3.12, $(\xi_4 a)$ is complex. The inner radius *a* is always a real, positive quantity, therefore complex $(\xi_4 a)$ implies complex ξ_4. However, as was discussed in chapter 2, if ξ_4 is complex then $W_1(\xi_4 a) = J_1(\xi_4 a)$. This is contradictory. So $W_1(\xi_4 a) \neq I_1(\xi_4 a)$. If $W_1(\xi_4 a) = J_1(\xi_4 a)$ then $x_1, x_2, x_3, \ldots$, are all real. This means $(\xi_4 a)$ is real and, since the inner radius *a* is always a real, positive quantity, ξ_4 is real and is equal to α. Therefore, from equation 3.11, we have

$$J_1(\alpha a) = 0, \tag{3.13}$$

and, from equation 3.12, we have

$$\alpha a = 3.832, 7.016, 10.173, \ldots. \tag{3.14}$$

Equation 3.14 is the frequency equation of a hypothetical fluid column with a pressure-release boundary condition.

3.3.2 Displacement-free boundary conditions

The case of a cylindrical fluid column with radial displacement-free boundary conditions requires that u_r^f must vanish at the inner radius of the cylinder while the pressure remains arbitrary. This must be true for all θ, z, and t, and equation 2.57, at the inner radius and n=1, reduces to

$$[W_1(\xi_4 r)_{,r}]_{r=a} = 0. \tag{3.15}$$

Using a similar argument as above, $W_1(\xi_4 a) \neq I_1(\xi_4 a)$ because the zeros of $I_1(\xi_4 r)_{,r}$ are all complex (Abramowitz and Stegun 1972). If $W_1(\xi_4 a) = J_1(\xi_4 a)$ then the roots of $[J_1(\xi_4 r)_{,r}]_{r=a}$ are all real, $\xi_4 = \alpha$, and equation 3.15 becomes

$$J_1(\alpha a) - \alpha a J_2(\alpha a) = 0, \tag{3.16}$$

or,

$$\alpha a = 1.841, 5.331, 8.536, \ldots. \tag{3.17}$$

Equation 3.17 is the frequency equation of a hypothetical fluid column with a displacement-free boundary condition.

Equations 3.14 and 3.17 represent families of hyperbolas with finite cut-off fre-

quencies. The first two cut-off frequencies, for each of the two boundary conditions and for s=0.8, normalized to the shear wave velocity in rubber, are

$\Omega \cong 19.98, 36.58$, pressure-release boundary conditions
$\Omega \cong 9.61, 27.8$, displacement-free boundary condtions.

The first two cut-off frequencies, for each of the two boundary conditions and for s=0.8, normalized to the shear wave velocity in steel, are

$\Omega \cong 0.9465, 0.8176$, pressure-release boundary conditions
$\Omega \cong 0.2146, 0.6213$, displacement-free boundary conditions.

3.3.3 Frequency spectra

The first two branches, corresponding to each of the two sets of boundary conditions and normalized to the shear wave velocity in rubber and of steel, are shown in figures 4 and 5, respectively. The normalization to the shear wave velocity in each of the materials facilitates the comparison of these results to other results. The curves labeled l_1 and l_2 represent solutions of equations 3.14, while the curves labeled L_1 and L_2 represent solutions of equations 3.17.

From a comparison of figures 2 and 4, we note that the fluid modes, figure 4, exist at wavenumbers and frequencies greater than the solid modes of a rubber cylinder, figure 2. This means that the fluid modes will not couple with the solid modes, at least in the wavenumber and frequency domains of interest. However, from a comparison of figures 3 and 5, we note that the fluid modes, figure 5, exist within the same wavenum-

ber and frequency domains as the solid modes of a steel cylinder, figure 3. The implications of this overlap or intersection of fluid and solid modes will be discussed further in the next section.

Sinha *et al.* (1992) investigated the dispersion curves for the axisymmetric wave propagation in a hypothetical fluid column, with stress-free and with displacement-free boundary conditions, and normalized their results to the shear wave velocity in steel. They found that the lowest order dispersion curve for the displacement-free boundary condition had a zero cut-off frequency. Kumar (1971) derived the frequency equation of the n=1 modes of nonaxisymmetric wave propagation in a hypothetical fluid column, for stress-free and for displacement-free boundary conditions. However, he did not develop the dispersion curves.

3.4 A FLUID-FILLED CYLINDER

The next case to be investigated is that of a fluid-filled cylinder. For this set of boundary conditions, the frequency equation is

$$|L| = \begin{vmatrix} L_{11} & L_{12} & L_{13} & L_{14} & L_{15} & L_{16} & L_{17} \\ L_{21} & L_{22} & L_{23} & L_{24} & L_{25} & L_{26} & L_{27} \\ L_{31} & L_{32} & L_{33} & L_{34} & L_{35} & L_{36} & L_{37} \\ L_{41} & L_{42} & L_{43} & L_{44} & L_{45} & L_{46} & L_{47} \\ L_{51} & L_{52} & L_{53} & L_{54} & L_{55} & L_{56} & L_{57} \\ L_{61} & L_{62} & L_{63} & L_{64} & L_{65} & L_{66} & L_{67} \\ L_{71} & L_{72} & L_{73} & L_{74} & L_{75} & L_{76} & L_{77} \end{vmatrix} = 0. \qquad (3.18)$$

In the limiting case of zero wavenumber, this frequency equation separates into the product of two sub-determinants

$$Det_1 Det_2 = 0 \tag{3.19}$$

where

$$Det_1 = \begin{vmatrix} L_{13} & L_{14} & L_{15} & L_{16} & L_{17} \\ L_{33} & L_{34} & L_{35} & L_{36} & L_{37} \\ L_{43} & L_{44} & L_{45} & L_{46} & L_{47} \\ L_{53} & L_{54} & L_{55} & L_{56} & L_{57} \\ L_{73} & L_{74} & L_{75} & L_{76} & L_{77} \end{vmatrix} \tag{3.20}$$

and where

$$Det_2 = \begin{vmatrix} L_{21} & L_{22} \\ L_{61} & L_{62} \end{vmatrix} \tag{3.21}$$

is the same as equation 3.10.

In the case of a hollow cylinder without any fluid loading, we noted that the only

material variable in Det_2 was the shear wave velocity in the solid material. Inspection of the components of equation 3.21 shows that Det_2 is also independent of the internal fluid parameters. This means that the normalized cut-off frequencies for the axial shear modes, found from setting 3.10 or 3.21 equal to zero, are the same for empty and for fluid-filled cylinders of any isotropic material.

3.4.1 Cut-off frequencies for the rubber cylinder

The normalized cut-off frequencies for the S_1, S_2, and S_3 modes for the fluid-filled rubber cylinder are

$$\Omega \cong 0,\ 0.223,\ 0.431,$$

respectively.

As expected, the presence of the internal fluid has not affected the normalized cut-off frequency of the S_2 mode. However, the presence of the internal fluid has reduced the cut-off frequency of the S_3 mode by approximately 28%. No additional cut-off frequencies, which can be traced back to fluid modes, exist within the normalized frequency band of 0 to π. The absence of any additional cut-off frequencies means that the internal fluid does not introduce additional modes in the coupled system, consisting of the inner fluid and the cylinder, within the normalized frequency band of interest.

3.4.2 Frequency spectrum for the rubber cylinder

The frequency spectrum for the fluid-filled rubber cylinder is shown in figure 6. From a comparison of figure 6 to figure 2, we note that the phase velocity of the S_1 mode of the fluid-filled cylinder is less than that of the S_1 mode of the empty cylinder for all wavenumbers. For instance, at $\delta = 0.2\pi$, the phase velocity of the S_1 mode is re-

duced approximately 36% when fluid is added to the inside of the cylinder.

The phase velocity of the S_2 mode is reduced somewhat for $\delta/\pi < 0.3$. At higher wavenumbers, the phase velocity of this mode is unaffected by the fluid and is asymptotic to the shear wave velocity in rubber. The phase velocity of the S_3 mode is reduced over all wavenumbers as compared to the phase velocity of the hollow cylinder without an internal fluid.

3.4.3 Cut-off frequencies for the steel cylinder

The normalized cut-off frequencies for the S_1, S_2, L_1, S_3, and L_2 modes for a fluid-filled steel cylinder are

$$\Omega \cong 0, 0.223, 0.228, 0.516, 0.644,$$

respectively.

The normalized cut-off frequencies of each of these modes can be traced back to the normalized cut-off frequencies of the modes for each of the separate components of the coupled system. For instance, the cut-off frequency for the S_3 mode is somewhat reduced from the cut-off frequency for the "breathing" mode of the empty cylinder. The cut-off frequencies for the modes labeled L_1 and L_2 can be similarly traced back to the cut-off frequencies of the hypothetical fluid column with the radial displacement-free boundary condition. As expected, the cut-off frequency of the S_2 mode has been unaffected by the presence of the fluid.

The presence of the additional cut-off frequencies for the $L_1$and L_2 modes means that the internal fluid has introduced two more modes in the coupled system, consisting of a the inner fluid and the cylinder, at least within the normalized frequency band of 0

to π.

3.4.4 Frequency spectrum for the steel cylinder

The frequency spectrum for the fluid-filled steel cylinder is shown in figure 7. These results are dramatically different from those shown in figure 6. The fluid-based modes and the solid-based modes are greatly perturbed in the coupled system as evidenced by large changes in the phase velocities from those of the individual components of the system and by an alternating "weak coupling" between the S_3 and L_1 modes and between the S_3 and L_2 modes. Weak coupling of modes is evidenced by regions in the frequency spectrum where branches come close together (Armenakas *et al.* 1969).

The phenomenon of coupling between fluid and solid modes was observed for the cases of axisymmetric motion of a fluid-filled steel cylinder by Sinha *et al.* (1992) and for the case of nonaxisymmetric motion of a fluid-filled steel cylinder by Kumar (1971).

A comparison of the frequency spectrum of a fluid-filled steel and hard rubber cylinders was made by Fuller and Fahy (1982) on the basis of a thin-shell theory. In their analysis the ratio of the cylinder wall thickness to the mean radius was 0.05, and the shear wave velocity in the hard rubber was approximately 785 m/sec. The results shown in figures 6 and 7 are for a ratio of the cylinder wall thickness to the mean radius of approximately 0.22, and for a shear wave speed in the soft rubber of approximately 72 m/sec.

To the author's knowledge, this is the first time that a direct comparison of the wave propagation characteristics of a thick, fluid-filled steel and soft rubber cylinder has been

made on the basis of the theory of elasticity.

3.5 A CYLINDER THAT IS FLUID-FILLED AND IMMERSED IN FLUID

The final case to be investigated, in this chapter, is that of a fluid-filled cylinder that is immersed in an infinite inviscid fluid. For this set of boundary conditions, the frequency equation is

$$|L| = \begin{vmatrix} L_{11} & L_{12} & L_{13} & L_{14} & L_{15} & L_{16} & L_{17} & L_{18} \\ L_{21} & L_{22} & L_{23} & L_{24} & L_{25} & L_{26} & L_{27} & L_{28} \\ L_{31} & L_{32} & L_{33} & L_{34} & L_{35} & L_{36} & L_{37} & L_{38} \\ L_{41} & L_{42} & L_{43} & L_{44} & L_{45} & L_{46} & L_{47} & L_{48} \\ L_{51} & L_{52} & L_{53} & L_{54} & L_{55} & L_{56} & L_{57} & L_{58} \\ L_{61} & L_{62} & L_{63} & L_{64} & L_{65} & L_{66} & L_{67} & L_{68} \\ L_{71} & L_{72} & L_{73} & L_{74} & L_{75} & L_{76} & L_{77} & L_{78} \\ L_{81} & L_{82} & L_{83} & L_{84} & L_{85} & L_{86} & L_{87} & L_{88} \end{vmatrix} = 0. \qquad (3.22)$$

In the limiting case of zero wavenumber, this frequency equation separates into the product of two sub-determinants

$$Det_1 Det_2 = 0 \qquad (3.23)$$

where

$$Det_1 = \begin{vmatrix} L_{13} & L_{14} & L_{15} & L_{16} & L_{17} & L_{18} \\ L_{33} & L_{34} & L_{35} & L_{36} & L_{37} & L_{38} \\ L_{43} & L_{44} & L_{45} & L_{46} & L_{47} & L_{48} \\ L_{53} & L_{54} & L_{55} & L_{56} & L_{57} & L_{58} \\ L_{73} & L_{74} & L_{75} & L_{76} & L_{77} & L_{78} \\ L_{83} & L_{84} & L_{85} & L_{86} & L_{87} & L_{88} \end{vmatrix} \tag{3.24}$$

and where

$$Det_2 = \begin{vmatrix} L_{21} & L_{22} \\ L_{61} & L_{62} \end{vmatrix} \tag{3.25}$$

is the same as equations 3.10 and 3.21. Inspection of the components of equation 3.25 shows that Det_2 is also independent of the external fluid parameters. Therefore, the normalized cut-off frequencies for the axial shear modes, found from setting equations 3.10, 3.21, or 3.25 equal to zero, are the same for any isotropic cylinders that are empty, fluid-filled, or fluid-filled and immersed in fluid.

3.5.1 Cut-off frequencies for the rubber cylinder

The normalized cut-off frequencies for the S_1, S_2, and S_3, modes for a rubber cylinder that is fluid-filled and immersed in fluid are

$$\Omega \cong 0, 0.223, 0.431,$$

respectively.

The cut-off frequencies for the S_3 mode is essentially unaffected by the addition of the external fluid loading. All the cut-off frequencies are real.

3.5.2 Frequency spectrum for the rubber cylinder

The frequency spectrum for the rubber cylinder that is fluid-filled and immersed in fluid is shown in figure 8. From a comparison of figures 6 and 8, we note that the low wavenumber behavior of the S_1 and S_3 modes is virtually unaffected by the addition of the external fluid loading. There is some reduction in phase velocity of the S_1 mode at the higher wavenumbers. The reduction in phase velocity of the S_3 mode at the higher wavenumbers is more pronounced. The S_2 mode is not affected by the external fluid loading. It should be noted, that the branches are real. This means that the external fluid has not introduced any damping into the modes of wave propagation in the coupled system.

3.5.3 Cut-off frequencies for the steel cylinder

The normalized cut-off frequencies for the S_1, S_2, L_1, S_3, and L_2 modes for a steel cylinder that is fluid-filled and immersed in fluid are

$$\Omega \cong 0, 0.223, 0.228 - 0.0014i, 0.515 - 0.010i, 0.6433\text{-}0.0035i,$$

respectively.

The most notable effect of the external fluid loading on the cut-off frequencies of the coupled system is that the cut-off frequencies for the L_1, S_3, and L_2 modes are complex. At zero wavenumber, these modes are rigid body modes. Therefore, the presence of the external fluid has introduced damping in these modes of vibration.

3.5.4 Frequency spectrum for the steel cylinder

In figure 9 we show the real part of the frequency spectrum for the steel cylinder that is fluid-filled and immersed in fluid. From a comparison of figures 9 and 7 we find that the real part of branches are very similar to the branches for the fluid-filled steel cylinder. That is, except some very small changes in the phase velocity of the S_1 mode, the presence of the external fluid has had little effect on the real part of the cut-off frequencies or the phase velocities of any of the modes.

In figure 10 we show the imaginary part of the frequency spectrum. The presence of the imaginary part of a complex frequency indicates that the external fluid has introduced damping in the coupled system. What is most important to note in figure 10 is the nontrivial behavior of the imaginary term as a function of wavenumber and of mode type. At zero wavenumber, the S_1 and S_2 modes are undamped and the cut-off frequencies are unaffected by the presence of the internal or external fluids. The S_1 mode remains lightly damped or undamped over the wavenumber domain of interest. The S_3 mode has the highest amount of damping at zero wavenumber while the damping in the L_2 mode is somewhat greater than the damping in the L_1 mode. This means, as rigid body modes, only the S_1 (harmonic transverse vibration) and S_2 modes (harmonic longitudinal vibration) will exist for all time.

Attenuation of displacements, particle velocities, stresses, etc., due to the damping in the system, can be examined by rewriting the complex exponential as

$$e^{-i(\omega t - kz)} = e^{-i(x+iy)t} e^{ikz} = e^{yt} e^{-i(xt-kz)} \tag{3.26}$$

where x is the real part and y is the imaginary part of the complex frequency. If y is positive, the cylinder displacements (for instance) increase without bounds with increasing time. This is physically unrealistic. Therefore, the imaginary term must be negative, which is true for our results.

Chandra and Kumar (1976) investigated the axisymmetric modes of wave propagation in a brass cylinder that was fluid-filled and immersed in fluid. They found that the percent reduction in phase velocity of the various modes increased with a decrease in the wall thickness of the cylinder. Sinha, *et al.* (1992) investigated the axisymmetric modes of wave propagation in a steel cylinder that was fluid-filled and immersed in fluid. They found the presence of the external fluid introduced damping in the system through the presence of complex frequencies as solutions of the frequency equation.

To the author's knowledge, this dissertation represents the first time the frequency spectrum of the n=1 modes of nonaxisymmetric wave propagation in isotropic cylinders (of any material), with internal and external fluid loading, has been studied within the framework of the theory of elasticity.

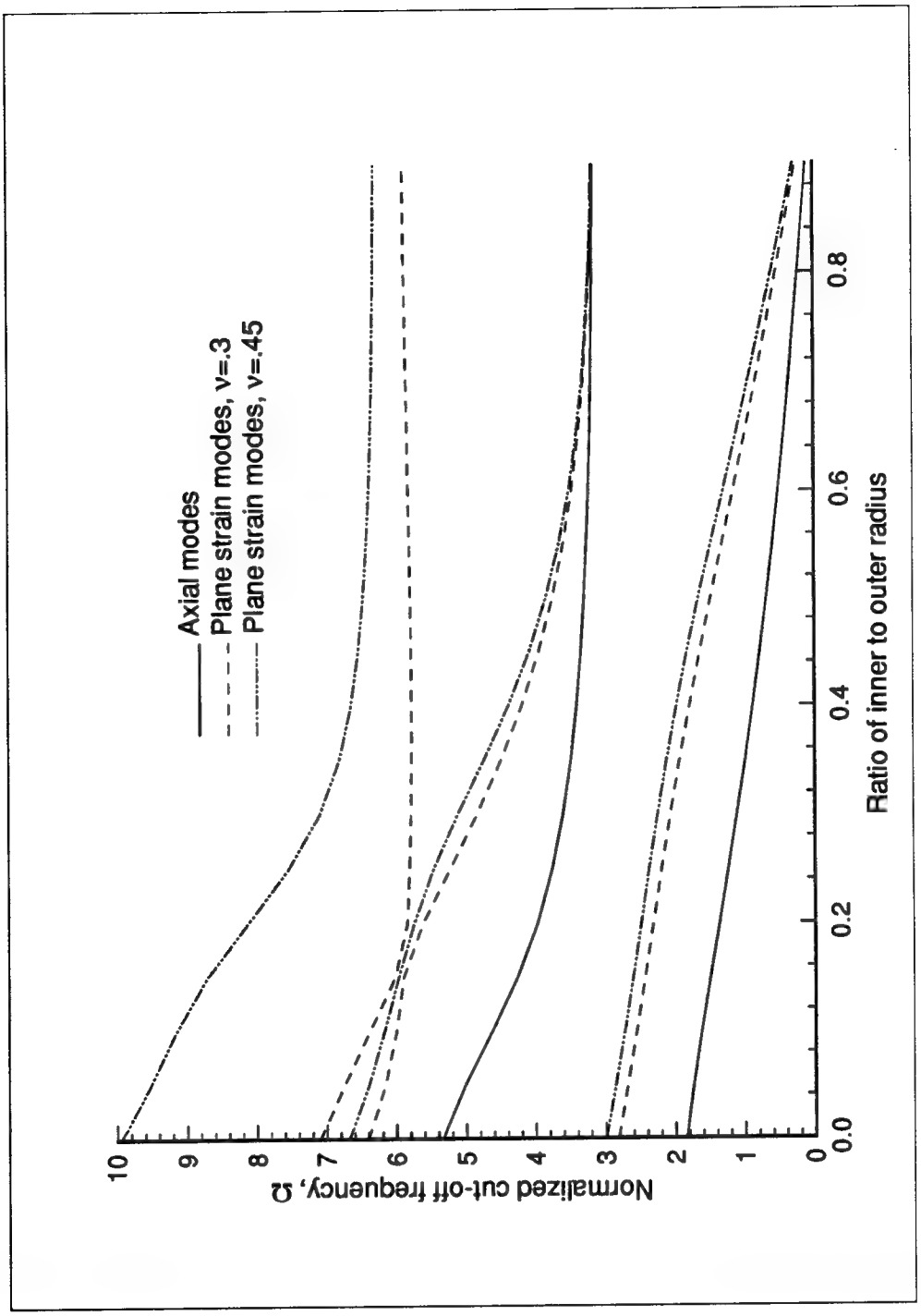

Figure 1. Comparison of the normalized cut-off frequencies of the steel cylinder and of the rubber cylinder, as functions of the ratio of the inner to the outer radius

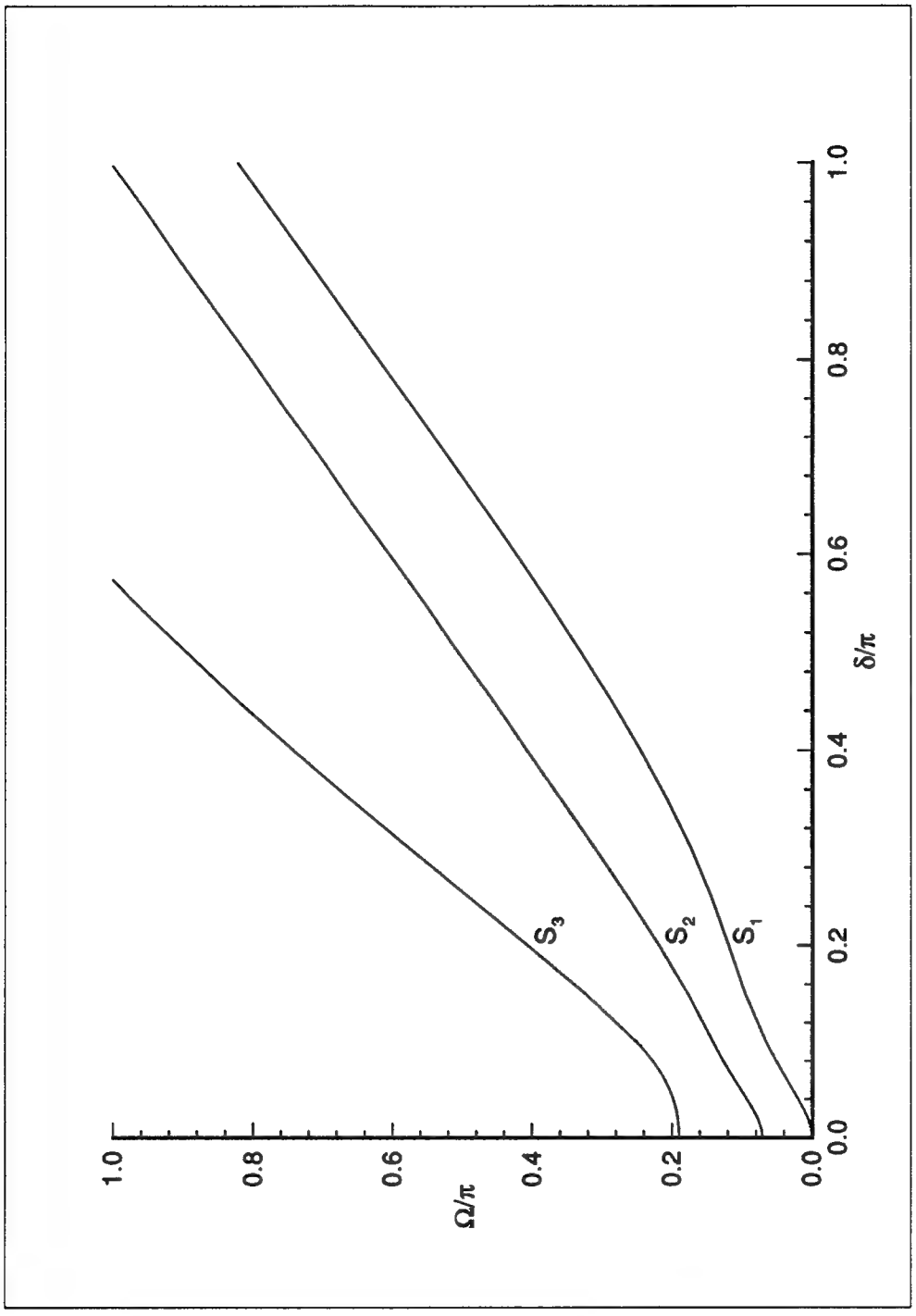

Figure 2. Frequency spectrum of the rubber cylinder in a vacuum

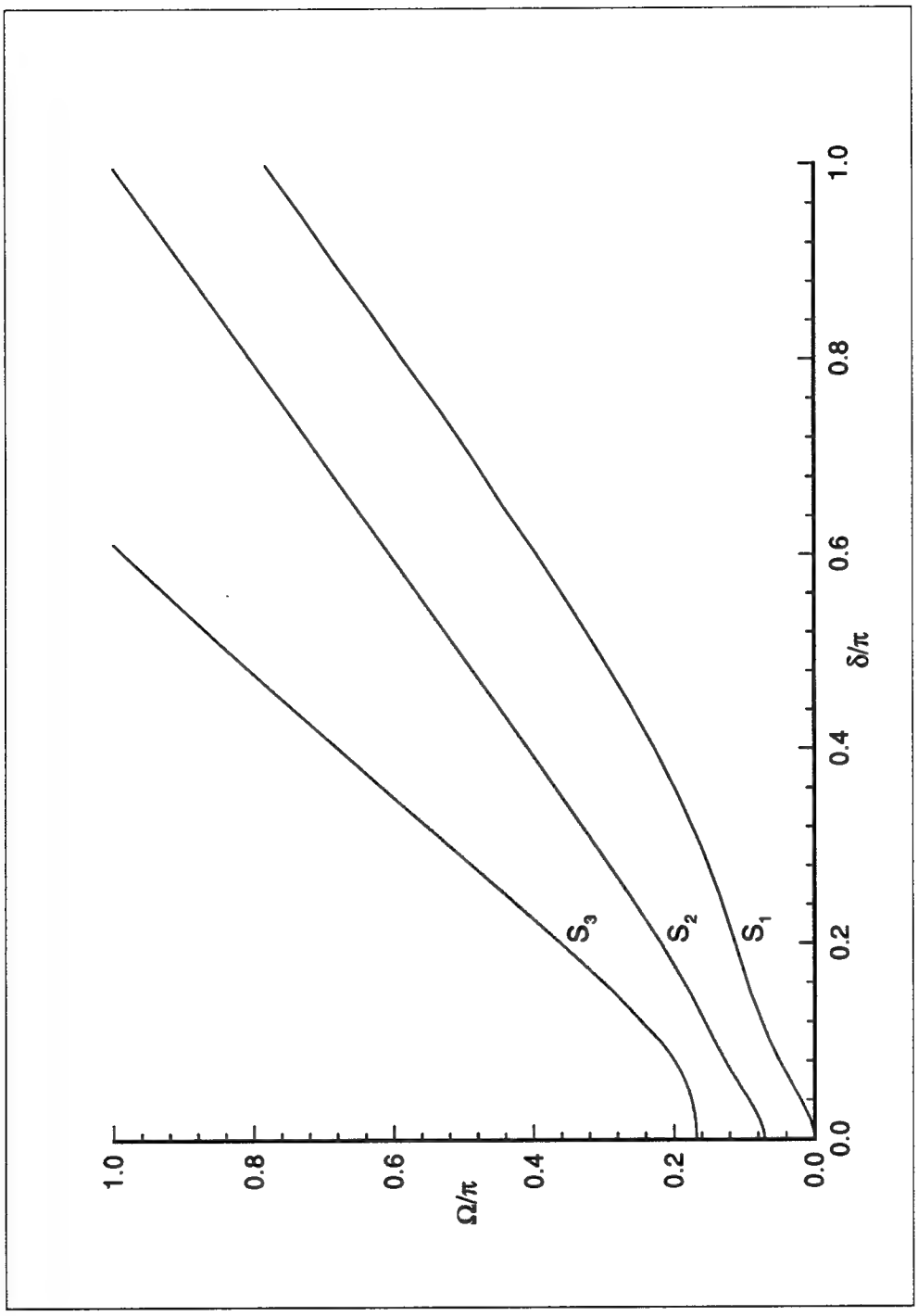

Figure 3. Frequency spectrum of the steel cylinder in a vacuum

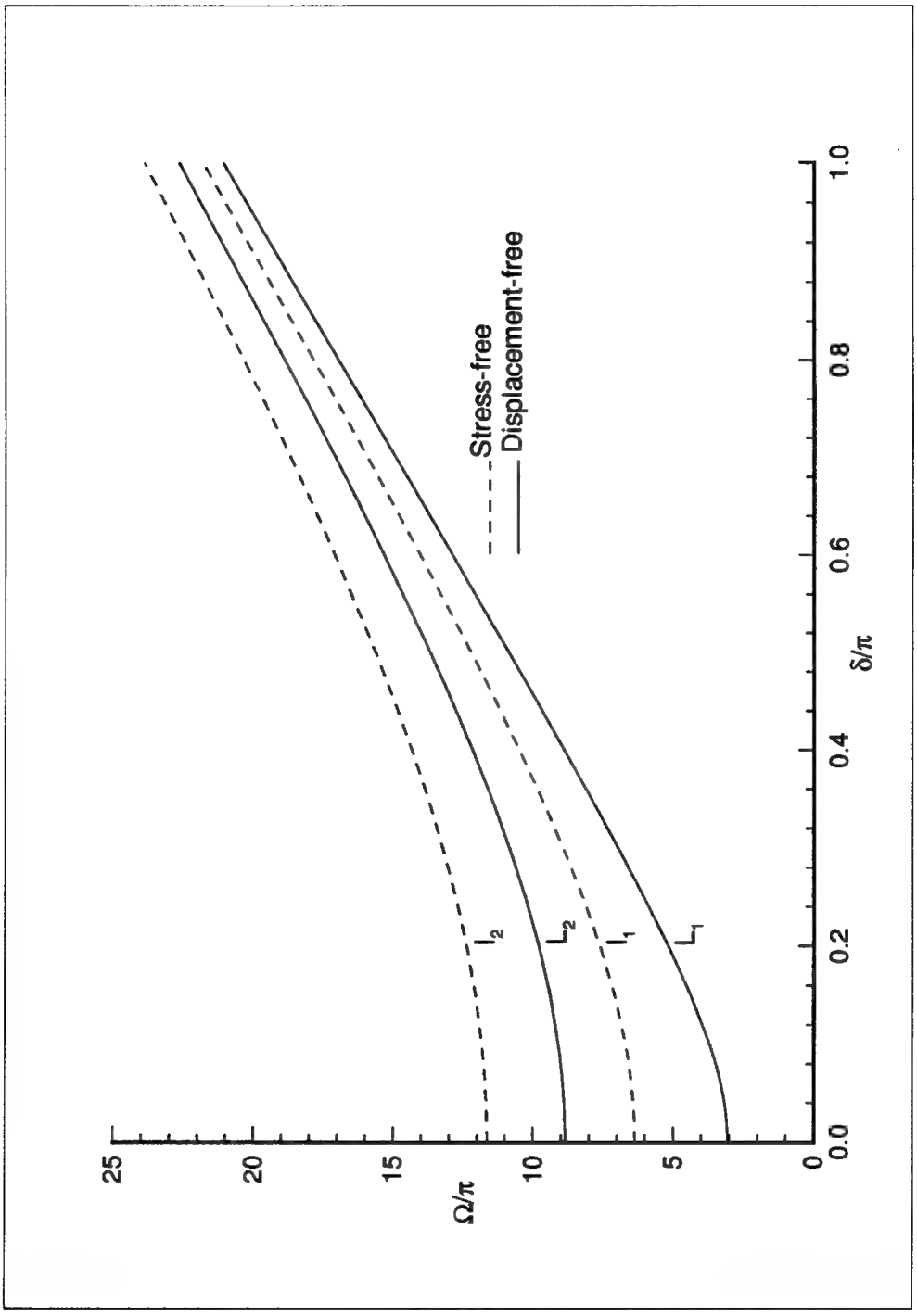

Figure 4. Frequency spectrum of the hypothetical fluid column normalized to the shear wave velocity in rubber

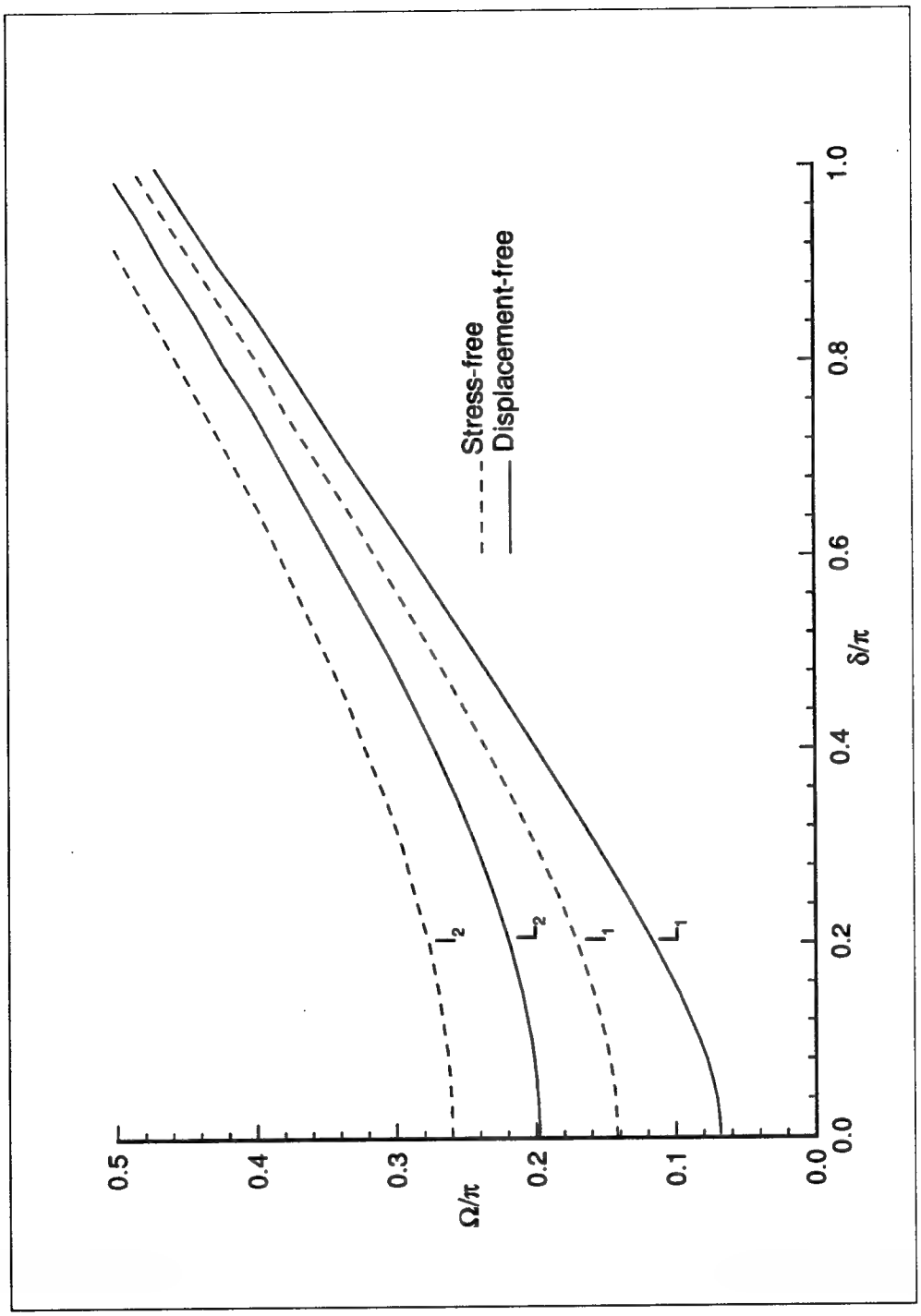

Figure 5. Frequency spectrum of the hypothetical fluid column normalized to the shear wave velocity in steel

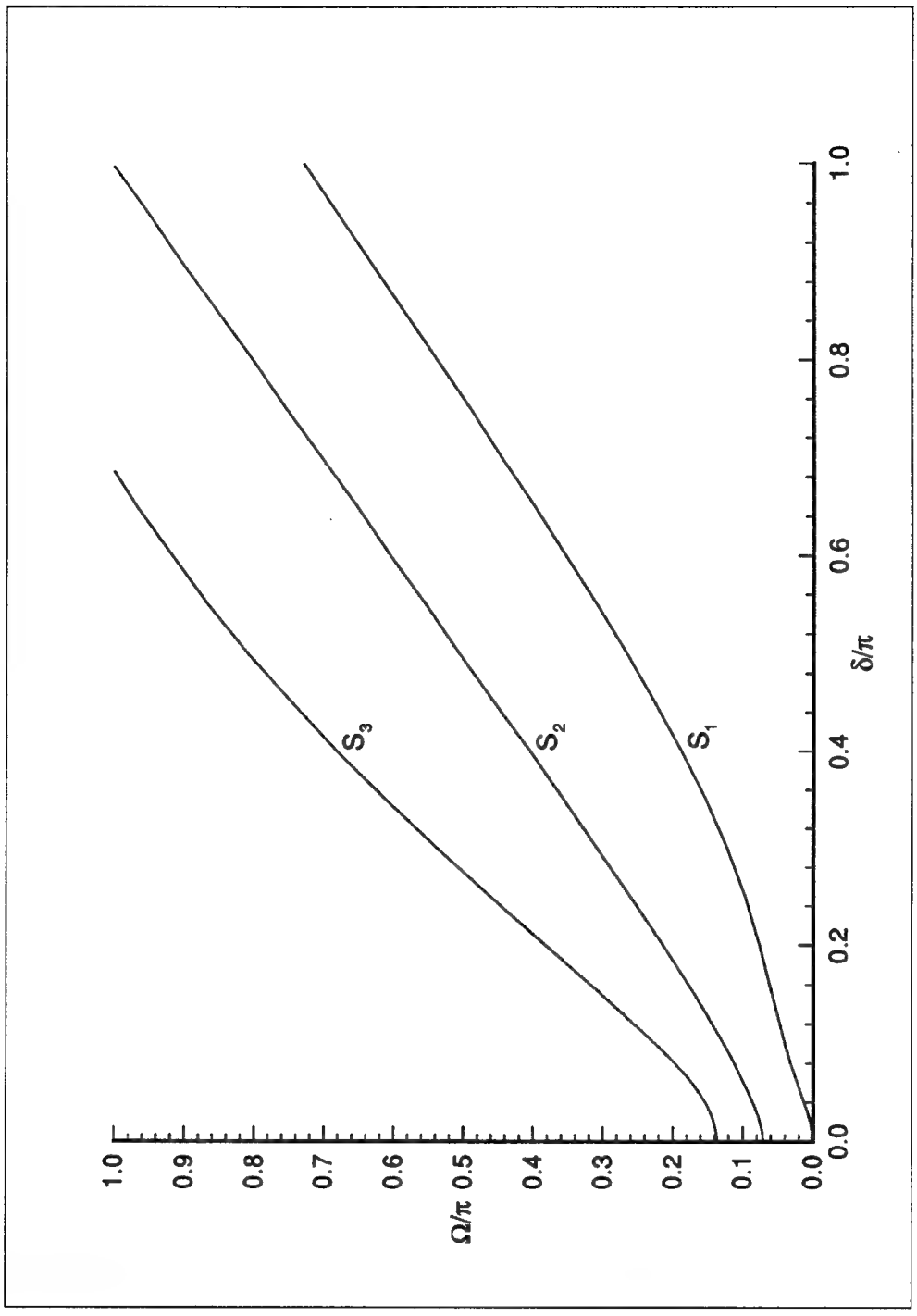

Figure 6. Frequency spectrum of the fluid-filled rubber cylinder

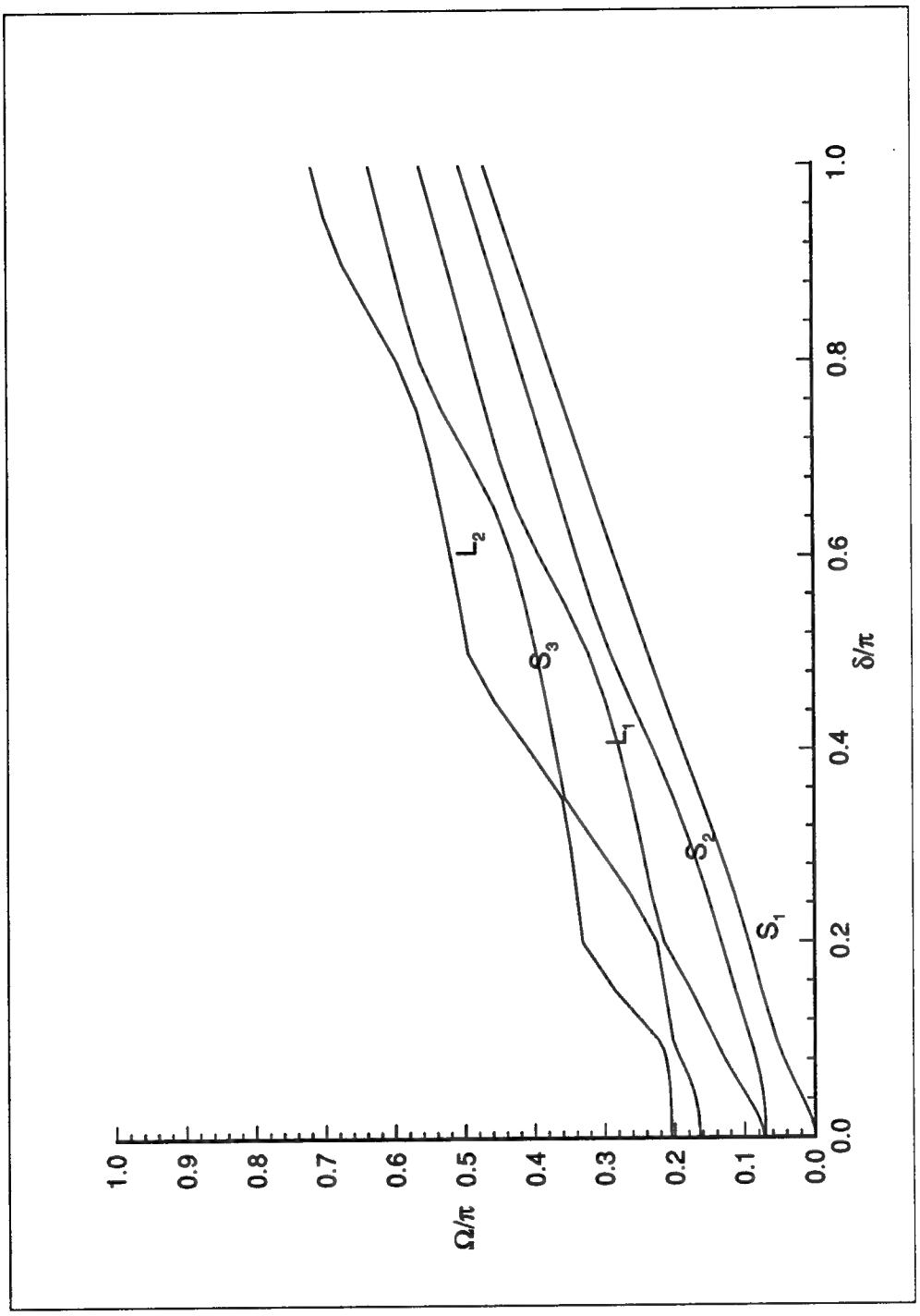

Figure 7. Frequency spectrum of the fluid-filled steel cylinder

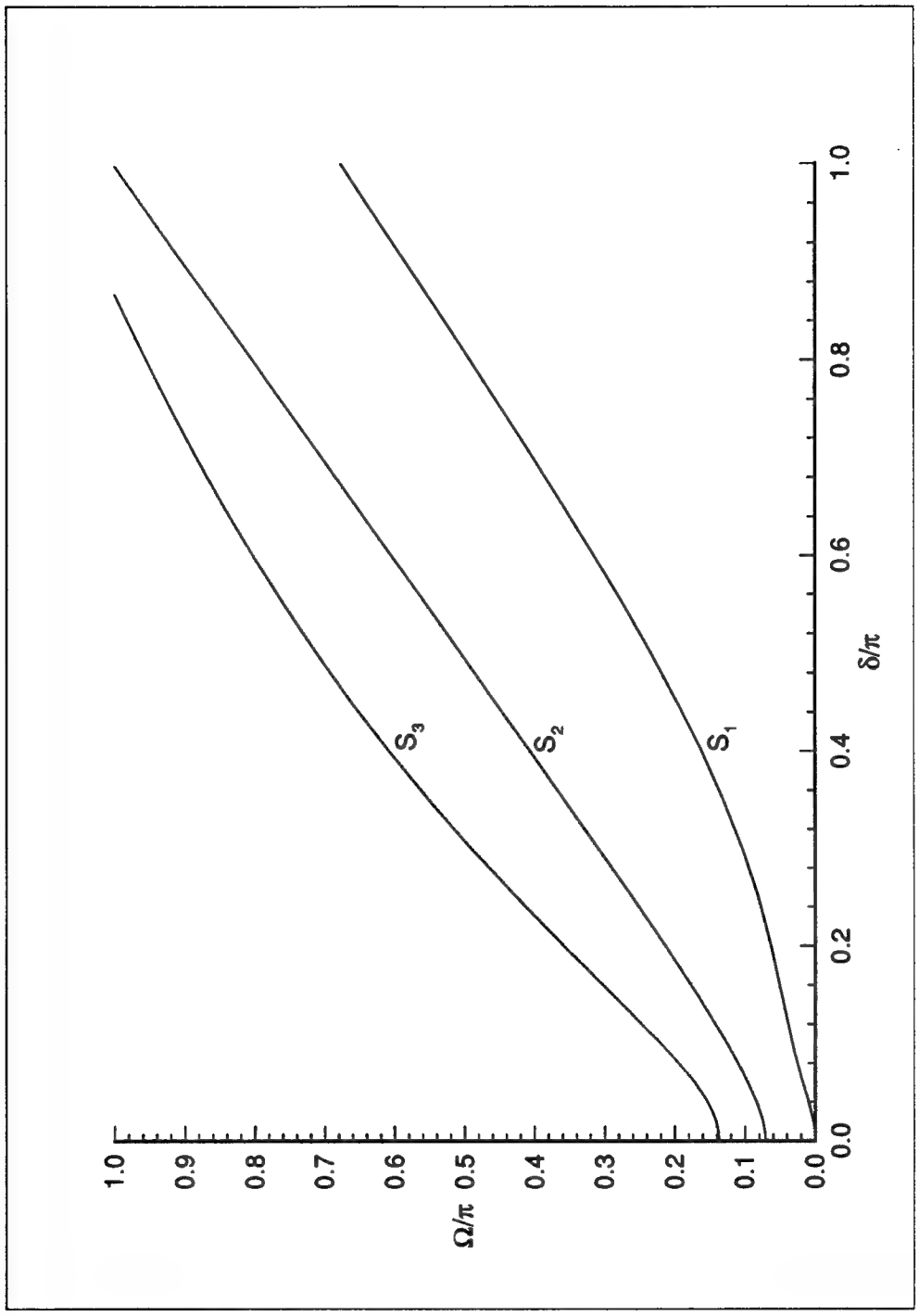

Figure 8. Frequency spectrum of the rubber cylinder that is fluid-filled and immersed in fluid

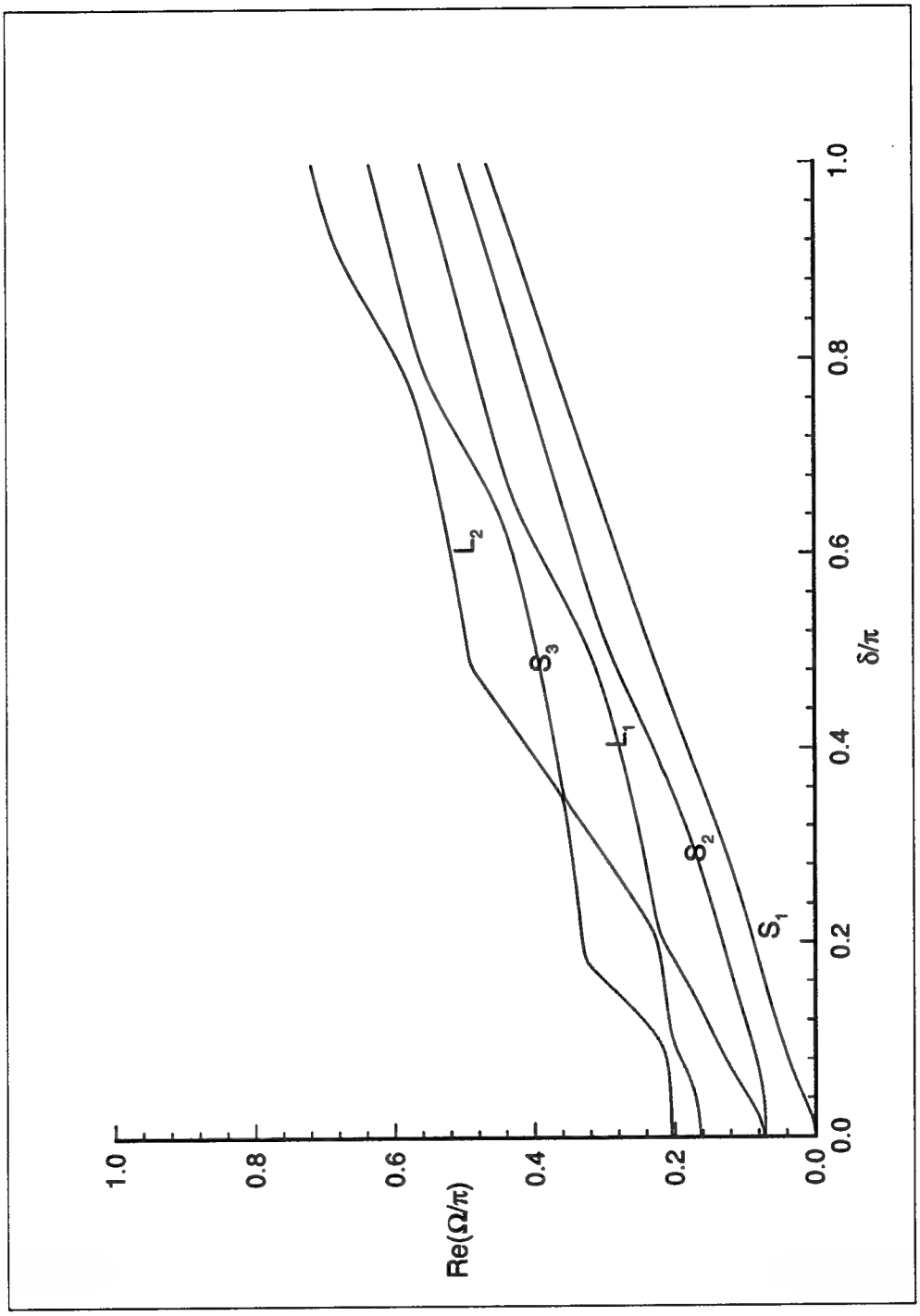

Figure 9. Real part of the frequency spectrum of the steel cylinder that is fluid-filled and immersed in fluid

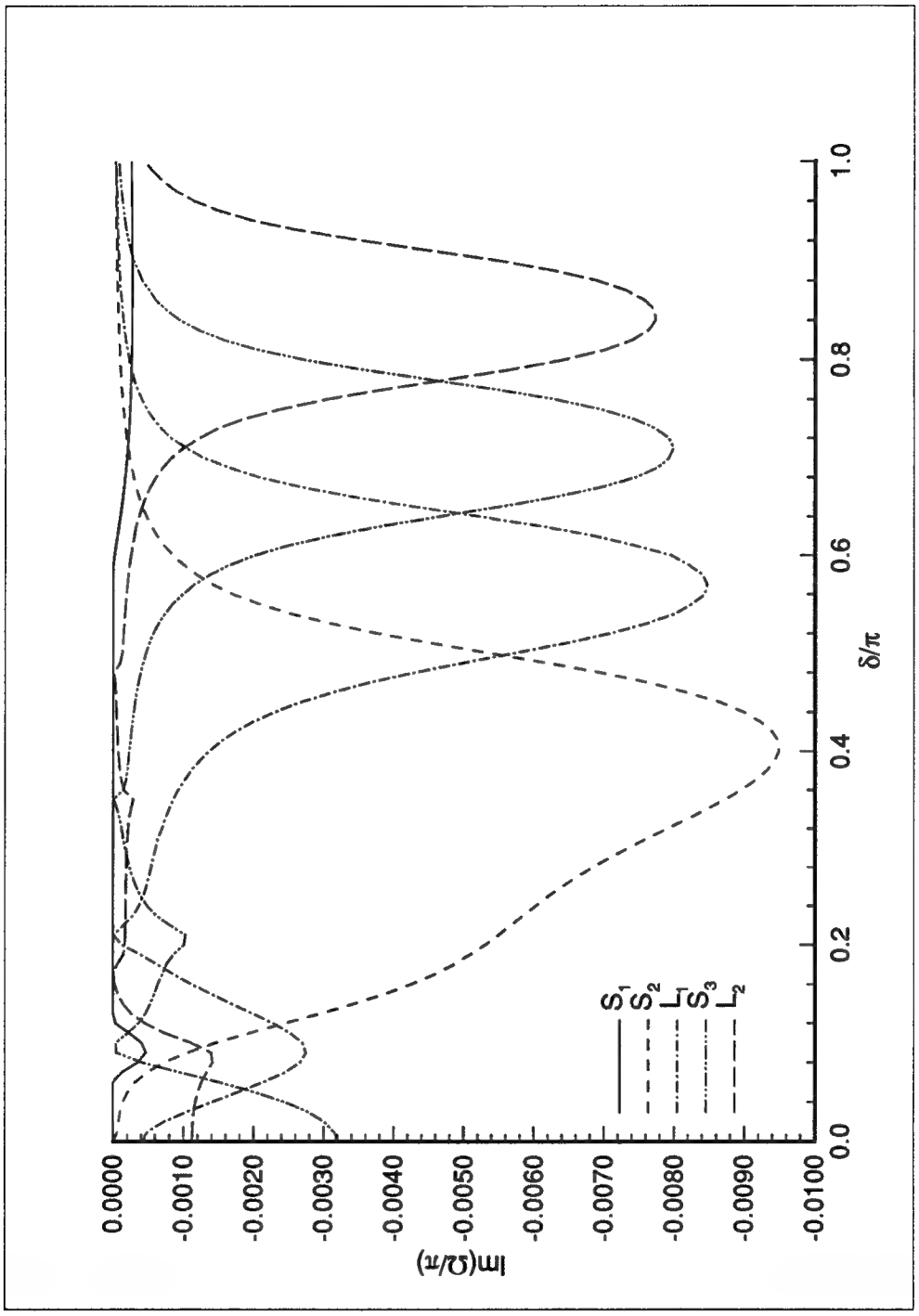

Figure 10. Imaginary part of the frequency spectrum of the steel cylinder that is fluid-filled and immersed in fluid

4. COMPUTATIONAL RESULTS FOR A HOMOGENEOUS, TRANSVERSELY ISOTROPIC CYLINDER

In this chapter, the n=1 modes of nonaxisymmetric wave propagation in a fluid-loaded, homogeneous, transversely isotropic cylinder are investigated. The cut-off frequencies are computed for a ratio of cylinder inner to outer radius s ranging from 0 to 0.9. The frequency spectrum is computed for a cylinder with a ratio of inner to outer radius of 0.8 and consisting of a fiber-reinforced matrix material in which the fibers are aligned parallel to the longitudinal axis of the cylinder.

The matrix material is a soft rubber with the same material properties as in the case of the rubber isotropic cylinder. The fibers are nylon cords and the fiber volume fraction is 10%. The material properties of the rubber matrix material and nylon cords are provided in appendix C.

Numerical results for the same sequence of cases of boundary conditions are obtained in this chapter as were obtained in chapter 3. These cases are a hollow cylinder in a vacuum, a hypothetical fluid column with pressure-release and with displacement-free boundary conditions, a fluid-filled cylinder, and a cylinder that is fluid-filled and immersed in fluid.

The numerical results are presented in and discussed as functions of normalized frequency Ω, normalized wavenumber δ, normalized phase velocity Ω/δ, and the ratio of the cylinder's inner to outer radius s. These normalized variables were defined in chapter 3, but are redefined here for completeness as

a = inner radius,

b = outer radius,

$s = \frac{a}{b}$, ratio of inner and outer radius,

$h = b - a$, cylinder thickness,

$\Omega = \frac{\omega h}{c_T}$, normalized frequency,

$\delta = kh$, normalized wavenumber,

$\hat{c} = \frac{\Omega}{\delta} = \frac{c}{c_T}$, normalized phase velocity,

where we define the shear wave velocity in the transversely isotropic material as

$$c_T^2 = \frac{c_{44}}{\rho}. \tag{4.1}$$

4.1 EFFECTIVE ELASTIC CONSTANTS

For this investigation, we use the definitions derived by Jones (1975) for the effective engineering constants of the fiber-reinforced cylinder. These definitions are

$$
\begin{aligned}
G_T &= \frac{E_T}{2(1+\nu_T)} \\
G_L &= \frac{(G_m G_f)}{(V_m G_f + V_f G_m)} \\
E_L &= V_f E_f + V_m E_m \\
E_T &= \frac{(E_m E_f)}{(V_m E_f + V_f E_m)} \\
\nu_L &= V_f \nu_f + V_m \nu_m \\
\rho &= \rho_f V_f + \rho_m V_m ,
\end{aligned}
\tag{4.2}
$$

where E_m, G_m, ν_m, ρ_m, and V_m are the Young's modulus, shear modulus, Poisson's ratio, density and volume fraction of the matrix material, and where E_f, G_f, ν_f, ρ_f, and V_f are the Young's modulus, shear modulus, Poisson's ratio, density and volume fraction of the fiber, respectively, and where

B_T = the transverse bulk modulus,

G_L = the longitudinal shear modulus,

G_T = the transverse shear modulus,

E_L = the longitudinal Young's modulus,

E_T = the transverse Young's modulus,

ν_L = the longitudinal Poisson's ratio,

ν_T = the transverse Poisson's ratio,

In these definitions, "transverse" refers to properties in the plane of isotropy, and "longitudinal" refers to properties along the material preferred direction.

The transverse bulk modulus is defined by Hashin (1979) as

$$2B_T = \frac{E_T}{1 - \nu_T - 2\nu_L^2 \frac{E_T}{E_L}}. \tag{4.3}$$

Substitution of the material properties of the matrix material (soft rubber) and the reinforcing fibers (nylon cord), along with a 10% fiber volume fraction of fiber, into equations 4.2 and 4.3, results in

$$\begin{aligned}
B_T &= 1.54 \times 10^7 \ \text{N/m}^2 \\
G_L &= 5.75 \times 10^6 \ \text{N/m}^2 \\
G_T &= 5.75 \times 10^6 \ \text{N/m}^2 \\
E_L &= 5.64 \times 10^8 \ \text{N/m}^2 \\
E_T &= 1.67 \times 10^7 \ \text{N/m}^2 \\
\nu_L &= 0.42 \\
\nu_T &= 0.45 \\
\rho &= 1014 \ \text{kg/m}^3.
\end{aligned}$$

Sutcu (1992) analyzed the constraints on the engineering constants for a transversely isotropic material and reported them as

$$G_L, G_T, E_L, E_T > 0,$$

$$-1 < \nu_T < 1, \tag{4.4}$$

$$\nu_L^2 \leq \frac{(1-\nu_T)}{2}\frac{E_L}{E_T}.$$

The effective engineering constants of the fiber-reinforced cylinder, computed from the definitions by Jones (1975), fall within the allowable bounds of equations 4.4.

Substitution of the effective engineering constants into the definitions of the elastic constants, equations 2.11, results in

$$\begin{aligned} c_{11} &= 2.12 \times 10^7 \\ c_{12} &= 9.69 \times 10^6 \\ c_{13} &= 1.3 \times 10^7 \\ c_{33} &= 5.74 \times 10^8 \\ c_{44} &= 5.74 \times 10^6 \\ c_{44} &= 5.74 \times 10^6. \end{aligned}$$

When these elastic constants are normalized to c_{44}, we have

$$c_{11} \cong 3.7 \times c_{44}$$
$$c_{12} \cong 1.7 \times c_{44}$$
$$c_{13} \cong 2.3 \times c_{44}$$
$$c_{33} \cong 100 \times c_{44}$$
$$c_{66} \cong c_{44} .$$

It is important to take note at this time of how highly anisotropic the fiber-reinforced composite material is compared to naturally occurring hexagonal crystal materials. For instance, for the fiber-reinforced material, $c_{33} > 27 \times c_{11}$, while, from Payton (1983), we find that the elastic constants for beryllium are

$$c_{11} \cong 1.8 \times c_{44}$$
$$c_{12} \cong 0.16 \times c_{44}$$
$$c_{13} \cong 0.09 \times c_{44}$$
$$c_{33} \cong 2.1 \times c_{44}$$
$$c_{66} \cong 0.82 \times c_{44} ,$$

and, therefore, $c_{33} \cong 1.17 \times c_{11}$. Similarly, the elastic constants for ice are

$$c_{11} \cong 4.3 \times c_{44}$$
$$c_{12} \cong 2.1 \times c_{44}$$
$$c_{13} \cong 1.6 \times c_{44}$$
$$c_{33} \cong 4.6 \times c_{44}$$
$$c_{66} \cong 1.1 \times c_{44},$$

and, therefore, $c_{33} \cong 1.07 \times c_{11}$.

It is also interesting to compare the normalized elastic constants for the two isotropic materials used in chapter 3 to those for the fiber-reinforced material. Using equation 3.4 and $\nu = 0.45$ for the soft rubber cylinder we have

$$c_{11} = c_{33} = 11 \times c_{44}$$
$$c_{12} = c_{13} = 9 \times c_{44}$$
$$c_{66} = c_{44}.$$

Similarly, using equation 3.3 and $\nu = 0.3$ for the steel cylinder, we have

$$c_{11} = c_{33} = 3.5 \times c_{44}$$
$$c_{12} = c_{13} = 1.5 \times c_{44}$$
$$c_{66} = c_{44}.$$

The relationships of c_{11} and c_{12} to c_{44} in the fiber-reinforced material are very similar to those in steel. However, the relationships of c_{13} and c_{33} to c_{44} in the fiber-reinforced material are different from those in either steel or rubber. In particular, the relationship

of c_{33} to c_{44} is approximately an order of magnitude greater than in rubber. Therefore, we expect the numerical results for the transversely isotropic cylinder to be different from the results for either the rubber or the steel cylinder.

4.2 A HOLLOW CYLINDER IN A VACUUM

The frequency equation for this set of boundary equations was defined by equation 3.6. It is repeated here for completeness as

$$|L| = \begin{vmatrix} L_{11} & L_{12} & L_{13} & L_{14} & L_{15} & L_{16} \\ L_{21} & L_{22} & L_{23} & L_{24} & L_{25} & L_{26} \\ L_{31} & L_{32} & L_{33} & L_{34} & L_{35} & L_{36} \\ L_{51} & L_{52} & L_{53} & L_{54} & L_{55} & L_{56} \\ L_{61} & L_{62} & L_{63} & L_{64} & L_{65} & L_{66} \\ L_{71} & L_{72} & L_{73} & L_{74} & L_{75} & L_{76} \end{vmatrix} = 0. \qquad (4.5)$$

4.2.1 Cut-off frequencies

We first examine the solutions of equation 4.5 in the limiting case of zero wave-number. When the wavenumber is zero, equations 2.23, 2.26 and 2.38, simplify to

$$\zeta_1^2 \to \frac{\rho\omega^2}{c_{11}} = \left(\frac{c_{44}}{c_{11}}\right)\frac{\omega^2}{c_T^2}$$

$$\zeta_2^2 \to \frac{\rho\omega^2}{c_{44}} = \frac{\omega^2}{c_T^2}$$

$$q^2 \to \frac{\rho\omega^2}{c_{66}} = \left(\frac{c_{44}}{c_{66}}\right)\frac{\omega^2}{c_T^2} \qquad (4.6)$$

$$ik\eta_1 \to 0$$

$$ik\eta_2 \to \left(\frac{c_{11}-c_{44}}{c_{13}+c_{44}}\right)\frac{\rho\omega^2}{c_{44}} = \left(\frac{c_{11}-c_{44}}{c_{13}+c_{44}}\right)\frac{\omega^2}{c_T^2},$$

and $L_{21}, L_{22}, L_{25}, L_{26}, L_{61}, L_{62}, L_{65}$, and L_{66} are zero. Just as in the case of the isotropic cylinders, equation 4.6 separates into the product of two sub-determinants

$$Det_1 Det_2 = 0 \qquad (4.7)$$

where

$$Det_1 = \begin{vmatrix} L_{11} & L_{12} & L_{15} & L_{16} \\ L_{31} & L_{32} & L_{35} & L_{36} \\ L_{51} & L_{52} & L_{55} & L_{56} \\ L_{71} & L_{72} & L_{75} & L_{76} \end{vmatrix} \qquad (4.8)$$

and

$$\mathrm{Det}_2 = \begin{vmatrix} L_{23} & L_{24} \\ L_{63} & L_{64} \end{vmatrix}. \tag{4.9}$$

Equation 4.7 is satisfied when either Det_1 or Det_2 is equal to zero. As in the cases for isotropic cylinders, solutions of $\mathrm{Det}_1 = 0$ correspond to plane strain vibration, and solutions of $\mathrm{Det}_2 = 0$ correspond to axial shear vibration. When the variables in equations 4.6 are substituted into equation 4.9 using normalized elastic constants, we find that Det_2 is again only dependent on the shear wave velocity in the material.

When the relationships for isotropic materials, equations 3.2, are substituted into equations 4.6, and the results are substituted into equation 4.9, we find that equation 4.9 is equivalent to equation 3.10. Therefore, the normalized cut-off frequencies, corresponding to axial shear modes, for a transversely isotropic material are equal to the normalized cut-off frequencies for an isotropic material. This means that the normalized cut-off frequencies of the axial shear modes of vibration in the cylinder are dependent only on the shear wave velocity in the material, and are independent of any fluid-loading boundary conditions, at least when the cylinder is isotropic or transversely isotropic.

The normalized cut-off frequencies for the second, third, and fourth plane strain

modes of the fiber-reinforced cylinder were computed and are compared to the normalized cut-off frequencies of the soft rubber and steel cylinders in figure 11. (Note that figures 11-15 are located at the end of chapter 4, starting on page 94). The cut-off frequencies are normalized to the shear wave velocity in each material. Using the material properties for rubber, for steel, and for the fiber-reinforced material, along with equation 3.1, the shear wave velocities in the three materials are

$$c_T = 72 \text{ m/sec, for rubber}$$
$$c_T = 3218 \text{ m/sec, for steel}$$
$$c_T = 75 \text{ m/sec, for fiber-reinforced composite.}$$

In general, the normalized cut-off frequencies of the fiber-reinforced cylinder are very similar to the normalized cut-off frequencies of the steel cylinder. For the second and third plane strain modes, the normalized cut-off frequencies are essentially equal for cylinders with a ratio of inner to outer radius s greater than or equal to approximately 0.7. This means that, at zero wavenumber and for $s \geq 0.7$, the hollow fiber-reinforced cylinder has essentially the same resonant frequencies for these plane strain, rigid body modes (i.e. no longitudinal motion) as the steel cylinder.

4.2.2 Frequency spectrum

The frequency spectrum for the first two plane strain modes and the first axial shear mode of the fiber-reinforced cylinder with a ratio of the inner radius to the outer radius of 0.8, and for real wavenumbers from 0 to π, is shown in figure 12. (Note that the ap-

parent piecewise smooth behavior of the branches in figure 12 and subsequent figures is due to conducting the root searches of the frequency equation at discrete wavenumbers). Again we have labeled the branch corresponding to the first plane strain mode S_1, the branch corresponding to the first axial shear mode S_2, and the branch corresponding to the second plane strain mode S_3. The normalized cut-off frequency for the S_2 mode is

$$\Omega \cong 0.223$$

and the normalized cut-off frequency for the S_3 mode is

$$\Omega \cong 0.5331 .$$

The normalized cut-off frequency for the S_3 mode is about 1% greater than the normalized cut-off frequency for this mode in the steel cylinder.

At low wavenumbers, the normalized phase velocity of the S_1 mode is approximately one-half the shear wave velocity in the composite material. As wavenumber is increased, the phase velocity of this mode asymptotically approaches the shear wave velocity from below.

The group velocity of the S_3 mode is essentially zero below $\delta/\pi = 0.01$. Above this wavenumber, the phase velocity of this mode is approximately equal to the longitudinal wave velocity in the composite, where the longitudinal wave velocity is defined as

$$c_L = \sqrt{\frac{c_{33}}{\rho}}. \tag{4.10}$$

The characteristics of the S_2 mode are quite different from those of the isotropic materials studied in chapter 3. At low wavenumbers, this mode exhibits weak coupling to the S_3 mode and the normalized phase velocity is somewhat greater than the longitudinal wave velocity. As wavenumber is increased, the group velocity approaches zero. At wavenumbers above $\delta/\pi = 0.1$, the phase velocity of this mode asymptotically approaches the shear wave velocity from above.

Mirsky (1965) studied the axisymmetric and nonaxisymmetric modes of wave propagation in transversely isotropic cylinders and compared the results to a thick shell theory. In his analysis, the dynamic behavior of beryllium and magnesium was compared to that of steel. The results showed that, for thin cylinders, ($s = 0.9672$), the frequency spectra for the steel, beryllium and magnesium cylinders were very similar. However, for thick cylinders, ($s = 0.3333$), the frequency spectrum for the beryllium cylinder was somewhat different from that of the steel or magnesium cylinder. It should be noted that in the low frequency region of the frequency spectrum for the beryllium cylinder, where the frequency equation contained Bessel functions with complex arguments, Mirsky (1965) substituted numerical results from a thick shell theory for numerical results from the elasticity theory.

To the author's knowledge, a comparison of the dynamic behavior of a thick rubber cylinder, a thick steel cylinder, and a highly anisotropic, thick fiber-reinforced cylinder has not been made before within the framework of the theory of elasticity.

4.3 A HYPOTHETICAL FLUID COLUMN

Next, we consider the cut-off frequencies and dispersion curves of a hypothetical, cylindrical fluid column with pressure-release (stress-free) and with radial displacement-free boundary conditions.

4.3.1 Pressure-release boundary conditions

The frequency equation of a hypothetical fluid column, within the transversely isotropic cylinder, with a pressure-release boundary condition is identical to equation 3.13, that is

$$J_1(\alpha a) = 0, \tag{4.11}$$

or,

$$\alpha a = 3.832, 7.016, 10.172, \ldots. \tag{4.12}$$

4.3.2 Displacement-free boundary conditions

The frequency equation of a hypothetical fluid column, within the transversely iso-

tropic cylinder, with a displacement-free boundary condition is identical to equation 3.16, that is

$$J_1(\alpha a) - \alpha a J_2(\alpha a) = 0, \tag{4.13}$$

or,

$$\alpha a = 1.841, 5.331, 8.536, \ldots. \tag{4.14}$$

Equations 4.12 and 4.14 represent families of hyperbolas with finite cut-off frequencies. The first two cut-off frequencies, for each of the two boundary conditions and $s = 0.8$, normalized to the shear wave velocity in the composite material, are

$\Omega \cong 19.08, 34.94$, pressure-release boundary conditions
$\Omega \cong 9.17, 26.55$, displacement-free boundary conditions.

These normalized cut-off frequencies are very similar to those for a hypothetical fluid column in the rubber cylinder.

4.3.3 Frequency spectrum

The first two branches, corresponding to each of the two sets of boundary condi-

tions and normalized to the shear wave velocity in the composite material, are shown in figure 13. The curves labeled l_1 and l_2 represent solutions of equations 4.12, while the curves labeled L_1 and L_2 represent solutions of equations 4.14, respectively.

From a comparison of figures 12 and 13, we note that the fluid modes exist at wavenumbers and frequencies greater than the solid modes of the cylinder. This means that the fluid modes will not couple with the solid modes, at least in the wavenumber and frequency domains of interest. This is similar to the relationship of the fluid modes and solid modes of the rubber cylinder.

4.4 A FLUID-FILLED CYLINDER

The next case to be investigated is that of a fluid-filled cylinder. The frequency equation for this set of boundary conditions was given in equation 3.18. Again, in the limit of zero wavenumber, this frequency equation separates into two sub-determinants. The solution of setting one sub-determinant to zero corresponds to the axial shear modes, which as stated before, are found to be dependent only on the shear wave velocity in the material, and independent of any fluid-loading boundary conditions.

4.4.1 Cut-off frequencies

The normalized cut-off frequencies for the S_1, S_2, and S_3 modes for the fluid-filled fiber-reinforced cylinder are

$$\Omega \cong 0,\ 0.223, \text{ and } 0.398\ ,$$

respectively.

The presence of the internal fluid has reduced the cut-off frequency of the S_3 mode

by approximately 25%. No additional cut-off frequencies, corresponding to the addition of fluid modes, exist within the normalized frequency band of 0 to π. The degree of reduction of the cut-off frequency of the S_3 mode, and the absence of the addition of any fluid modes, are similar to the characteristics of the fluid-filled rubber cylinder.

4.4.2 Frequency spectrum

The frequency spectrum for the fluid-filled fiber-reinforced cylinder is shown in figure 14. From a comparison of figure 14 to figure 12, we note that the phase velocity of the S_1 mode of the fluid-filled cylinder is less than the phase velocity of this mode of the empty cylinder, for all wavenumbers. For example, at $\delta = 0.2\pi$ the phase velocity of the S_1 mode is reduced approximately 35% when fluid is added to the inside of the cylinder.

The phase velocity of the S_3 mode at wavenumbers greater than $\delta/\pi = 0.01$ is virtually unaffected by the presence of the fluid. The S_2 mode still exhibits weak coupling to the S_3 mode at low wavenumbers. The phase velocity of the S_2 mode in the fluid-filled cylinder is less than the phase velocity of this mode in the empty cylinder at wavenumbers between $0.02 < \delta/\pi < 0.5$. At wavenumbers greater than $\delta/\pi = 0.5$ the phase velocity of the S_2 mode is virtually unchanged and asymptotically approaches the shear wave velocity in the composite material from above.

4.5 A CYLINDER THAT IS FLUID-FILLED AND IMMERSED IN FLUID

The final case to be investigated is that of a cylinder that is fluid-filled and immersed in an infinite inviscid fluid. The frequency equation for this set of boundary conditions is equation 3.22. Again, in the limit of zero wavenumber, this frequency

equation separates into two sub-determinants corresponding to the axial shear modes and plane strain modes. The solution of the cut-off frequencies corresponding to the axial shear modes remain constant, when normalized to the shear wave velocity in the material, and independent of fluid-loading boundary conditions. The lowest, non-zero cut-off frequency, corresponding to a plane strain mode, is the cut-off frequency for the S_3 mode.

4.5.1 Cut-off frequencies

The normalized cut-off frequencies for the S_1, S_2, and S_3 modes for a fiber-reinforced cylinder that is fluid-filled and immersed in fluid are

$$\Omega \cong 0, 0.223, \text{ and } 0.394.$$

The cut-off frequency of the S_3 mode is essentially unaffected by the addition of the external fluid loading.

4.5.2 Frequency spectrum

The dispersion curves for the fiber-reinforced cylinder that is fluid-filled and immersed in fluid are shown in figure 15. From a comparison of figures 14 and 15, we note that the S_2 mode is essentially unaffected by the addition of the external fluid loading. The phase velocity of the S_1 mode is reduced over all wavenumbers. For example, at $\delta/\pi = 0.2$ the phase velocity has been reduced by approximately 18%.

At wavenumbers less than $\delta/\pi = 0.05$, the dispersion characteristics of the S_3 mode are unaffected by the addition of the external fluid. However, at higher wavenum-

bers the phase velocity is reduced significantly. For example, at $\delta/\pi = 0.1$ the phase velocity is reduced by 46% with the addition of the external fluid. These results are very different from the results for the rubber cylinder and steel cylinder.

The effect of the external fluid on the dynamic behavior of the fluid-filled, fiber-reinforced cylinder is very different than on the dynamic behavior of the fluid-filled rubber and steel cylinder. For instance, all of the cut-off frequencies and branches of the frequency spectrum for the fiber-reinforced cylinder are real. That is, unlike the results for the fluid-filled steel cylinder, the addition of the external fluid has not introduced any damping in the coupled system. Also, unlike the results for the fluid-filled rubber cylinder, the addition of an external fluid resulted in significant reductions in the phase velocities for the S_1 and S_3 modes.

As a final comment, and to the author's knowledge, the results shown in figures 14 and 15 represent the first time the cut-off frequencies and frequency spectra of the n=1, nonaxisymmetric modes of wave propagation in a fluid-filled cylinder and for a fluid-filled cylinder immersed in fluid, have been computed for a homogeneous, transversely isotropic cylinder.

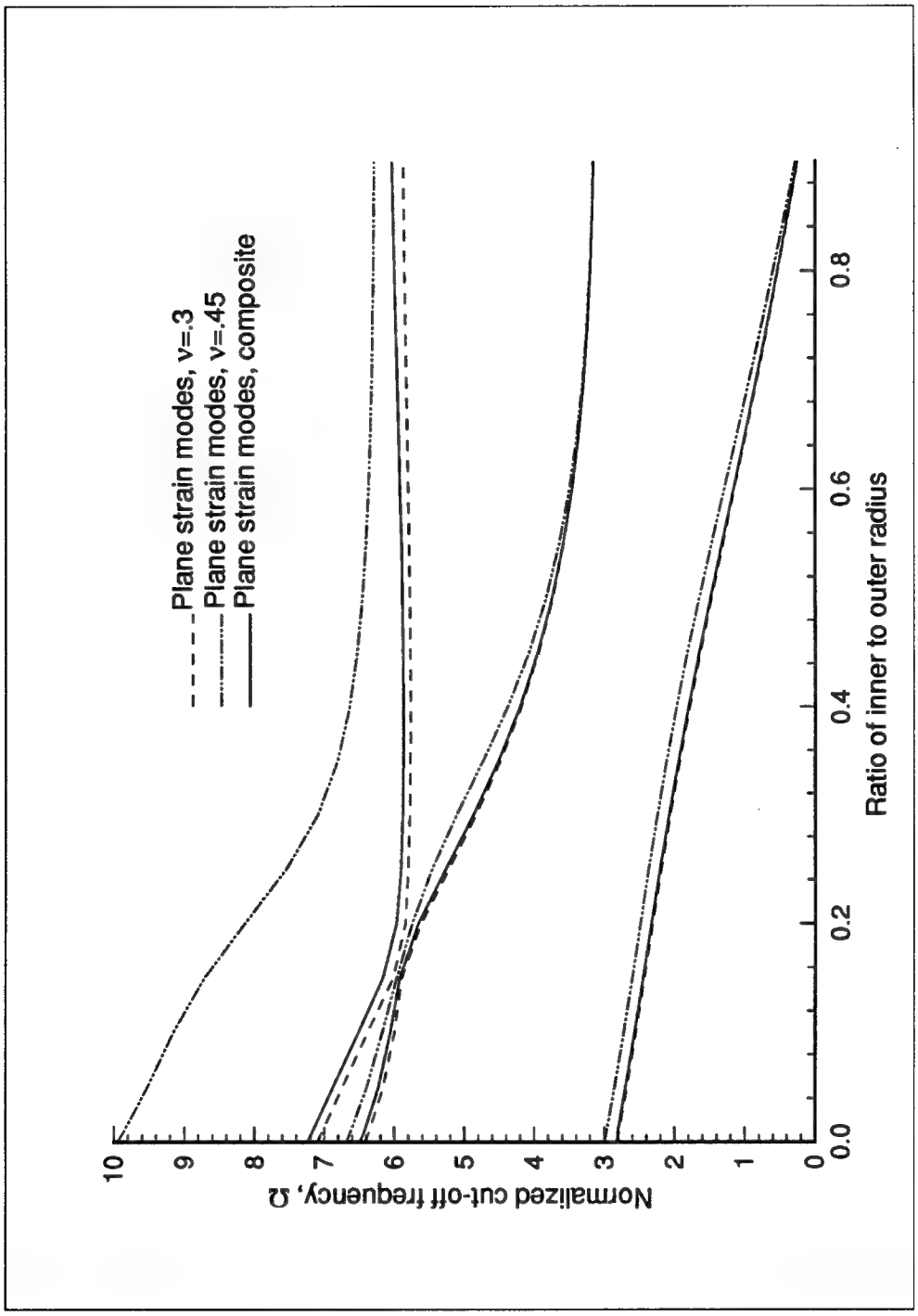

Figure 11. Comparison of the cut-off frequencies of the plane strain modes in a rubber, steel, and transversely isotropic cylinder as functions of the ratio of inner to outer radius

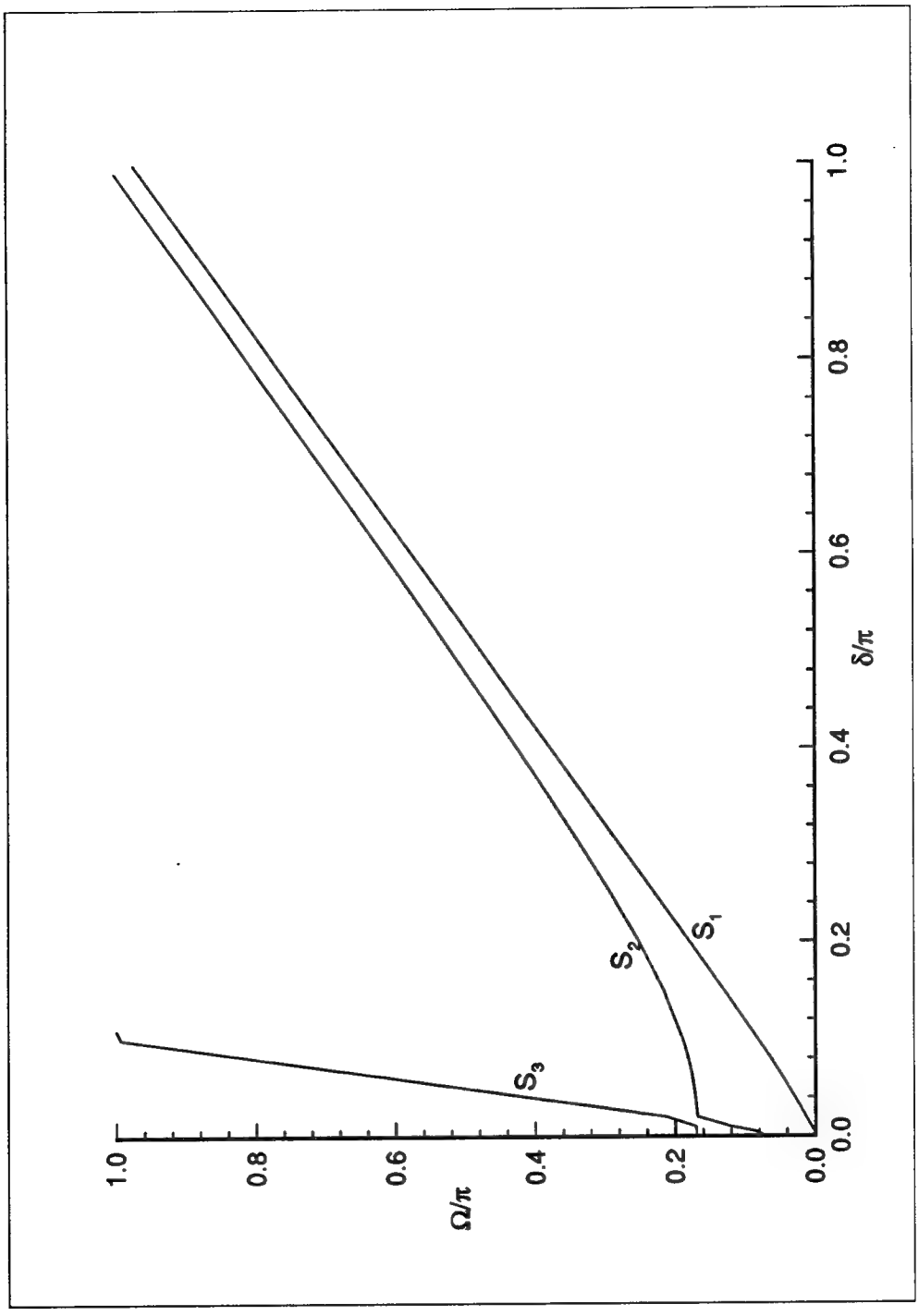

Figure 12. Frequency spectrum of the transversely cylinder in a vacuum

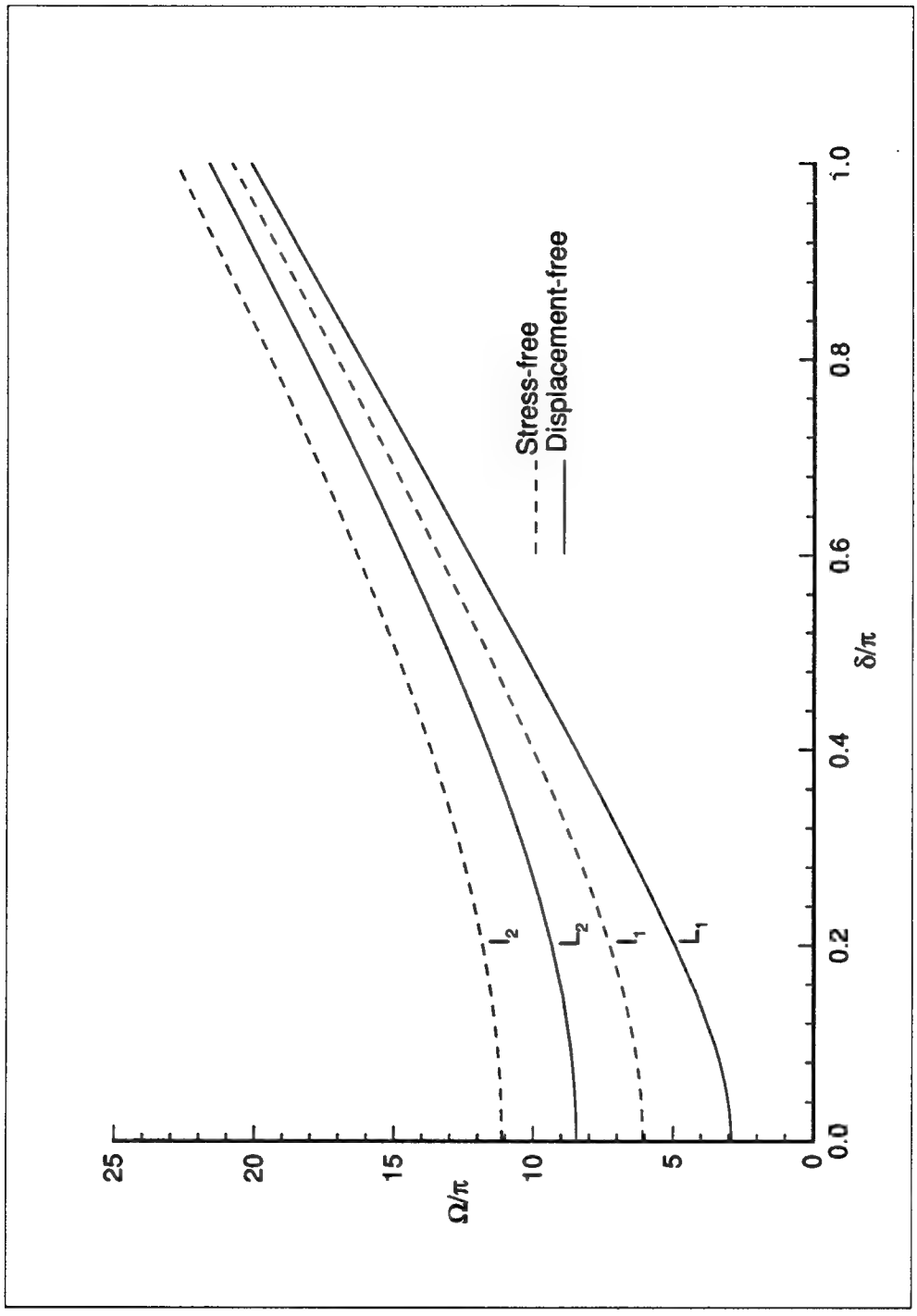

Figure 13. Frequency spectrum of the hypothetical fluid column normalized to the shear wave velocity in the composite material

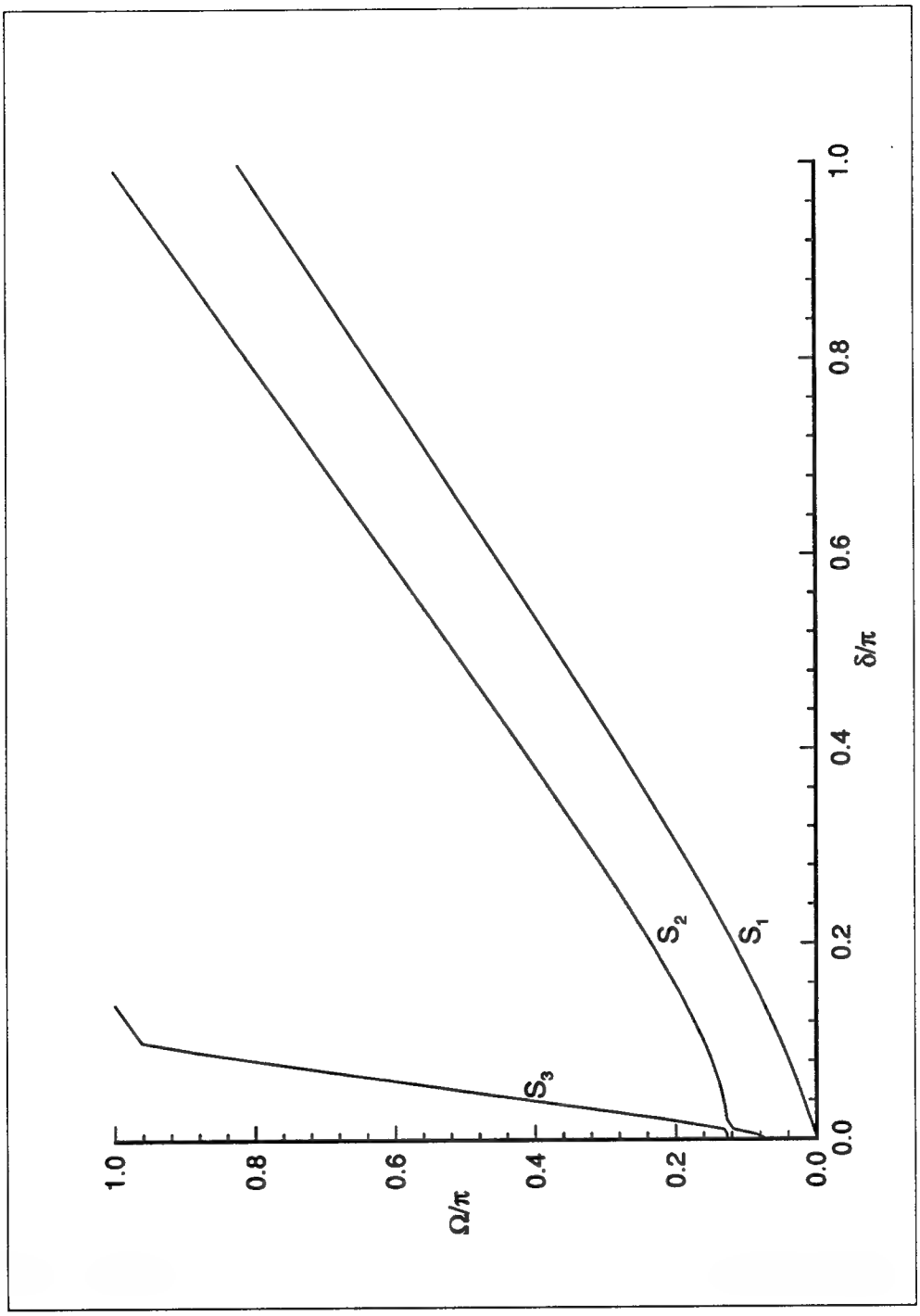

Figure 14. Frequency spectrum of the fluid-filled transversely isotropic cylinder

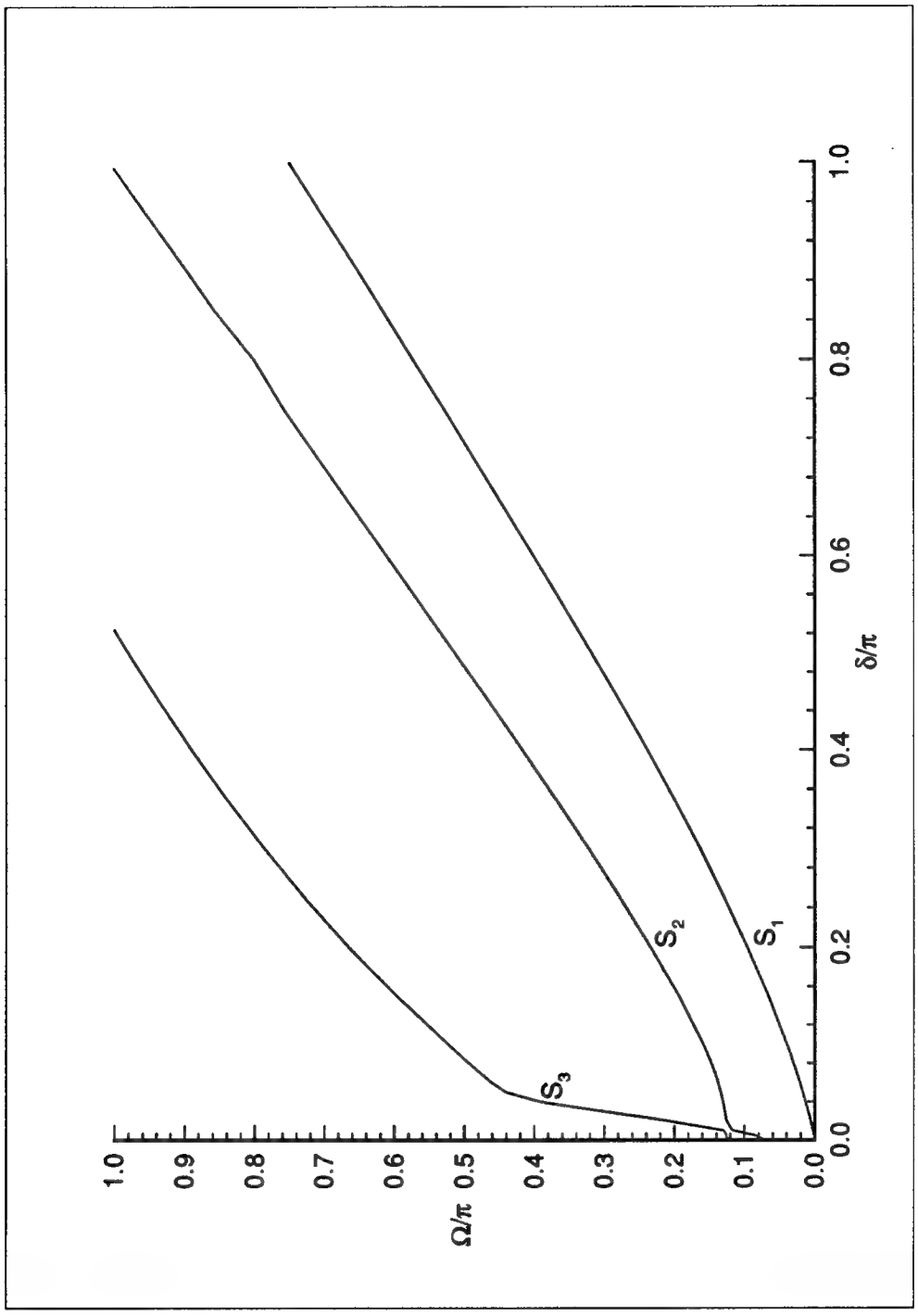

Figure 15. Frequency spectrum of the transversely isotropic cylinder that is fluid-filled and immersed in fluid

5. SUMMARY AND CONCLUSIONS

The frequency equation of wave propagation in a transversely isotropic cylinder, that is fluid-filled and immersed in fluid, was developed from the three-dimensional equations of elasticity and the assumptions of perfect-slip boundary conditions at the fluid-solid interfaces. This equation is general in axial wavenumber k, circumferential wavenumber n, wall thickness h, and radian frequency ω.

The frequency equation was verified by specializing the variables for the cases of isotropic cylinders and n = 1 nonaxisymmetric modes and comparing the normalized cut-off frequencies and frequency spectra to previous results for hollow cylinders in a vacuum and for fluid-filled cylinders.

The frequency spectrum for the n = 1 modes in fluid-filled, isotropic cylinders immersed in fluid were computed and compared to previous results for similar geometries and for the n = 0 modes. It was found that the effects of the presence of the inner and outer fluids on the steel cylinder, for the n = 1 modes, were similar to the effects for the n = 0 modes. That is, the inner fluid introduced additional modes in the fluid-filled cylinder that were not present in the cylinder in a vacuum. The outer fluid introduced damping into the system as evidenced by the presence of the imaginary term in the complex frequency.

The effects of the inner and outer fluids on the soft rubber cylinder, for the n = 1 modes, were quite different from the effects on the steel cylinder. For instance, the inner fluid reduced the normalized cut-off frequencies and phase velocities of the plane strain

modes in the soft rubber cylinder significantly more than in the steel cylinder. However, the inner fluid did not introduce any additional modes within the wavenumber and frequency domains of interest. The external fluid did not have any significant additional effect on normalized cut-off frequencies or phase velocities, and, unlike the case for the steel cylinder, did not introduce any damping into the system.

To the author's knowledge, the cut-off frequencies and frequency spectra for the $n = 1$ modes in isotropic cylinders, with fluid loading on the inner and on outer surfaces, have not been computed before within the framework of the theory of elasticity

Next, the frequency equation was specialized for the cases of a fiber-reinforced, transversely isotropic cylinder. When the relationships among the elastic constants of the fiber-reinforced cylinder were compared to those of some naturally occurring hexagonal crystals, the fiber-reinforced cylinder was found to be highly anisotropic.

New results for nonaxisymmetric ($n = 1$) wave propagation in a transversely isotropic cylinder were obtained for the cases of a fluid-filled cylinder and a cylinder that is fluid-filled and immersed in fluid. The normalized cut-off frequencies and frequency spectra for these geometries were computed and compared to those for the soft rubber cylinder and the steel cylinder. It was found that the effects of the inner fluid on the wave propagation characteristics of the fiber-reinforced cylinder were similar to the effects on the fluid-filled rubber cylinder, as evidenced by the reductions in the normalized cut-off frequencies and in the phase velocities of the plane strain modes. However, the effects of the outer fluid on the two types of cylinders were different. Contrary to the case of the soft rubber cylinder, the presence of the outer fluid on the fluid-filled,

fiber-reinforced cylinder further reduced the phase velocities of the plane strain modes by a significant amount.

It was noted that normalized cut-off frequencies corresponding to axial shear modes are dependent only on the shear wave velocity in the material and are independent of any internal or external fluid loading condition. This means, at zero wavenumber (corresponding to rigid body motion), the normalized resonant frequency for harmonic longitudinal vibration is the same for isotropic and transversely isotropic cylinders, regardless of whether they are fluid filled or immersed in fluid or both.

In conclusion, the characteristics of wave propagation in highly anisotropic cylinders, with or without fluid loading, may be markedly different from the characteristics of wave propagation in isotropic cylinders. Predictions of the normalized cut-off frequencies and, in particular, phase velocities of various modes in a transversely isotropic cylinder, based on results for isotropic cylinders, can be seriously inaccurate.

6. RECOMMENDATIONS FOR CONTINUED INVESTIGATIONS

1. The flexural mode is often the mode of greatest interest in nonaxisymmetric wave propagation. A simplified, low wavenumber model for this mode should be developed using small argument approximations for the Bessel functions in the frequency equation. This would provide a method to quickly analyze the effects of changes in material properties of the transversely isotropic material on the phase velocity of this mode.

2. The numerical computations performed in this dissertation were for a relatively thick cylinder. A similar study of the nonaxisymmetric wave propagation characteristics in fluid loaded, thin, transversely cylinders should also be conducted and compared to thin shell theory.

3. Displacement and stress distributions in the fluids and the cylinder wall should be computed over a range of wavenumbers and frequencies in order to analyze the degree of coupling of the radial, circumferential and longitudinal motions in the cylinder and the pressure distributions in the inner and outer fluids.

4. The matrix material of the fiber-reinforced cylinder was assumed to be linearly elastic. Fiber-reinforced materials are often composed of a linearly viscoelastic matrix material. The frequency equation for the fluid-loaded cylinder should be expanded to include the effects of linear viscoelasticity.

APPENDIX A. BOUNDARY EQUATIONS

The boundary equations, which were formulated in chapter 2, are

$$[L]\{c\} = 0. \tag{A.1}$$

Equations A.1 constitute a system of eight, linear, homogeneous algebraic equations in the wave amplitudes $\{c\}$, where

$$\{c\} = (A_1, B_1, A_2, B_2, A_3, B_3, D_1, D_2), \tag{A.2}$$

and where the components of $[L]$ are given below. The γ_i's are +1 or -1, depending upon the type of Bessel function that W_n represents. This bookkeeping variable is needed due to the differing recursion formulas for the derivatives of the Bessel functions. For instance, $\gamma_i = -1$, when W_n represents J_n, K_n, or H_n^1, and $\gamma_i = 1$ when W_n represents I_n.

$$L_{11} = \left[2c_{66}n(n-1) + \left(c_{44}k^2 - \rho\omega^2 - ic_{44}\eta_1 k\right)a^2\right]W_n(\xi_1 a) - \gamma_1 2c_{66}\xi_1 a W_{n+1}(\xi_1 a) \tag{A.3}$$

$$L_{12} = \left[2c_{66}n(n-1) + \left(c_{44}k^2 - \rho\omega^2 - ic_{44}\eta_1 k\right)a^2\right]Z_n(\xi_1 a) + 2c_{66}\xi_1 a Z_{n+1}(\xi_1 a) \tag{A.4}$$

$$L_{13} = \left[2c_{66}n(n-1) + \left(c_{44}k^2 - \rho\omega^2 - ic_{44}\eta_2 k\right)a^2\right]W_n(\xi_2 a) - \gamma_2 2c_{66}\xi_2 a W_{n+1}(\xi_2 a) \tag{A.5}$$

$$L_{14} = \left[2c_{66}n(n-1) + \left(c_{44}k^2 - \rho\omega^2 - ic_{44}\eta_2 k\right)a^2\right]Z_n(\xi_2 a) + 2c_{66}\xi_2 a Z_{n+1}(\xi_2 a) \tag{A.6}$$

$$L_{15} = 2c_{66}n\left[(n-1)W_n(\xi_3 a) + \gamma_3\xi_3 a W_{n+1}(\xi_3 a)\right] \quad (A.7)$$

$$L_{16} = 2c_{66}n\left[(n-1)Z_n(\xi_3 a) - \xi_3 a Z_{n+1}(\xi_3 a)\right] \quad (A.8)$$

$$L_{17} = \rho_1\omega^2 a^2 F_n(\xi_4 a) \quad (A.9)$$

$$L_{18} = 0 \quad (A.10)$$

$$L_{21} = (\eta_1 + ik)a\left[nW_n(\xi_1 a) + \gamma_1\xi_1 a W_{n+1}(\xi_1 a)\right] \quad (A.11)$$

$$L_{22} = (\eta_1 + ik)a\left[nZ_n(\xi_1 a) - \xi_1 a Z_{n+1}(\xi_1 a)\right] \quad (A.12)$$

$$L_{23} = (\eta_2 + ik)a\left[nW_n(\xi_2 a) + \gamma_2\xi_2 a W_{n+1}(\xi_2 a)\right] \quad (A.13)$$

$$L_{24} = (\eta_2 + ik)a\left[nZ_n(\xi_2 a) - \xi_2 a Z_{n+1}(\xi_2 a)\right] \quad (A.14)$$

$$L_{25} = inkaW_n(\xi_3 a) \quad (A.15)$$

$$L_{26} = inkaZ_n(\xi_3 a) \quad (A.16)$$

$$L_{27} = 0 \quad (A.17)$$

$$L_{28} = 0 \quad (A.18)$$

$$L_{31} = -2n\left[(n-1)W_n(\xi_1 a) + \gamma_1\xi_1 a W_{n+1}(\xi_1 a)\right] \quad (A.19)$$

$$L_{32} = -2n\left[(n-1)Z_n(\xi_1 a) - \xi_1 a Z_{n+1}(\xi_1 a)\right] \quad (A.20)$$

$$L_{33} = -2n\left[(n-1)W_n(\xi_2 a) + \gamma_2\xi_2 a W_{n+1}(\xi_2 a)\right] \quad (A.21)$$

$$L_{34} = -2n\left[(n-1)Z_n(\xi_2 a) - \xi_2 a Z_{n+1}(\xi_2 a)\right] \quad (A.22)$$

$$L_{35} = \left(q^2a^2 - 2n(n-1)\right)W_n(\xi_3 a) + 2\gamma_3\xi_3 a W_{n+1}(\xi_3 a) \quad (A.23)$$

$$L_{36} = \left(q^2a^2 - 2n(n-1)\right)Z_n(\xi_3 a) - 2\xi_3 a Z_{n+1}(\xi_3 a) \quad (A.24)$$

$$L_{37} = 0 \quad (A.25)$$

$$L_{38} = 0 \quad (A.26)$$

$$L_{41} = nW_n(\xi_1 a) + \gamma_1\xi_1 a W_{n+1}(\xi_1 a) \quad (A.27)$$

$$L_{42} = nZ_n(\xi_1 a) - \xi_1 a Z_{n+1}(\xi_1 a) \quad (A.28)$$

$$L_{43} = nW_n(\xi_2 a) + \gamma_2 \xi_2 a W_{n+1}(\xi_2 a) \tag{A.29}$$

$$L_{44} = nZ_n(\xi_2 a) - \xi_2 a Z_{n+1}(\xi_2 a) \tag{A.30}$$

$$L_{45} = nW_n(\xi_3 a) \tag{A.31}$$

$$L_{46} = nZ_n(\xi_3 a) \tag{A.32}$$

$$L_{47} = -(nW_n(\xi_4 a) + \gamma_4 \xi_4 a W_{n+1}(\xi_4 a)) \tag{A.33}$$

$$L_{48} = 0 \tag{A.34}$$

$$L_{51} = \left[2c_{66}n(n-1) + \left(c_{44}k^2 - \rho\omega^2 - ic_{44}\eta_1 k\right)b^2\right]W_n(\xi_1 b) - \gamma_1 2c_{66}\xi_1 b W_{n+1}(\xi_1 b) \tag{A.35}$$

$$L_{52} = \left[2c_{66}n(n-1) + \left(c_{44}k^2 - \rho\omega^2 - ic_{44}\eta_1 k\right)b^2\right]Z_n(\xi_1 b) + 2c_{66}\xi_1 b Z_{n+1}(\xi_1 b) \tag{A.36}$$

$$L_{53} = \left[2c_{66}n(n-1) + \left(c_{44}k^2 - \rho\omega^2 - ic_{44}\eta_2 k\right)b^2\right]W_n(\xi_2 b) - \gamma_2 2c_{66}\xi_2 b W_{n+1}(\xi_2 b) \tag{A.37}$$

$$L_{54} = \left[2c_{66}n(n-1) + \left(c_{44}k^2 - \rho\omega^2 - ic_{44}\eta_2 k\right)b^2\right]Z_n(\xi_2 b) + 2c_{66}\xi_2 b Z_{n+1}(\xi_2 b) \tag{A.38}$$

$$L_{55} = 2c_{66}n[(n-1)W_n(\xi_3 b) + \gamma_3 \xi_3 b W_{n+1}(\xi_3 b)] \tag{A.39}$$

$$L_{56} = 2c_{66}n[(n-1)Z_n(\xi_3 b) - \xi_3 b Z_{n+1}(\xi_3 b)] \tag{A.40}$$

$$L_{57} = 0 \tag{A.41}$$

$$L_{58} = \rho_2 \omega^2 b^2 G_n(\xi_5 b) \tag{A.42}$$

$$L_{61} = (\eta_1 + ik)b[nW_n(\xi_1 b) + \gamma_1 \xi_1 b W_{n+1}(\xi_1 b)] \tag{A.43}$$

$$L_{62} = (\eta_1 + ik)b[nZ_n(\xi_1 b) - \xi_1 b Z_{n+1}(\xi_1 b)] \tag{A.44}$$

$$L_{63} = (\eta_2 + ik)b[nW_n(\xi_2 b) + \gamma_2 \xi_2 b W_{n+1}(\xi_2 b)] \tag{A.45}$$

$$L_{64} = (\eta_2 + ik)\, b\, [nZ_n(\xi_2 b) - \xi_2 b Z_{n+1}(\xi_2 b)\ ] \tag{A.46}$$

$$L_{65} = inkbW_n(\xi_3 b) \tag{A.47}$$

$$L_{66} = inkbZ_n(\xi_3 b) \tag{A.48}$$

$$L_{67} = 0 \tag{A.49}$$

$$L_{68} = 0 \tag{A.50}$$

$$L_{71} = -2n\,[\,(n-1)\,W_n(\xi_1 b) + \gamma_1 \xi_1 b W_{n+1}(\xi_1 b)\,] \tag{A.51}$$

$$L_{72} = -2n\,[\,(n-1)\,Z_n(\xi_1 b) - \xi_1 b Z_{n+1}(\xi_1 b)\,] \tag{A.52}$$

$$L_{73} = -2n\,[\,(n-1)\,W_n(\xi_2 b) + \gamma_2 \xi_2 b W_{n+1}(\xi_2 b)\,] \tag{A.53}$$

$$L_{74} = -2n\,[\,(n-1)\,Z_n(\xi_2 b) - \xi_2 b Z_{n+1}(\xi_2 b)\,] \tag{A.54}$$

$$L_{75} = \left(q^2 b^2 - 2n(n-1)\right) W_n(\xi_3 b) + 2\gamma_3 \xi_3 b W_{n+1}(\xi_3 b) \tag{A.55}$$

$$L_{76} = \left(q^2 b^2 - 2n(n-1)\right) Z_n(\xi_3 b) - 2\xi_3 b Z_{n+1}(\xi_3 b) \tag{A.56}$$

$$L_{77} = 0 \tag{A.57}$$

$$L_{78} = 0 \tag{A.58}$$

$$L_{81} = nW_n(\xi_1 b) + \gamma_1 \xi_1 b W_{n+1}(\xi_1 b) \tag{A.59}$$

$$L_{82} = nZ_n(\xi_1 b) - \xi_1 b Z_{n+1}(\xi_1 b) \tag{A.60}$$

$$L_{83} = nW_n(\xi_2 b) + \gamma_2 \xi_2 b W_{n+1}(\xi_2 b) \tag{A.61}$$

$$L_{84} = nZ_n(\xi_2 b) - \xi_2 b Z_{n+1}(\xi_2 b) \tag{A.62}$$

$$L_{85} = nW_n(\xi_3 b) \tag{A.63}$$

$$L_{86} = nW_n(\xi_3 b) \tag{A.64}$$

$$L_{87} = 0 \tag{A.65}$$

$$L_{88} = -\left(nW_n(\xi_5 b) + \gamma_5 \xi_5 b W_{n+1}(\xi_5 b)\right) \tag{A.66}$$

The solutions of A.1 are nontrivial when the determinant of the coefficients of the wave amplitudes $\{c\}$ vanishes, i.e., when

$$|L| = 0. \tag{A.67}$$

Equation A.67 is a complex algebraic equation. The real and imaginary parts must vanish simultaneously. To aid in the computation of the solutions of equation A.67, all the physical variables are normalized as follows,

$$\begin{aligned} a &= h\frac{s}{(1-s)} \\ b &= h\frac{1}{(1-s)}\text{, where} \\ h &= (b-a)\text{, and} \\ s &= \frac{a}{b}, \end{aligned} \tag{A.68}$$

and

$$\begin{aligned} &\Omega \equiv \frac{\omega h}{c_T}\text{, normalized frequency,} \\ &\delta \equiv kh\text{, normalized wavenumber,} \\ &\hat{c} \equiv \frac{\Omega}{\delta}\text{, normalized phase speed.} \end{aligned} \tag{A.69}$$

The branches of the frequency spectrum are calculated by selecting a real value of the normalized wavenumber and searching for the real or complex value of the normalized frequency. A Mathematica (Wolfram, 1991) program was developed to conduct the root searches using Mueller's method (Press *et al*, 1986). Mueller's method is an algorithm that finds a real or complex zero of a complex function, which in this case is equation A.67. An example Mathematica program is provided in appendix B.

APPENDIX B. MATHEMATICA PROGRAM TO CONDUCT ROOT SEARCHES OF THE FREQUENCY EQUATION

This is a Mathematica script file to conduct root searches using Mueller's method. The comments and instructions are in Italic. The Mathematica commands can be typed or cut and pasted into a Mathematica session.

The following define the ratio of inner to outer radius, the circumferential wavenumber, the elastic constants and density of the cylinder, and the densities and acoustic phase velocities of the inner and outer fluids.

```
s=.8;n=1;
c11 = 3.7 c44;
c12 = 1.7 c44;
c13 = 2.3 c44;
c33 = 100 c44;
c66 = c44;
rho = 1014;
rho1 = 1000;
rho2 = 1000;
c1 = 1500;
c2 = 1500;
```

The following Mathematica instructions simplify the arguments of the Bessel functions and their coefficients.

```
kappa1 = 1/2((c11+c44)/c11 omega^2 + (c13^2 + 2 c13 c44 - c11 c33)/(c11 c44) *
      delta^2);
kappa1 = Cancel[kappa1];
kappa1 = Simplify[kappa1];
kappa2 = (c44/c11 omega^2 - c33/c11 delta^2)(omega^2 - delta^2);
kappa3 = Simplify[kappa1 - Sqrt[kappa1^2 - kappa2]];
kappa3 = PowerExpand[kappa3];
kappa3 = Simplify[kappa3];
kappa4 = Simplify[kappa1 + Sqrt[kappa1^2 - kappa2]];
kappa4 = PowerExpand[kappa4];
kappa4 = Simplify[kappa4];
kappa5 = c44/c66 (omega^2 - delta^2);
```

```
kappa6 = -(c13+c44) delta^2 kappa3/(c44 omega^2 - c33 delta^2 - c44 kappa3);
kappa7 = (c44 delta^2 - c44 omega^2 + c11 kappa4)/(c13 + c44);


denom = c44 omega^2-c33 delta^2 -c44 kappa3;
denom = Collect[denom,c44];
denom = Simplify[denom];
num1 = (c33+c44) delta^2 omega^2 - c33 delta^4 - c44 omega^4 +
      (c44 omega^2 + c13 delta^2) kappa3;
num1 = Collect[num1,c44];
num1 = Simplify[num1];
num1= Cancel[num1/denom];
num2 = (c13(delta^2 - omega^2) -c11 kappa4)/(c13 + c44);
num2 = Cancel[num2];
num2 = Simplify[num2];
num3 = delta^2(c33 delta^2 - c44 omega^2 - c13 kappa3);
num3 = Collect[num3,c44];
num3 = Cancel[num3/denom];
num4 = (c11 kappa4 - c44 omega^2 - c13 delta^2)/(c13+c44);
num4 = Cancel[num4];
num4 = Simplify[num4];
c44 = 5.7*10^6;
alpha = c44/(rho*c1^2) omega^2 - delta^2;
beta = c44/(rho*c2^2) omega^2 - delta^2;

xi1 = Sqrt[kappa3];
xi2 = Sqrt[kappa4];
xi3 = Sqrt[kappa5];
xi4 = Sqrt[Abs[alpha]];
xi5 = Sqrt[Abs[beta]];
```

The next Mathematica instructions define the components of the determinant /L/.

```
L11 = (2c66/c44 n (n-1) + num1 (s/(1-s))^2)*
BesselJ[n,xi1 s/(1-s)] + 2c66/c44  xi1 s/(1-s) BesselJ[n+1,xi1 s/(1-s)];

L12 = (2c66/c44 n (n-1) + num1 (s/(1-s))^2)*
BesselY[n,xi1 s/(1-s)] + 2c66/c44 xi1 s/(1-s) BesselY[n+1,xi1 s/(1-s)];

L13 = ((2c66/c44 n (n-1) + num2 (s/(1-s))^2)*
BesselJ[n,xi2 s/(1-s)] + 2c66/c44 xi2 s/(1-s) BesselJ[n+1,xi2 s/(1-s)]);

L14 = ((2c66/c44 n (n-1) + num2 (s/(1-s))^2)*
```

```
BesselY[n,xi2 s/(1-s)] + 2c66/c44 xi2 s/(1-s) BesselY[n+1,xi2 s/(1-s)]);

L15 = 2c66/c44 n( (n-1) BesselJ[n,xi3 s/(1-s)] - xi3 s/(1-s)*
BesselJ[n+1,xi3 s/(1-s)]);

L16 = 2c66/c44 n( (n-1) BesselY[n,xi3 s/(1-s)] - xi3 s/(1-s)*
BesselY[n+1,xi3*s/(1-s)]);

L17 = (rho1/rho omega^2) (s/(1-s))^2 BesselI[n,xi4 s/(1-s)];

L18 = 0;

L21 = num3 (n BesselJ[n,xi1 s/(1-s)] - xi1 s/(1-s) BesselJ[
     n+1, xi1 s/(1-s)]);

L22 = num3 (n BesselY[n,xi1 s/(1-s)] - xi1 s/(1-s) BesselY[
     n+1, xi1 s/(1-s)]);

L23 = num4 (n BesselJ[n,xi2 s/(1-s)] - xi2 s/(1-s) BesselJ[
     n+1, xi2 s/(1-s)]);

L24 = num4 (n BesselY[n,xi2 s/(1-s)] - xi2 s/(1-s) BesselY[
     n+1, xi2 s/(1-s)]);

L25 = -n  delta^2 BesselJ[n,xi3 s/(1-s)];

L26 = -n  delta^2 BesselY[n,xi3 s/(1-s)];

L27 = 0;

L28 = 0;

L31 = c66/c44 (-2n((n-1) BesselJ[n,xi1 s/(1-s)] -
    xi1 s/(1-s) BesselJ[n+1,xi1 s/(1-s)]));

L32 = c66/c44 (-2n((n-1) BesselY[n,xi1 s/(1-s)] -
     xi1 s/(1-s) BesselY[n+1,xi1 s/(1-s)]));

L33 = c66/c44 (-2n((n-1) BesselJ[n,xi2 s/(1-s)] -
    xi2 s/(1-s) BesselJ[n+1,xi2 s/(1-s)]));

L34 = c66/c44 (-2n((n-1) BesselY[n,xi2 s/(1-s)] -
     xi2 s/(1-s) BesselY[n+1,xi2 s/(1-s)]));
```

```
L35 = c66/c44 ((kappa5 (s/(1-s))^2 - 2n (n-1)) BesselJ[n,xi3*
    s/(1-s)] -2 xi3 s/(1-s) BesselJ[n+1,xi3 s/(1-s)]);

L36 = c66/c44 ((kappa5 (s/(1-s))^2 - 2n (n-1)) BesselY[n,xi3*
    s/(1-s)] -2 xi3 s/(1-s) BesselY[n+1,xi3 s/(1-s)]);

L37 = 0;

L38 = 0;

L41 = n BesselJ[n,xi1 s/(1-s)] - xi1 s/(1-s) BesselJ[n+1,xi1 s/(1-s)];

L42 = n BesselY[n,xi1 s/(1-s)] - xi1 s/(1-s) BesselY[n+1,xi1 s/(1-s)];

L43 = n BesselJ[n,xi2 s/(1-s)] - xi2 s/(1-s) BesselJ[n+1,xi2 s/(1-s)];

L44 = n BesselY[n,xi2 s/(1-s)] - xi2 s/(1-s) BesselY[n+1,xi2 s/(1-s)];

L45 = n BesselJ[n,xi3 s/(1-s)];

L46 = n BesselY[n, xi3 s/(1-s)];

L47 = -(n BesselI[n,xi4 s/(1-s)] + xi4 s/(1-s) BesselI[n+1,xi4 s/(1-s)]);

L48 = 0;

L51 = (2c66/c44 n (n-1) + num1 (1/(1-s))^2)*
BesselJ[n,xi1 1/(1-s)] + 2c66/c44 xi1 1/(1-s) BesselJ[n+1,xi1 1/(1-s)];

L52 = (2c66/c44 n (n-1) + num1 (1/(1-s))^2)*
BesselY[n,xi1 1/(1-s)] + 2c66/c44 xi1 1/(1-s) BesselY[n+1,xi1 1/(1-s)];

L53 = ((2c66/c44 n (n-1) + num2 (1/(1-s))^2)*
BesselJ[n,xi2 1/(1-s)] + 2c66/c44 xi2 1/(1-s) BesselJ[n+1,xi2 1/(1-s)]);

L54 = ((2c66/c44 n (n-1) + num2 (1/(1-s))^2)*
BesselY[n,xi2 1/(1-s)] + 2c66/c44 xi2 1/(1-s) BesselY[n+1,xi2 1/(1-s)]);

L55 = 2c66/c44 n( (n-1) BesselJ[n,xi3 1/(1-s)] - xi3 1/(1-s) *
BesselJ[n+1,xi3 1/(1-s)]);

L56 = 2c66/c44 n( (n-1) BesselY[n,xi3 1/(1-s)] - xi3 1/(1-s) *
```

```
BesselY[n+1,xi3 1/(1-s)]);

L57 = 0;

L58 = (rho2/rho) omega^2 (1/(1-s))^2 BesselK[n,xi5 1/(1-s)];

L61 = num3 (n BesselJ[n,xi1 1/(1-s)] - xi1 1/(1-s) BesselJ[
    n+1, xi1 1/(1-s)]);

L62 = num3 (n BesselY[n,xi1 1/(1-s)] - xi1 1/(1-s) BesselY[
    n+1, xi1 1/(1-s)]);

L63 = num4 (n BesselJ[n,xi2 1/(1-s)] - xi2 1/(1-s) BesselJ[
    n+1, xi2 1/(1-s)]);

L64 = num4 (n BesselY[n,xi2 1/(1-s)] - xi2 1/(1-s) BesselY[
    n+1, xi2 1/(1-s)]);

L65 = -n delta^2 BesselJ[n,xi3 1/(1-s)];

L66 = -n delta^2  BesselY[n,xi3 1/(1-s)];

L67 = 0;

L68 = 0;

L71 =  c66/c44 (-2n((n-1) BesselJ[n,xi1 1/(1-s)] - xi1 1/(1-s)*
    BesselJ[n+1,xi1 1/(1-s)]));

L72 =  c66/c44 (-2n((n-1) BesselY[n,xi1 1/(1-s)] - xi1 1/(1-s) *
    BesselY[n+1,xi1 1/(1-s)]));

L73 =  c66/c44 (-2n((n-1) BesselJ[n,xi2 1/(1-s)] - xi2 1/(1-s)*
    BesselJ[n+1,xi2 1/(1-s)]));

L74 =  c66/c44 (-2n((n-1) BesselY[n,xi2 1/(1-s)] - xi2 1/(1-s)*
    BesselY[n+1,xi2 1/(1-s)]));

L75 =  c66/c44 ((kappa5 (1/(1-s))^2 - 2n (n-1)) BesselJ[n,xi3*
    1/(1-s)] -2 xi3 1/(1-s) BesselJ[n+1,xi3 1/(1-s)]);

L76 = c66/c44 ((kappa5 (1/(1-s))^2 - 2n (n-1)) BesselY[n,xi3*
    1/(1-s)] -2 xi3 1/(1-s) BesselY[n+1,xi3 1/(1-s)]);
```

```
L77 = 0;

L78 = 0;

L81 = n BesselJ[n,xi1 1/(1-s)] - xi1 1/(1-s) BesselJ[n+1,xi1 1/(1-s)];

L82 = n BesselY[n,xi1 1/(1-s)] - xi1 1/(1-s) BesselY[n+1,xi1 1/(1-s)];

L83 = n BesselJ[n,xi2 1/(1-s)] - xi2 1/(1-s) BesselJ[n+1,xi2 1/(1-s)];

L84 = n BesselY[n,xi2 1/(1-s)] - xi2 1/(1-s) BesselY[n+1,xi2 1/(1-s)];

L85 = n BesselJ[n,xi3 1/(1-s)];

L86 = n BesselY[n,xi3 1/(1-s)];

L87 = 0;

L88 = -(n BesselK[n,xi5 1/(1-s)] - xi5 1/(1-s) BesselK[n+1,xi5 1/(1-s)]);
```

"Myroot" is a Mathematica program (somewhat like a subroutine) that is called with the arguments x, y, z. These arguments are the "first guess" root locations. This program uses Mueller's method to locate the closest root to the first guess. If a root is not found after 25 iterations, the program stops. The criteria for convergence is that the difference between the current value of a possible root and the last calculated value is less than 1x10^-10.

```
myroot := For[i=1,i<25,i++,(
q = (z-y)/(y-x);
omega = x;
xi1 = Sqrt[kappa3];
xi2 = Sqrt[kappa4];
xi3 = Sqrt[kappa5];
xi4 = Sqrt[Abs[alpha]];
xi5 = Sqrt[Abs[beta]];
matrix = {{N[L11],N[L12],N[L13],N[L14],N[L15],N[L16],N[L17],N[L18]},
      {N[L21],N[L22],N[L23],N[L24],N[L25],N[L26],N[L27],N[L28]},
      {N[L31],N[L32],N[L33],N[L34],N[L35],N[L36],N[L37],N[L38]},
      {N[L41],N[L42],N[L43],N[L44],N[L45],N[L46],N[L47],N[L48]},
      {N[L51],N[L52],N[L53],N[L54],N[L55],N[L56],N[L57],N[L58]},
      {N[L61],N[L62],N[L63],N[L64],N[L65],N[L66],N[L67],N[L68]},
      {N[L71],N[L72],N[L73],N[L74],N[L75],N[L76],N[L77],N[L78]},
```

```
      {N[L81],N[L82],N[L83],N[L84],N[L85],N[L86],N[L87],N[L88]}};
px = Det[matrix];
omega = y;
xi1 = Sqrt[kappa3];
xi2 = Sqrt[kappa4];
xi3 = Sqrt[kappa5];
xi4 = Sqrt[Abs[alpha]];
xi5 = Sqrt[Abs[beta]];
matrix = {{N[L11],N[L12],N[L13],N[L14],N[L15],N[L16],N[L17],N[L18]},
      {N[L21],N[L22],N[L23],N[L24],N[L25],N[L26],N[L27],N[L28]},
      {N[L31],N[L32],N[L33],N[L34],N[L35],N[L36],N[L37],N[L38]},
      {N[L41],N[L42],N[L43],N[L44],N[L45],N[L46],N[L47],N[L48]},
      {N[L51],N[L52],N[L53],N[L54],N[L55],N[L56],N[L57],N[L58]},
      {N[L61],N[L62],N[L63],N[L64],N[L65],N[L66],N[L67],N[L68]},
      {N[L71],N[L72],N[L73],N[L74],N[L75],N[L76],N[L77],N[L78]},
      {N[L81],N[L82],N[L83],N[L84],N[L85],N[L86],N[L87],N[L88]}};
py = Det[matrix];
omega = z;
xi1 = Sqrt[kappa3];
xi2 = Sqrt[kappa4];
xi3 = Sqrt[kappa5];
xi4 = Sqrt[Abs[alpha]];
xi5 = Sqrt[Abs[beta]];
matrix = {{N[L11],N[L12],N[L13],N[L14],N[L15],N[L16],N[L17],N[L18]},
      {N[L21],N[L22],N[L23],N[L24],N[L25],N[L26],N[L27],N[L28]},
      {N[L31],N[L32],N[L33],N[L34],N[L35],N[L36],N[L37],N[L38]},
      {N[L41],N[L42],N[L43],N[L44],N[L45],N[L46],N[L47],N[L48]},
      {N[L51],N[L52],N[L53],N[L54],N[L55],N[L56],N[L57],N[L58]},
      {N[L61],N[L62],N[L63],N[L64],N[L65],N[L66],N[L67],N[L68]},
      {N[L71],N[L72],N[L73],N[L74],N[L75],N[L76],N[L77],N[L78]},
      {N[L81],N[L82],N[L83],N[L84],N[L85],N[L86],N[L87],N[L88]}};
pz = Det[matrix];
a = q pz - q (1+q) py + q^2 px;
b = (2q + 1) pz - (1 + q)^2 py + q^2 px;
c = (1 + q) pz;
den1 = b + Sqrt[b^2 - 4 a c];
den2 = b - Sqrt[b^2 - 4 a c];
d = Abs[den1];
e = Abs[den2];
If[d > e, denom = den1, denom = den2];
next = Chop[z - (z - y) (2 c/ denom),10^-6];
x = y; y = z; z = next;
f = Chop[z-y];
```

```
If[f != 0, Continue[], Return[next]];
omega = next;
xi1 = Sqrt[kappa3];
xi2 = Sqrt[kappa4];
xi3 = Sqrt[kappa5];
xi4 = Sqrt[Abs[alpha]];
xi5 = Sqrt[Abs[beta]];
matrix = {{N[L11],N[L12],N[L13],N[L14],N[L15],N[L16],N[L17],N[L18]},
      {N[L21],N[L22],N[L23],N[L24],N[L25],N[L26],N[L27],N[L28]},
      {N[L31],N[L32],N[L33],N[L34],N[L35],N[L36],N[L37],N[L38]},
      {N[L41],N[L42],N[L43],N[L44],N[L45],N[L46],N[L47],N[L48]},
      {N[L51],N[L52],N[L53],N[L54],N[L55],N[L56],N[L57],N[L58]},
      {N[L61],N[L62],N[L63],N[L64],N[L65],N[L66],N[L67],N[L68]},
      {N[L71],N[L72],N[L73],N[L74],N[L75],N[L76],N[L77],N[L78]},
      {N[L81],N[L82],N[L83],N[L84],N[L85],N[L86],N[L87],N[L88]}};
g = Chop[Det[matrix]];
If[g != 0,Continue[],Return[next]])]
```

The following is a representative set of Mathematica instructions to locate two roots for two branches. Typically, a root if found in 6 or 7 iterations. Several of these sets of instructions can be input at once to run the root searches unattended. The answers, which are displayed on the screen, and can be saved in a text file, are shown in Italics.

```
delta = N[.005*Pi]
x=.26;y=.27;z=.28;myroot
omega = 0.2705293700078156
x=.39;y=.395;z=.4;myroot
omega = 0.3950075764334804
```

The numerical computations were performed using machine precision numbers, where precision refers to the total number of significant decimal digits. In the case of the computers used to compute the results shown in the body of the dissertation, the machine precision was 16. The accuracy of a root is the number of significant decimal digits to the right of the decimal point.

APPENDIX C. MATERIAL PROPERTIES

Steel

Young's modulus: 21×10^{10} N/m^2

Poisson's ratio: 0.3

Density: 7800 kg/m^3

Rubber

Young's modulus: 1.5×10^7 N/m^2

Poisson's ratio: 0.45

Density: 1000 kg/m^3

Inner and Outer Fluids

Acoustic phase velocity: 1500 m/sec^2

Density: 1000 kg/m^3

Composite material matrix

Young's modulus: 1.5×10^7 N/m^2

Poisson's ratio: 0.45

Density: 1000 kg/m^3

Volume fraction: 0.9

Composite material reinforcing fibers

Young's modulus: 5.5×10^9 N/m^2

Poisson's ratio: 0.15

Density: 1140 kg/m^3

Volume fraction: 0.1

APPENDIX D. MATHEMATICA PROGRAM TO DETERMINE THE EFFECTIVE ELASTIC CONSTANTS

This is a Mathematica script file to determine the elastic constants of a homogeneous, transversely isotropic material. The comments and instructions in Italic are not Mathematica commands. The Mathematica commands can be typed or cut and pasted into a Mathematica session to produce the results shown in Italics.

First, we define Kronecker's delta, the unit vector {m}, and the symmetry of the components of the strain tensor.

```
kroneckerDelta[i_,j_] := If[i==j,1,0]

m[p_,q_] := m[p] m[q]

eps[2,1]=eps[1,2]
eps[1,3]=eps[3,1]
eps[3,2]=eps[2,3]
```

The following is equation 2.6.

```
stress[i_,j_] := Expand[ kroneckerDelta[i,j] (c1 Sum[eps[k,k],{k,1,3}] +
    c2 Sum[m[p,q] eps[p,q],{p,1,3},{q,1,3}]) + m[i,j] (c2 Sum[eps[k,k],{k,1,3}] +
    c3 Sum[m[p,q] eps[p,q], {p,1,3},{q,1,3}]) + c4 eps[i,j] +
    c5 (Sum[m[i,p] eps[p,j], {p,1,3}] + Sum[m[j,p] eps[p,i],{p,1,3}]) ];
```

When the direction cosines are defined as m[1] = 0, m[2] = 0, m[3] = 1, the elastic constants are found from the equations below.

```
m[1] = 0
m[2] = 0
m[3] = 1


c11 = Simplify[Coefficient[stress[1,1],eps[1,1]]]
c12 = Simplify[Coefficient[stress[1,1],eps[2,2]]]
c13 = Simplify[Coefficient[stress[1,1],eps[3,3]]]
c14 = Simplify[Coefficient[stress[1,1],eps[2,3]]]
```

```
c15 = Simplify[Coefficient[stress[1,1],eps[3,1]]]
c16 = Simplify[Coefficient[stress[1,1],eps[1,2]]]

c21 = Simplify[Coefficient[stress[2,2],eps[1,1]]]
c22 = Simplify[Coefficient[stress[2,2],eps[2,2]]]
c23 = Simplify[Coefficient[stress[2,2],eps[3,3]]]
c24 = Simplify[Coefficient[stress[2,2],eps[2,3]]]
c25 = Simplify[Coefficient[stress[2,2],eps[3,1]]]
c26 = Simplify[Coefficient[stress[2,2],eps[1,2]]]

c31 = Simplify[Coefficient[stress[3,3],eps[1,1]]]
c32 = Simplify[Coefficient[stress[3,3],eps[2,2]]]
c33 = Simplify[Coefficient[stress[3,3],eps[3,3]]]
c34 = Simplify[Coefficient[stress[3,3],eps[2,3]]]
c35 = Simplify[Coefficient[stress[3,3],eps[3,1]]]
c36 = Simplify[Coefficient[stress[3,3],eps[1,2]]]

c41 = Simplify[Coefficient[stress[2,3],eps[1,1]]]
c42 = Simplify[Coefficient[stress[2,3],eps[2,2]]]
c43 = Simplify[Coefficient[stress[2,3],eps[3,3]]]
c44 = Simplify[Coefficient[stress[2,3],eps[2,3]]/2]
c45 = Simplify[Coefficient[stress[2,3],eps[3,1]]/2]
c46 = Simplify[Coefficient[stress[2,3],eps[1,2]]/2]

c51 = Simplify[Coefficient[stress[3,1],eps[1,1]]]
c52 = Simplify[Coefficient[stress[3,1],eps[2,2]]]
c53 = Simplify[Coefficient[stress[3,1],eps[3,3]]]
c54 = Simplify[Coefficient[stress[3,1],eps[2,3]]/2]
c55 = Simplify[Coefficient[stress[3,1],eps[3,1]]/2]
c56 = Simplify[Coefficient[stress[3,1],eps[1,2]]/2]

c61 = Simplify[Coefficient[stress[1,2],eps[1,1]]]
c62 = Simplify[Coefficient[stress[1,2],eps[2,2]]]
c63 = Simplify[Coefficient[stress[1,2],eps[3,3]]]
c64 = Simplify[Coefficient[stress[1,2],eps[2,3]]/2]
c65 = Simplify[Coefficient[stress[1,2],eps[3,1]]/2]
c66 = Simplify[Coefficient[stress[1,2],eps[1,2]]/2]
```

The answers are as follows:

c11 = c1 + c4
c12 = c1
c13 = c1 + c2

c33 = c1 + 2c2
c44 = (c4 + c5)/2
c66 = c4/2

When the following relationships between the constants c1, c2, c3, c4, and c5 and the more familiar engineering constants are defined,

c1 = bt - gt
c2 = (2 vl - 1)bt + gt
c3 = El + (2 vl - 1)^2 bt- 4 gl + gt
c4 = 2 gt
c5 = 2 gl - 2 gt

the elastic constants, in terms of the engineering constants simplify to:

c11 = bt + gt
c12 = bt - gt
c13 = 2 bt vl
c33 = El + 4 bt vl^2
c44 = gl
c66 = gt

When the cylinder is made from a fiber reinforced matrix, the effective properties can be found from

El = Ef Vf + Em Vm
Et = (Ef Em)/(Vm Ef + Vf Em)
vl = Vm vm + Vf vf
vt = vm
gl = (gm gf)/(Vm gf + Vf gm)
gt = Et/(2(1+vt))
rho = pf Vf + pm Vm
bt = .5 Et/(1-vt-2vl^2 Et/El)

The following properties were used for a soft rubber matrix reinforced with nylon cords

Ef = 5.5*10^9
Em = 1.5*10^7
vm = 0.45
vf = 0.15
gm = Em/(2(1+vm))
gf = Ef/(2(1+vf))

pm = 1000
pf = 1140
Vf = 0.10
Vm = 0.90

The resultant effective properties are

*El = 5.635*10^8*
*Et = 1.66616*10^7*
vl = 0.42
vt = 0.45
*gl = 5.74575*10^6*
*gt = 5.74539*10^6*
*bt = 1.54398*10^7*
rho = 1014

The elastic constants become

rho = 1014
*c11 = 2.11851*10^7*
*c12 = 9.69438*10^6*
*c13 = 1.29694*10^7*
*c33 = 5.74394*10^8*
*c44 = 5.74575*10^6*
*c66 = 5.74539*10^6*

The above components are normalized for numerical computations

*c11 = 3.6871 c44 = 3.7*c44*
*c12 = 1.68723 c44 = 1.7*c44*
*c13 = 2.25722 c44 = 2.3*c44*
*c33 = 99.9686 c44 = 100*c44*
c66 = 0.999937 c44 = c44

BIBLIOGRAPHY

Abramowitz, M., Stegun, I. E., eds, (1972) *Handbook of mathematical functions with formulas, graphs, and mathematical tables*, National Bureau of Standards Applied Mathematics, Series 55, Tenth Printing, Dept. of Commerce, Washington, D. C.

Achenbach, J. D. (1990) *Wave propagation in elastic solids*, Sixth printing, Elseivier Science Publishing Company, Inc., New York, NY.

Armenakas, A. E., Gazis, D. C., and Herrmann, G. (1969) *Free vibrations of circular cylindrical shells*, Pergamon Press, Inc., New York.

Armenakas, A. E., Reitz, E. S. (1973) Propagation of harmonic waves in orthotropic circular cylindrical shells, *J. Appl. Mech.* **40**, 168-174.

Bird, J. F. (1960) Vibrations of thick-walled hollow cylinders: Approximate theory, *J. Acoust. Soc. Am.* **32**, 1413-1419.

Bird, J. F., Hart, R. W., McClure, F. T. (1960) Vibrations of thick-walled hollow cylinders: Exact numerical solutions, *J. Acoust. Soc. Am.* **32**, 1404-1413.

Bleich, H. H., Baron, M. L. (1954) Free and forced vibrations of an infinitely long cylindrical shell in an infinite acoustic medium, *J. Acoust. Soc. Am.* **21**, 167-177.

Chandra, J., Kumar, R. (1976) Dispersion of axially symmetric waves in cylindrical shells, immersed in an acoustic medium, *Acustica* **35**, 1-10.

Chree, C. (1890) *On the longitudinal vibrations of aeolotropic bars with one axis of material symmetry*, Quart. J. Math. **24**, 340-354.

Christensen, R. M. (1979) *Mechanics of Composite Materials*, John Wiley & Sons, New York.

Cooper, R. M., Naghdi, P. M. (1957) Propagation of nonaxially symmetric waves in elastic cylindrical shells, *J. Acoust. Soc. Am.* **29**, 1365-1375.

Fay, R. D., Brown, R. L., Fortier, O. V. (1947) Measurement of acoustic impedances of surfaces in water, *J.Acoust. Soc. Am.* **19**, 850-856.

Fraser, W. B. (1980) Separable equations for a cylindrical anisotropic elastic waveguide, *J. Sound Vib.* **72**, 151-157.

Fuller, C. R., Fahy, F. J. (1982) Characteristics of wave propagation and energy distribution in cylindrical elastic shells filled with fluid, *J. Sound Vib.* **81**, 501-518.

Gazis, D. C. (1958) Exact analysis of the plane-strain vibrations of thick-walled hollow cylinders, *J. Acoust. Soc. Am.* **30**, 786-794.

Gazis, D. C. (1959a) Three-dimensional investigation of the propagation of waves in hollow circular cylinders. I. Analytical foundation, *J. Acoust. Soc. Am.* **31**, 568-573.

Gazis, D. C. (1959b) Three-dimensional investigation of the propagation of waves in hollow circular cylinders. II. Numerical results, *J. Acoust. Soc. Am.* **31**, 573-578.

Greenspon, J. E. (1960) Axially symmetric vibrations of a thick cylindrical shell in an acoustic medium, *J. Acoust. Soc. Am.* **32**, 1017-1025.

Greenspon. J. E. (1961) Vibrations of thick and thin cylindrical shells surrounded by water, *J. Acoust. Soc. Am.* **33**, 1321-1328.

Hashin, Z. (1979) Analysis of properties of fiber composites with anisotropic constituents, *J. Appl. Mech.* **46**, 543-550.

Hashin, Z. (1983) Analysis of composite materials - a survey, *J. Appl. Mech.* **50**, 481-505.

Herrmann, G., Mirsky, I. (1956) Three-dimensional and shell-theory analysis of axially symmetric motions of cylinders, *J. Appl. Mech.* **23**, 563-568.

Jacobi, W. J. (1949) Propagation of sound waves along liquid cylinders, *J. Acoust. Soc. Am.* **21**, 120-127.

Jones, R. M. (1975) *Mechanics of composite materials*, Scripta Book Company, Washington, D.C.

Junger, M. C. (1952a) Radiation loading of cylindrical and spherical surfaces, *J. Acoust. Soc. Am.* **24**, 288-289.

Junger, M. C. (1952b) Vibrations of elastic shells in a fluid medium and the associated radiation of sound, *J. Appl. Mech.* **19**, 439-445.

Junger, M. C. (1953) The physical interpretation of the expression for an outgoing wave in cylindrical coordinates, *J. Acoust. Soc. Am.* **25**, 40-?

Junger, M. C., Feit, D (1986) *Sound, structures and their interaction*, Second Edition, The MIT Press, Cambridge, MA.

Junger, M. C., Rosato, F. J. (1954) The propagation of elastic waves in thin-walled cylindrical shells, *J. Acoust. Soc. Am.* **26**, 709-713.

Kreyszig, E. (1972) *Advanced engineering mathematics*, Third Edition, John Wiley and Sons, Inc., New York, NY.

Kumar, R. (1971) Flexural vibrations of fluid-filled circular cylindrical shells, *Acustica* **24**, 137-146.

Kumar, R. (1972) Dispersion of axially symmetric waves in empty and fluid-filled cylindrical shells, *Acustica* **27**, 317-329.

Kumar, R., Stephens, R. W. B. (1972) Dispersion of flexural waves in circular cylindrical shells, *Proc. R. Soc. London* **329** (A), 283-297.

Lin, T. C., Morgan, G. W. (1956a) A study of axisymmetric vibrations of cylindrical shells as affected by rotary inertia and transverse shear, *J. Appl. Mech.* **23**, 255-261.

Lin, T. C., Morgan, G. W. (1956b) Wave propagation through fluid contained in a cylindrical, elastic shell, *J. Acoust. Soc. Am.* **28**, 1165-1176.

Love, A. E. H., (1944) *A Treatise on the mathematical theory of elasticity*, Fourth Edition, Dover Publications, New York, N. Y.

McFadden, J. A. (1954) Radial vibrations of thick-walled hollow cylinders, *J. Acoust. Soc. Am.* **26**, 714-715.

McNiven, H. D., Shah, A. H., Sackman, J. L. (1966a) Axially symmetric waves in hollow, elastic rods: Part I, *J. Acoust. Soc. Am.* **40**, 784-792.

McNiven, H. D., Sackman, J. L., Shah, A. H. (1966b) Axially symmetric waves in hollow, elastic rods: Part II, *J. Acoust. Soc. Am.* **40**, 1072-1076.

Mirsky, I. (1964) Axisymmetric vibrations of orthotropic cylinders, *J. Acoust. Soc. Am.* **36**, 2106-2112.

Mirsky, I. (1965a) Wave propagation in transversely isotropic circular cylinders, Part I: Theory, *J. Acoust. Soc. Am.* **37**, 1016-1021.

Mirsky, I. (1965b) Wave propagation in transversely isotropic circular cylinders, Part

II: Numerical results, *J Acoust. Soc. Am.* **37**, 1022-1026.

Mirsky, I., Herrmann, G. (1957) Nonaxially symmetric motions of cylindrical shells, *J. Acoust. Soc. Am.* **29**, 1116-1123.

Mirksy, I., Herrmann, G. (1958) Axially symmetric motions of thick cylindrical shells, *J. Appl. Mech.* **25**, 97-102.

Morse, R. W. (1954) Compressional waves along an anisotropic circular cylinder having hexagonal symmetry, *J. Acoust. Soc. Am.* **26**, 1018-1021.

Naghdi, P. M., Berry, J. G. (1954) On the equations of motion of cylindrical shells, *J. Appl. Mech.* **21**, 160-166.

Naghdi, P. M., Cooper, R. M. (1956) Propagation of elastic waves in cylindrical shells, including the effects of transverse shear and rotary inertia, *J. Acoust. Soc. Am.* **28**, 56-63.

Payton, R. G. (1983) *Elastic wave propagation in transversely isotropic media*, Martinus Nijhoff Publishers, The Hague, The Netherlands.

Plona, T. J., Sinha, B. K., Kostek. S. Chang, S. K. (1992) Axisymmetric wave propagation in fluid-loaded cylindrical shells. II: Theory versus experiment, *J. Acoust. Soc. Am.* **92**, 1144-1155.

Press, W. H., Flannery, B. P., Teukolsky, S. A., Vettering, W. T. (1986) *Numerical recipes: The art of scientific computing*, Cambridge University Press, New York, NY.

Sinha, B. K., Plona, T. J., Kostek. S., Chang S. K. (1992) Axisymmetric wave propagation in fluid-loaded cylindrical shells. I: Theory, *J. Acoust. Soc. Am.* **92** (2), 1132-1143.

Skalak, R. (1966) Wave propagation in blood flow, *Biomechanics, Proc. Symp. Appl. Mech. Div. (ed. Y. C. Fung)*, New York.

Sokolnikoff, I. S. (1987) *Mathematical theory of elasticity*, Reprint Edition, Krieger Publishing Company, Malabar, FL.

Sutcu, M. (1992) Orthotropic and transversely isotropic stress-strain relations with built-in coordinate transformations, *Int. J. Solids Structures* **29**, 503-518.

Thomson, W. T. (1953) Transmission of pressure waves in liquid filled tubes, *Proc. of the First U.S. National Congress on Appl. Mech.*, Chicago, IL, 922-933.

Wolfram, S. (1991) *Mathematica: A system for doing mathematics by computer*, Second Edition, Addison-Wesley Publishing Company, Inc., Redwood City, CA.

Young, T. (1808) Hydraulic investigations, subservient to an intended croonian lecture on the motion of the blood, *Phil. Trans. Roy. Soc. London* **98**, 164-186.

INITIAL DISTRIBUTION LIST

Addressee	No. of Copies
Defense Technical Information Center	12
Office of Naval Research (Code 321 SS: K. G. Dial, R. Varley)	2
Technology Services Corporation (L. Brooks)	1
Cambridge Acoustical Associates (J. M. Garrelick, J. E. Cole)	2
Bolt Beranek & Newman, Cambridge (B. Watters)	1
Applied Measurement Systems, Inc., New London (J. Diggs)	1
Defence Research Establishment, Atlantic (J. B. Franklin, P. Barry)	2